Aggregated scale modelling of tidal inlets of the Wadden Sea

Morphological response to the closure of the Zuiderzee

N.G. Kragtwijk

Supervisors:
prof.dr.ir. M.J.F. Stive
dr.ir. Z.B. Wang
ir. T.J. Zitman
ir. H.A.H. Petit

June 2001

Preface

The present report forms my Master of Science thesis and is carried out within the framework of my study Civil Engineering and Geosciences, Division of Hydraulics and Offshore Engineering at the Delft University of Technology. The present study has been carried out at WL | Delft Hydraulics and was funded by Delft Cluster Projects Coast 03.01.03.

This study concerns long-term modelling of the morphological development of tidal inlets due to human interferences, such as the closure of the Zuiderzee.

I would like to thank my supervisors prof.dr.ir. M.J.F. Stive (Delft University of Technology and WL | Delft Hydraulics), dr.ir. Z.B. Wang (Delft University of Technology and WL | Delft Hydraulics), ir. H.A.H. Petit (Delft University of Technology and WL | Delft Hydraulics) and especially ir. T.J. Zitman (Delft University of Technology) for sharing their knowledge and for their support during this study. Furthermore I would like to thank my temporary colleagues and fellow graduate students at WL | Delft Hydraulics for the pleasant stay. Finally, I would like to thank my family and friends for their support during the years I spent in Delft.

Nicole Kragtwijk
Delft, June 2001

Contents

List of Figures

List of Tables

Summary

A large part of the coastline of the world consists of barrier islands separated by tidal inlets, just like the Dutch Wadden islands. These inlets play an important role in the sediment budget of the coastal zone and thereby influence the long-term development of the coasts.

In 1932 the Zuiderzee was closed from sea, by completing the construction of the Afsluitdijk. The tidal inlets of the Wadden Sea evolve towards an equilibrium state that matches the situation that has arisen as a result of the closure. At this moment little knowledge is available on the morphological behaviour of these inlets since the closure and the future equilibrium state.

The objective of this study is to obtain more insight into the long-term morphological behaviour of tidal inlets as a consequence of large scale interventions calibrating Asmita for the closure of the Zuiderzee.

In order to analyse the long-term development of tidal inlets, we have to consider a high level of aggregation. At such a level of aggregation we can distinguish three elements in a tidal system: the ebb-tidal delta, the channel and the tidal flat. Empirical equilibrium relations exist which describe the relation between the (wet or dry) equilibrium volumes of these elements and the tidal volume. The equilibrium state is the starting-point of the model formulation of Asmita. Asmita is a behaviour-oriented model which describes the evolution of a tidal system that is brought out of its equilibrium, towards its equilibrium state.

To calibrate Asmita for the closure of the Zuiderzee, the Asmita equations have been linearised. In this way, the morphological development of a tidal inlet has been expressed explicitly in time-scales. The evolution of each element is described by a combination of three system time-scales, which depend on geometric and exchange characteristics of the system (input parameters of Asmita). These linearised equations give insight into the morphological response of a tidal system to disturbances. In particular, it can be demonstrated that in some situations an element does not evolve monotonously towards its equilibrium state, but first overshoots its equilibrium or initially moves away from it. Finally, the linearised equations pointed out that in the case of a system like the Marsdiep the equilibrium volumes, diffusion coefficients and equilibrium concentration have a large influence on the system time-scales compared to the other Asmita parameters. These formed important parameters in the calibration.

Analysis of the tide and of digitised maps of bed topography point out that the inlets Vlie and Marsdiep are suitable for calibration purposes as in these inlets significant changes have occurred in both the hydrodynamics and morphology. The character of the tidal wave along the basin changed from a more propagating character in the former Zuiderzee, into a more standing character after closure. Before closure the tidal range decreased from sea towards Nijkerk and after closure the tidal range increased from sea towards the Afsluitdijk. As a result, the tidal volume in these inlets increased instantaneously due to the closure of the Zuiderzee. Based on digitised maps of bed topography (1933-1998), volumetric data of the elements of these inlets have been computed by Biegel (1993) and additional volumes for

recent years have been computed in this study. For both inlets it holds that the volume of the flats shows an increase due to the reduction in area. The channel volume shows a decrease, because the sedimentation in the back of the basin dominated the erosion near the throat. The delta volumes relative to a time-invariable reference coastal profile show a decrease, while an increase is expected based on the equilibrium relation. The difference can be explained from a regression of the coast adjacent to the delta. This regression has been neglected unjustly in interpreting field data on delta evolution.

The delta volumes have been adjusted for the retreated coastal profile by adding an extra term to the sediment balance for the delta. With this addition we have included the relation between the sediment demand of the tidal inlet and the regression of the coast to the Asmita formulation. The delta volumes from field data till 1990 have been adjusted, as since then the coastline has been maintained at its position by nourishments.

A plausible calibration of Asmita for the morphological development of Vlie and Marsdiep inlet is possible. All elements show the development as derived from the data analysis. Only the delta of the Marsdiep shows an unexpected, invariable development. A possible explanation for this effect is that the delta volume before closure already exceeded its equilibrium value, due to storm surges in the former Zuiderzee, which enlarged the tidal volume.

Regarding both Marsdiep and Vlie inlets, the channel is the element which reacts the slowest. At present, the deltas and flats are close to their estimated equilibrium state. It will take at least a century before the channel, and hence the total tidal inlet system, reaches its equilibrium. About 170 million m^3 of sediment will be transported into the Vlie and Marsdiep basin. Beach nourishments slow down this process, since these prevent the delta to grow geometrically and the sediment available for the channel decreases.

Uncertainties in the total calibration process are expected with respect to the boundary interpretation of the elements (especially the delta) and the height and width measures of the delta and coast segments which are used for the adjustment of the delta volume to coastal regression.

Samenvatting (in Dutch)

In 1932 werd de Zuiderzee afgesloten van zee door de bouw van de afsluitdijk. De getijde-inlaten van de Waddenzee streven naar een evenwichtssituatie die past bij de veranderde situatie na de afsluiting. Op dit moment is er weinig bekend over het morfologisch gedrag van deze getijde-inlaten en de toekomstige evenwichtssituatie.

Het doel van deze studie is om meer inzicht te verkrijgen in de lange termijn ontwikkeling van getijde-inlaten en daarnaast specifiek om de ontwikkelingen als gevolg van de afsluiting van de Zuiderzee te beschrijven en te voorspellen met het Asmita model.

Om het lange termijn gedrag te kunnen beschrijven moeten we zowel in tijd als in ruimte een hoog aggregatieniveau beschouwen. Op zo'n niveau kunnen we een getijde-inlaat onderverdelen in 3 morfologische elementen: de ebgetijde delta, de geul en de plaat. Er bestaan empirische evenwichtsrelaties die de relatie beschrijven tussen de (natte of droge) evenwichtsvolumes van deze elementen en het getijdevolume. De basisaanname in het Asmita model is dat er een evenwichtstoestand gedefinieerd kan worden voor elk van de elementen. Asmita is een gedragsgeoriënteerd model die de asymptotische ontwikkeling van de elementen naar een evenwichtstoestand beschrijft.

Om inzicht te krijgen in het morfologische gedrag van een getijde-inlaat zijn de Asmita vergelijkingen gelineariseerd. Op deze manier is de morfologische ontwikkeling van getijde-inlaten expliciet uitgedrukt in systeem tijdschalen. Deze systeem tijdschalen zijn karakteristiek voor een bepaalde inlaat en geven inzicht in de morfologische responses op een willekeurige verstoring (bijv. een afsluiting). Zo is er aangetoond dat in sommige situaties een element niet rechtstreeks naar een evenwichtssituatie ontwikkeld, maar eerst zijn evenwichtswaarde voorbijschiet of er vanaf ontwikkeld. De analyse van de gelineariseerde vergelijkingen heeft de kalibratie van het Asmita model ondersteund.

Analyse van getijdegegevens en van de gedigitaliseerde bodemkaarten (periode 1933-1998) hebben aangetoond dat in de Vlie en Marsdiep inlaten significante hydrodynamische en morfologische veranderingen zijn opgetreden als gevolg van de afsluiting van de Zuiderzee. Het karakter van de getijdegolf langs het bassin is veranderd van een lopende golf in de voormalige Zuiderzee in een min of meer staande golf na de afsluiting. Het gevolg van de afsluiting was een directe toename van het getijdevolume. Volumetrische data van de Marsdiep en Vlie inlaten zijn verzameld en berekend. Voor beide inlaten geldt dat het plaatvolume is toegenomen en het geulvolume is afgenomen. De deltavolumes, ten opzichte van een tijdsinvariant referentie kustprofiel, laten een afname zien, terwijl een toename te verwachten is op basis van de evenwichtsrelatie met het getijdevolume. Dit verschil wordt veroorzaakt doordat de kustachteruitgang ongerechtvaardigd is verwaarloosd in de interpretatie van de veldgegevens. Asmita is uitgebreid om het effect van de kustachteruitgang op het deltavolume in rekening te brengen.

Een plausibele kalibratie van het Asmita model is bewerkstelligd voor de morfologische ontwikkeling van de Marsdiep en Vlie inlaten over de periode 1933-1998. Alle elementen laten de ontwikkeling zien zoals die is afgeleid uit de data-analyse. Alleen de delta van het

Marsdiep laat een onverwachte invariabele ontwikkeling zien. Een mogelijke verklaring hiervoor is het feit dat het deltavolume voor de afsluiting groter was dan de evenwichtswaarde door de stormen in de voormalige Zuiderzee, welke een vergroting van het getijdevolume veroorzaakten.

Voor zowel de Marsdiep als de Vlie inlaat geldt in dit geval dat de geul het element is met de grootste aanpassingstijd. Op dit moment zijn de delta's en de platen dicht bij hun evenwichtswaarde. Het zal tenminste een eeuw duren voordat de geulen, en dus de getijde-inlaten, een dynamisch evenwicht bereikt zullen hebben. Hiervoor zal circa 170 miljoen m3 sediment het Vlie en Marsdiep bassin in worden getransporteerd. Strandsuppleties vertragen dit proces, omdat dan de delta niet meer geometrisch groeit waardoor de beschikbare hoeveelheid sediment voor de geulen afneemt.

1 Introduction

1.1 Background

A large part of the coastline of the world consists of barrier islands separated by tidal inlets, just like the Dutch Wadden islands. These inlets play an important role in the sediment budget of the coastal zone and thereby influence the long-term development of the coasts.

The Wadden Sea forms a complex, dynamic morphological system and it hosts a unique ecosystem. Its state and evolution are effected by a wide variety of socio-economic activities, such as navigation, recreation, fishing, sand mining, gas mining, land reclamation and flood protection.

Especially land reclamation and flood protection works have had a major impact on the morphological evolution of the Wadden area. A considerable part of the present northern part of the province of Noord-Holland is the result of extensive land reclamation over de past centuries. That applies also for the northern edges of the provinces of Friesland and Groningen. Such interventions affect the size and shape of the basins behind the gorge between the barrier islands and hence, they influence the morphology of the entire Wadden Sea area.

The closure of the Zuiderzee with a 36 km long dam, completed in 1932, was probably one of the most substantial interventions in the system. It was designed to have a minimal morphological impact. Considering the knowledge and means available at that time to predict morphological changes, the design was highly successful. Nevertheless, there is still some measurable effect.

At present there are plans to restore parts of the tidal dynamics around the closure dam of the Zuiderzee. Although this plan is part of the policy to extend the well-being of the local ecosystem, its possible impact may not be overlooked. Similar plans exist for the Lauwerszee that was closed off in 1969 as part of the Delta project (a nation wide flood protection project, initiated after the flooding in 1953). It is to be expected that such interventions will continue in future and in order to evaluate their morphological impact it is essential to develop insight into long-term morphological behaviour of tidal inlets.

The knowledge on morphological behaviour of tidal inlets is still limited, because of the complex dynamic interaction of waves, currents and bed topography. Understanding and predicting this behaviour means that we have to deal with different time spans and space scales. First an overview is given on time spans and space scales.
Stive et al.(1990) ordered the following division for scales:

very long-term (mega-scale)	time span: centuries to millennia
	space-scale: 100 km and more
long-term (macro-scale):	time span: decades to centuries
	space scale: 10-100 km

middle term (meso-scale): time span: years to decades
space scale: 1-5 km
short term (micro-scale): time span: hours to years
space scale: 10m-1km

A correlation between time spans and space scales exist. In most cases long term processes have effect on large areas and short term processes have effect in smaller areas. For example when looking on a geological time spans (i.e. thousands of years) coastal behaviour in relation to sea level rise requires understanding of the origin and development of the coast in the past. However, for a time span of 10 to 100 years, it is not the geological trend, but the fluctuations around the trend that are important for the development of the coastline. On a relative short time scales these fluctuations may even be opposite to the long-term trend.

The meso- and micro-scale levels concern phenomena like: surf zone bar cycles, and the consequence of shore nourishments. These can be modelled with process-based models. These models are based on physical processes like waves, currents and related sediment transport. To work at this level, information is needed on the complex interaction due to these processes. At this level, it is not possible to cover large time-spans as long-term variations in tide and waves will occur and we are unable to model this properly yet as there is shortage in available information. So, modelling on a long-term (macro-scale) requires empirical information as well.

Since the empirical information is not available at a very detailed scale, it is important to work at a high level of aggregation, for example in terms of principal system elements: basin, gorge, ebb-tidal delta and island coasts. In this way it might be possible to improve the predictability of long-term modelling: based on knowledge of the system's behaviour on smaller scale, another model is formulated at the higher scale, without attempting to describe every detail at the lower-scale level. In this way semi-empirical models have been developed, which are based on knowledge on physical processes, but include empirical knowledge.

An example of a semi-empirical model is the behavioural model Asmita (Aggregated Scale Morphological Interaction between a Tidal inlet and the Adjacent coast, Stive and Wang 1996). This model has opportunities to predict the morphological behaviour after an interference like the closure of the Zuiderzee.

1.2 Area of interest

The area of interest is the Western Wadden Sea. This comprises four barrier islands within between four tidal inlets; the Marsdiep (1), Eierlandse gat (2), the Vlie (3) and the Borndiep (4), see figure 2.1. Each inlet consists of three main morphological elements: a tidal basin, containing channels and flats, and an ebb-tidal delta just off-shore the islands. These elements will be explained in chapter 3.

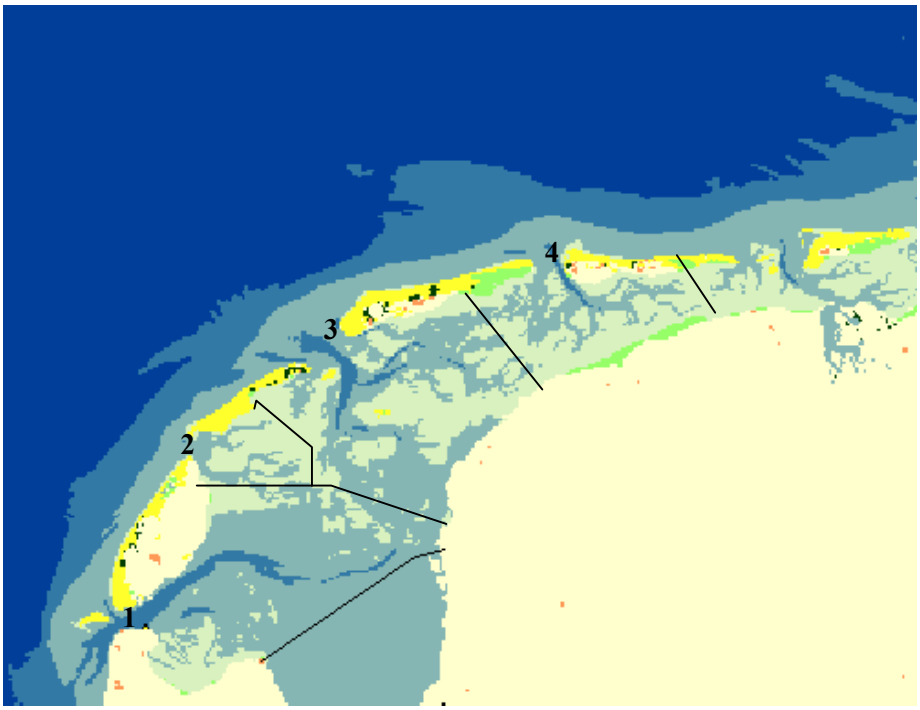

Figure 1-1 Overview tidal inlets Western Wadden Sea.

1.3 Problem analysis

In 1932 the Zuiderzee was closed from sea, by completing the construction of the Afsluitdijk. As a result of the damming of the Zuiderzee many changes have occurred in the water motions and the bed topography of the Western Wadden Sea. The tidal inlets of the Wadden Sea evolve towards an equilibrium state that matches the situation that has arisen as a result of the closure. At this moment, little is known on the morphological behaviour of these inlets since the closure, and the future equilibrium state.

The morphological response of inlets in the western Wadden Sea to closure of a part of the corresponding basin, manifests itself on a macro-scale (decades to centuries, see chapter 1).

One way to model responses at this scale, is the so-named behaviour-oriented approach. It is based on the assumption that in this case a tidal inlet evolves towards an equilibrium state that depends on some general characteristics of sediment management and tidal intrusion. Partial closure of the tidal basin, for instance, affects the tidal intrusion and hence it will divert the evolution of the inlet towards another equilibrium than the one it would have reached without the closure.

One such behavioural-oriented models is Asmita (Aggregated Scale Morphological Interaction between a Tidal inlet and the Adjacent coast, Stive and Wang 1996). It is a semi-empirical model, based on elementary physics on sediment exchange between the elements, and includes the empirical knowledge on equilibrium conditions. The equilibrium state is the starting point, and then, the adaptation process after an imposed disturbance can be simulated with this model. This model has proved to be a valuable elementary model for estimating long-term effects of subsidence due to gas mining (see Buisman 1997), but still

uncertainties arise on the fundamental behaviour of tidal inlets which are represented by several parameters in this model.

Problem definition

There is lack of insight into morphological behaviour of tidal inlets as a consequence of interventions like the closure of the Zuiderzee. Asmita could possibly describe this behaviour, but there are some uncertain parameters.

1.4 Objective

The objectives of the present study are:

- to obtain more insight into the morphological behaviour of tidal inlets as a consequence of the closure of the Zuiderzee.
- to extend the knowledge on the fundamental behaviour of tidal inlets with the Asmita model.

The approach to achieve these objectives are as follows. Obtaining insight into morphological behaviour of the inlets in the Western Wadden Sea is realised, based on analysis of both Asmita, and the available data since the closure of the Zuiderzee. This will provide knowledge to come to a proper calibration of Asmita. Then Asmita is calibrated and more information on future development of the Wadden Sea inlets may be derived. It must be noted that calibrating Asmita and obtaining insight into morphological behaviour is an interaction process, which finally leads to more understanding on both these fields.

In the Reader the structure of this study is described.

1.5 Reader

The outline of this study is as follows:

In the following chapter a description of the Wadden system is given on different scales, which were distinguished in the first chapter. The historical background on mega-scale is given and then we will zoom to the scale of interest (macro-scale) where the tidal system and related forcings are described. In chapter 3 the principles and formulation of the behaviour orientated model Asmita are explained. Subsequently, the linearised approximation of Asmita is considered in chapter 4. We have analysed different possibilities of the use of this linearisation to help the calibration of Asmita. Chapter 5 contains an analysis of available data of the area affected since the closure of the Zuiderzee. These comprise tide-data and maps of bed topography of the period 1933-1998. Also the volumetric data, which are of interest for Asmita are derived and analysed. Finally in chapter 6, Asmita is calibrated to the morphological development due to the closure of the Zuiderzee. In this way the (future) morphological development of the Vlie and Marsdiep inlet is analysed and at the same time the Asmita model is tested. We have concluded this study with some conclusions and recommendations, which are presented in chapter 7.

2 Morphodynamics of the Wadden Sea

2.1 Introduction

The Dutch Wadden Sea comprises 10 tidal basins which are divided by water sheds. These basins were created by breakthroughs and flooding of coastal planes as sea level rose. Moreover, human interferences have caused subsidence which encouraged the creation of these basins. The tidal basins consist of channels, shallow tidal flats and salt marshes. Together with the island coasts and the ebb-tidal deltas they form the Wadden system. The elements of this system react dynamically to forcings like tides, waves and wind by exchanging water and sediment. The net transport of sediment, which causes the change of the bottom with time, is called *morphological development* (morph=shape). Because there is a constant interaction between forcings and morphological changes, we speak of the *morphodynamics* of the Wadden Sea.

In this chapter a historical overview on the morphological development of the inlets of the Wadden Sea will be given as a frame of the present study. For this, the mega-scale, which means centuries or millennia, will be considered. Subsequently, we will zoom to the scale of interest, macro-scale. The forcings on a tidal inlet and the elements of a tidal inlet are explained. (These same elements will be used in the Asmita model, which is explained in the following chapter). Furthermore, a closer look is taken on the morphological development of the elements of an inlet as a consequence of these forcings. Finally, the closure of the Zuiderzee will be briefly discussed as this will be used as a case for this study.

2.2 Wadden Sea on mega-scale

The Wadden Sea is a geologically young landscape, which did not take on its current form until the warm period after the last ice age (ca. 10.000 years ago). In this section we will describe the historical development of the Wadden Sea, based on different literature.

First some background information will be given on geological sea level changes, then a theory is discussed for the formation of barrier islands and finally these two developments explain the probable development of the barrier islands of the Wadden Sea.

2.2.1 Geological evolution and sea level changes.

Natural preconditions have played a substantial role in the morphological development of the Wadden Sea and the formatting of the surrounding barrier islands. During the Tertiary and Quarternary, subsidence of the North Sea bottom has been dominant, but as soon as the Holocene began about 10.000 years ago, the sea level rise began to play a significant role. Nevertheless, speculation about widespread coastal subsidence can be traced back to 1837 (Forchhammer, 1837). Scientists assumed subsidence was the reason for the apparent rise in sea level. The eustatic consequences of melting glaciers and ice sheets on sea level was not

recognised until 1930 (Ramsay, 1930). Even then it was regarded as a causal mechanism for recent sea level changes. Dewers (Dewers, 1940) was the first to seriously question that eustatic sea level changes were negligible. After the Second World War, the coastal subsidence theory was soon refuted, because it was not possible to indicate any measurable subsidence.

Apart from eustatic movements, also tectonic movement can cause relative sea level rise. The Wadden Sea area experiences little tectonic activity and is rather stable. Therefore tectonic movement as cause for relative sea level rise can be neglected.

Since 1970, a new concept of sea level rise came up. The world-wide sea level change is not simultaneous as the eustasy definition claims. This is because of the connection between the sea level movement and the gravity change. The sea level is an equipotential surface of the earths gravity field, with a form of a geoid. This phenomenon did not play a big part in the sea level rise the past 10.000 years.

Summarising, it can be stated that melting glaciers and ice sheets have had an great impact on the relative sea level rise. Besides this, the gravity change and tectonic movements played a very small role. These factors have determined the development of the Wadden Sea and the barrier islands during the past 10.000 years.

2.2.2 Formation barrier islands

Barrier coasts like those of the North Sea are found, among other places along the east coast of the United States. In the American literature (e.g Leatherman, 1982), three different basic concepts of barrier island genesis have been considered for the North Sea coast.

1. Drowning coastal dune ridges.
2. Formation of spits, which were later breached by the sea.
3. Island development from emerging shoals

The first hypothesis fits in the theories of coastal subsidence. As a consequence of coastal subsidence barriers were believe to have formed (a.o. Haage (1899) and Wahnschaffe (1901)). After the theory of coastal subsidence was refuted, also this hypothesis was no longer valid. In 1944 the idea was promoted that shore parallel sand transport would have created the barrier (a.o. Gripp, 1944). However, as within the Wadden Sea area no major spit formation was observed (only in one island in the Eastern Wadden Sea, Isle of Sylt), this concept is not believed to be true either. From 1912 islands were believed to have formed as a result of emerging sand banks (a.o. Ordemann 1912). In the course of geological mapping the conclusion was drawn that the island chain had been built up by sediment supply from sea as follows:

1. Sand supply from the sea leads to the formation of sand banks near the coast.
2. Increasing sand supply causes the shoals to rise until they finally emerge during low tide
3. If accumulation continues, they eventually remain dry during ordinary floods.
4. Under influence of the wind, parts of the former shoal finally grow above spring tide level, forming an island.

2.2.3 Formation barrier islands Wadden Sea

The concept of the formation of barrier islands together with the geological evolution and sea level changes in the Holocene period resulted in the following description regarding the development of the Wadden Sea (o.a. Jelgersma 1979 and Zagzwijn, 1986).

Before 9200 BC (BC = Before Christ)
15000 years ago (beginning of Holocene), the sea level was 120 to 140 metres below the current level and the melting of the ice-caps cause the sea level to start rising.

9200-5800 BC (Zagwijn, 1986), see figure 2.1A
The relative sea level rapidly start rising at a rate of 80 cm up to a few metres per century. Erosion caused the coast to rapidly shift landwards and large parts of the Wadden Sea area were inundated. The first brackish lagoon was formed behind an offshore bar.

5800-3780 BC (Zagwijn, 1986), see figure 2.1B
Formation of a fairly stable coastline with tidal channels and, behind that, a zone with tidal flats, salt marshes and higher-lying peat bogs. The sea level was about 4 metres below NAP and rose by approximately 40 to 80 cm per century. Sediment was deposited at the same rate that the sea level rises. This means that the formation of the inland sea is not lost because of sea level rise. Here, the landward migration of the islands started, which still continues, though to a lesser extend.

3780-2100 BC (Zagwijn, 1986) see figure 2.1C
The sea level rose by between 40 and 20 centimetres per century. The coast was able to expand in seaward direction.

1700-1000 BC (Jelgersma, 1979)
The continuous coastal barrier was breached in several places. In the western part of the present Wadden Sea, minor tidal inlets with small drainage areas were formed.

300 BC (Jelgersma, 1979)
The freshwater lake, Lake Flevo was formed in the area of the present IJsselmeer. This Lake was later extended to form the Zuider Sea by the inundations of the early Middle Ages.

500-700 AD (Zagwijn, 1986) see figure 2.1D
The Wadden Sea area developed to the intertidal area as we knew it before the Zuider Sea was dammed. The sea level rise was about 5 to 30 cm per century.

700 AD - Present
The influence of humankind started. Acts of intervention include dike construction, empoldering, peat-cutting, as well as the damming off channels and parts of tidal basins (e.g the Zuider Sea and the Lauwers Sea).

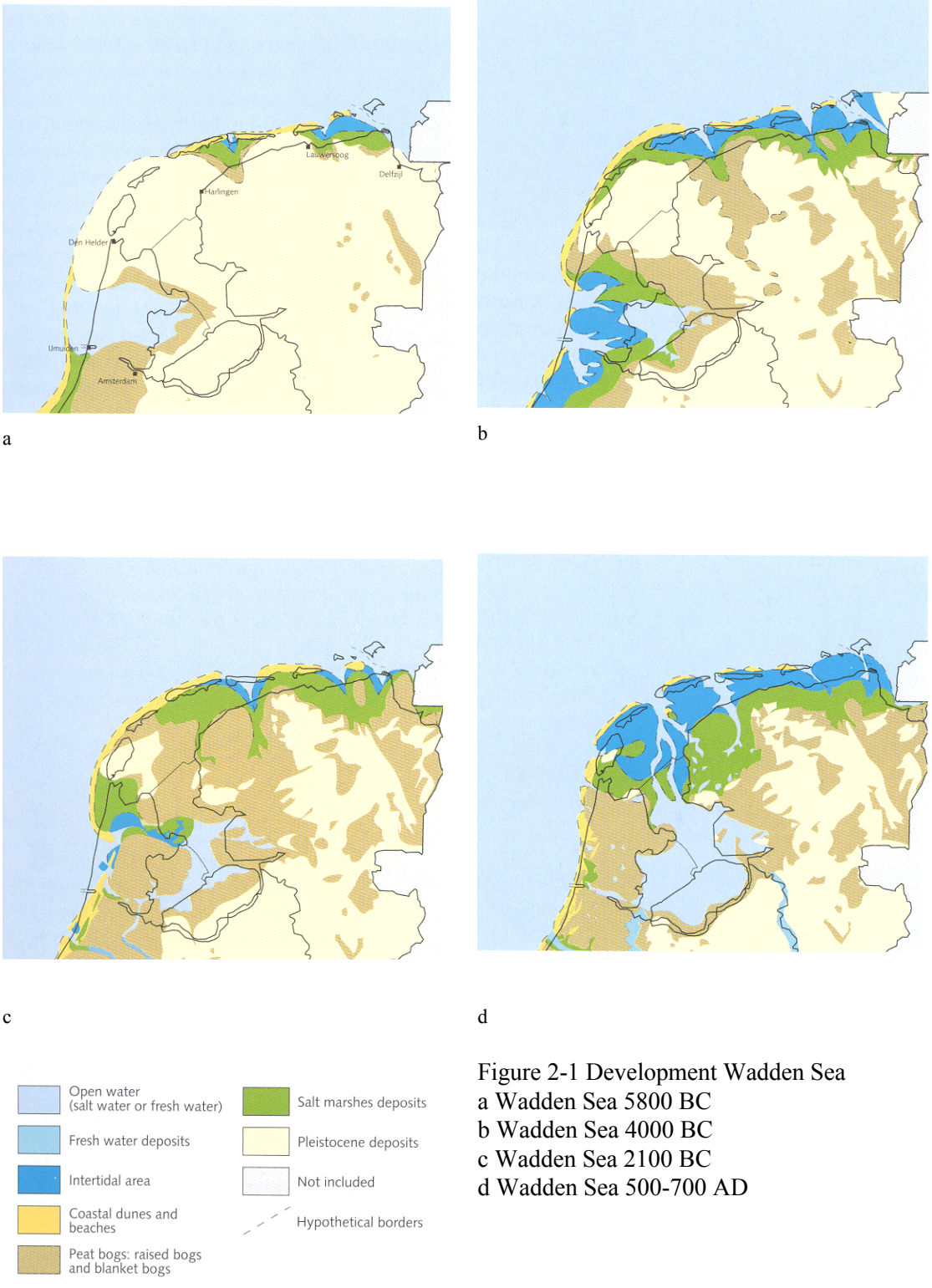

Figure 2-1 Development Wadden Sea
a Wadden Sea 5800 BC
b Wadden Sea 4000 BC
c Wadden Sea 2100 BC
d Wadden Sea 500-700 AD

Digging channels in order to drain and empolder as well as peat-cutting exposed the marshy area to flooding. Around 1000 AD the sea intruded the area and transformed it into tidal flats. Sand sources which made growth of barrier islands and flats possible were exhausted and as a consequence coastal inundation took place on large scale. The tidal basins increased in volume and the old peat in the Wadden area was swept away. The coasts of Noord-

Holland and the western islands were subjected to intense erosion due to the enlargement of the volume of the tidal basin.

During the past 100 years the coastline has been intensely regulated. In 1990 the decision was made to maintain the coastline at its then position. We have fixed the position of the islands coast and that of most of the mainland over the years, thus restraining the dynamics of the Wadden system. Consequently the Wadden system can respond to processes like sea level rise and other disturbances only within the current fixed boundaries of the Wadden Sea.

2.2.4 Sea level rise past century

Sea level rise is a natural form of large scale interference in the tidal sytem. From the previous section it became clear that the sea level rise decreased from about 140 cm per century to about 5 to 30 cm per century. According to the measurements of Rijkswaterstaat (Jaarboek 1998), the last 100 years the mean sea level (MSL) has developed as follows at Den Helder:

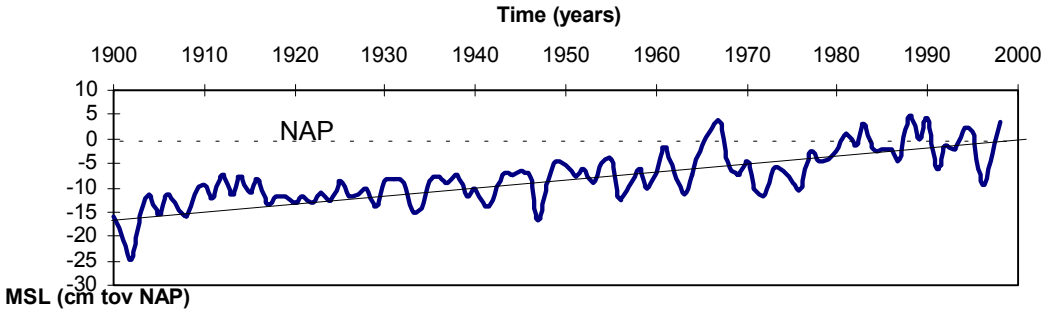

Figure 2-2 Mean sea level (MSL) development at Den Helder

The figure shows that the mean sea level rising has been constant for the last 100 years. The average sea level rise is approximately 17 cm per century, slightly dependent on the location (for Harlingen slightly different values are found compared to Den Helder) and the regression-line drawn between the measurements. The fluctuations around the trend are mainly due to wind influence.

As a consequence of sea level rise, the coast line is still receding. In the natural situation in which the Wadden Sea and the islands could react dynamically, the system always proved to reach a balance between the supply of sand from eroding islands, its size and the sand demand from the Wadden Sea to keep up with the sea level rise.

The sea level rise is a process which takes place over hundreds or thousands of years and is dominating on mega-scale (see chapter 1). At macro-scale, which is of interest in this study, sea level rise is a minor, though non-negligible forcing, which influences the morphological development of a tidal inlet. In the following section, the main forcings on a tidal inlet will be discussed.

2.3 Forcings on a tidal inlet

In the previous section we analysed the behaviour of the Wadden Sea on mega-scale (see chapter 1). Now, we will zoom to the scale of interest: macro-scale. We will consider the forcings on a tidal inlet.

2.3.1 Empirical correlation forcings and tidal inlets

The Wadden Sea is subjected constantly to all kinds of forcings. The most important ones are related to the astronomical tide and the wave action from sea. These forcings induce sediment transport in and out of the Wadden Sea. This leads to morphologic development (= change of bed topography), which in turn influences the forcings on the system. This looks like:

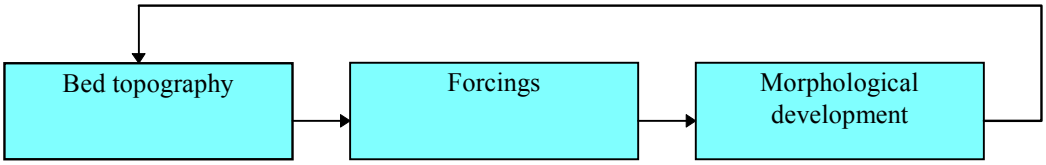

Figure 2-3 Cycle of morphological development

As indicated in chapter one, it is essential that these forcings will be analysed at the scale of interest. A classification was made by Hayes (Hayes, 1979) for tidal inlets, see figure 2.4. With this classification Hayes indicated a empirical correlation between the integrated characteristics of tide and the wave climate, and the morphological shape of inlets. The wave climate is generally characterised by the mean significant wave height, yearly averaged. The mean tide in an inlet is characterised by the mean tidal range or prism.

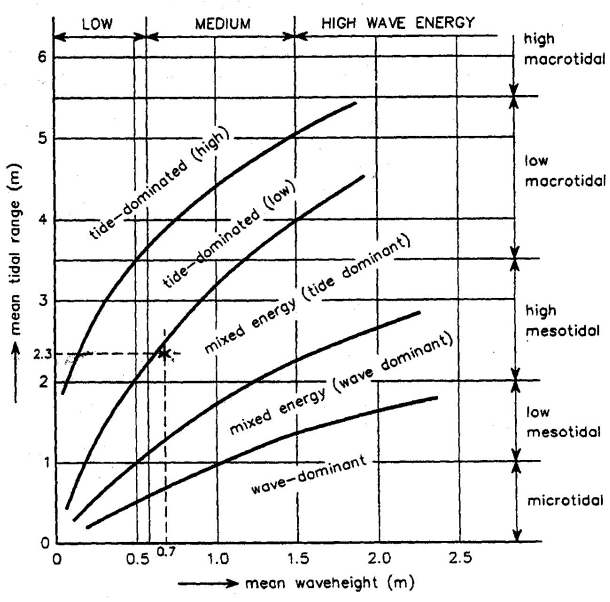

Figure 2-4 Classification tidal inlets

The Dutch Wadden Sea inlets come under Mixed energy inlets, where tide dominates. These inlets are characterised by abundant tidal inlets, relative large ebb-tidal deltas and usually drumstick barriers. In figure 2.3 an example is given of the Friesche Zeegat, which has an

average wave-height of 0.7 m and an mean tidal range of 2.3 m. In general a relationship exists between the length of the barrier and the tidal range. Large tidal ranges apparently result in shorter barrier islands and vice versa.

In the same way as Hayes, semi-empirical models like Asmita deal with forcings on a higher scale. In Asmita, for example, also empirical relations are used between the tide and wave climate, and the size of the basin. However, the barrier islands are not taken into account in Asmita, and therefore the classification of Hayes is not relevant for Asmita.

In the following section the process-based processes, which provide the base for the empirical relations will be made clear. It will be explained how these forcings influence the morphology of the elements of an inlet.

2.3.2 Process-based relation between forcings and inlet

Tide

Due to both a gravitational attraction between earth and moon and sun, and due to the rotating earth, tidal waves are generated in the oceans. A tidal wave enters the North Sea from the Atlantic Ocean and propagates anticlockwise, along the Dutch North Sea coast from south to north, further north-east to the German Bight. It takes about 11 hours for the tidal wave to travel from Vlissingen tot the German Bight. The tidal range (difference between high and low water level) diminishes from about 4 m near Vlissingen to 1.7 m at Hoek van Holland. A minimum value of less than 1.4 m is reached south of Den Helder. Then, further east along Wadden islands the amplitude gradually increases to 3 m. Because of the variation in tidal range, a longshore water suface gradient is generated at low and high water levels. As a consequence a tide-driven longshore current takes place along the coast (horizontal tide).

The tidal prism is defined as wet storage area between MLW and MHW For small basins, compared to the tidal wave length, the prism approximates the complete volume of water that enters an area during one tidal period (12hours 25minutes) and has a dimension m^3. The mean tidal prism (over several tides) depends on the shape of the basin and the tidal range.

The tidal current enters the Wadden Sea through the inlets. Two flood currents on both sides of the islands meet each other approximately in the middle behind the islands. Where these currents meet, watersheds can be recognised. Here the current-velocities are very low and ridges arise. These watersheds form the boundaries of the different tidal basins. They are not totally fixed, but move a little eastwards. Only under conditions with strong winds, drift currents will pass the watersheds during high water. Because of the presence of such watersheds, the Wadden system is a ‘chain’ of separated inlets. These inlets can be seen as independent units consisting of a basin (with flats and channels) and an ebb-tidal delta. This is a relevant aspect for the schematisation of Asmita (chapter 3).

The interaction between the tidal currents in the inlet and the tidal current along the North Sea coast determine (together with the wave influence) the geometry of the ebb-tidal delta

(see section 2.4). This because of the large sediment transport capacity of the tidal flow. In general the maximum flow velocities along the coast are very modest and increase to averaged velocities of about 1 m/s in the large channels (Eysink and Biegel, 1992).

Waves and wind

Wind induces waves and currents which causes sediment transport. Besides, wind influences the water-level near the coast due to set-ups or set-downs.

Waves induce an important forcing on a tidal inlet, mainly on the ebb-tidal delta. Waves induce shear-stress and therefore stir-up a lot of sediment. Most of the waves break on the shoals (area of relatively shallow water) of the ebb-tidal delta, at a depth of approximately twice their height. Because of this, hardly any waves enter the tidal basin. Only during a high storm flood, part of the waves will penetrate the Wadden Sea and break on the first tidal flats in the basin. The maximum wave-heights come from the north west. The common wave direction is the south-west.

Because waves approach the coast under an angle, they generate wave-induced currents in the breakerzone. The wave energy flux along the coast is mainly directed to the east or north-east, suggesting a net longshore drift in (north)easterly directions. These currents transport a lot of sediment, which is by-passed over the ebb-tidal delta. Also a considerable part of the sediment enters the tidal basin with the flood current, or is directly taken off shore by the ebb current. The wave patterns over channels and shoals are very complicated. The sediment transport process is discussed in section 2.4.1.

Wind generates shear stress at the water surface, which causes drift currents and wind waves. The flow-component of a drift current perpendicular to the coast is compensated by a slope in the water surface, which generates a return flow near the bottom. This slope grows due to the displacement of water by the wind causing a wind set-up or set-down. In a year with a lot of storms, the mean (high) water level will reach a considerable higher value.

Coriolis

The Coriolis forcing is a sham forcing which counters the effect of the rotating earth. This effect gives every moving particle on the northern hemisphere a tendency to bend to the right. The Coriolis forcings on the system are noticed at large scales, but also at smaller scales. The most obvious influence on macro scale is the tide. The propagation of the tidal wave in the North Sea is determined by the Coriolis forcing. On smaller scales the Coriolis forcing in curved tidal channels give rise to secondary flow components. The secondary flow is always directed to the shoal and, therefore assures the existence of the shoal. Apart from this, the Coriolis forcing gives rise to residual currents in wide tidal channels, because of the tidal asymmetry. These effects are not important here as this plays on meso and micro-scales. In this study we are considering the long-term development which corresponds to macro-scale (see chapter 1). Thus the Coriolis forcing only influences the morphological development indirectly on macro-scale via the tide.

2.4 Morphologic elements tidal system

As mentioned before, the present study is focused on describing the morphological behaviour of the inlet system on the basis of integral sediment exchange, erosion and deposition between and within the elements. The various types of forcings that play a role in this respect have been discussed in the previous section. In this section, we will look in to the element response to this forcing.

For the intended analysis and modelling, tidal inlets are schematised to a composition of three basic elements:

- ebb-tidal delta, also called: delta
- channel
- flat

As an illustration, this schematisation is applied to the Vlie inlet (see also figure 2.1) in figure 2.5. It shows the bottom topography of the inlet and surrounding areas together with an indication of the boundaries of the various elements.

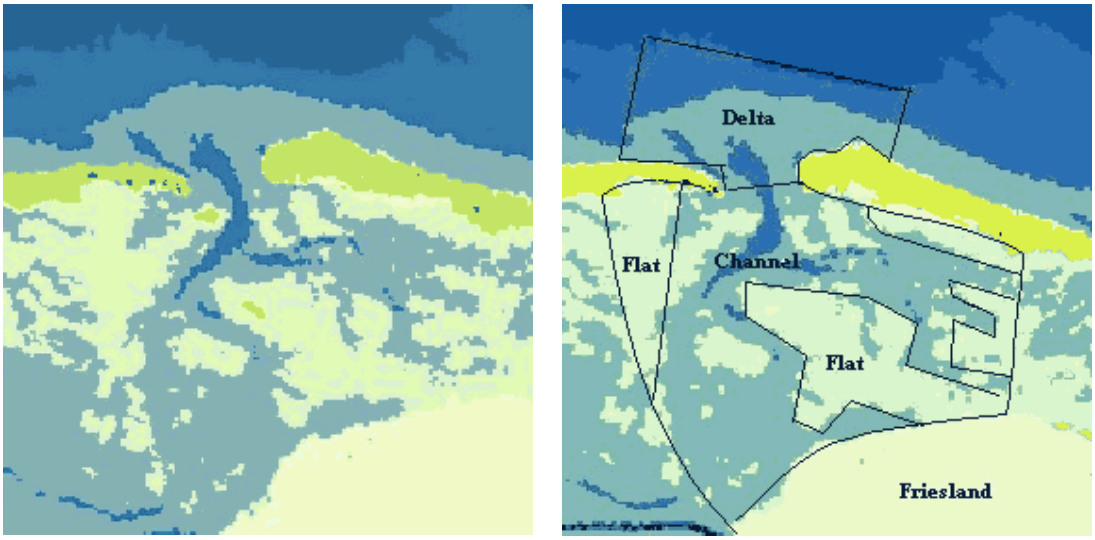

Figure 2-5 Overview elements tidal inlet, example Vlie inlet (see figure 1.1)

2.4.1 Ebb-tidal delta

Ebb-tidal deltas are sediment accumulations on the seaward side of, and morphologically and dynamically connected to, tidal inlets, and they form important morphological elements along the barrier islands (Sha, 1990). Ebb-tidal deltas are important as permanent and temporary sediment reservoirs. When the tidal inlet demands sediment, this is delivered by the ebb-tidal delta. If there is not enough sediment "available", this sediment will be delivered by the adjacent coast.

The name of this morphological unit is ebb-tidal delta, because the sediment accumulations are primarily deposited by ebb-tidal currents that decelerate when they leave the basin. A typical ebb-tidal delta includes a main ebb-channel, a terminal lobe, swash platforms and

bars and flood channels. The terminal lobe is a rather steep seaward-sloping body of sand, which forms the outer end of the ebb-tidal delta. The main ebb-channel is surrounded by swash platforms, which are broad sheets of sand. On these swash platforms, isolated swash bars can be recognised, built up by waves. Flood channels usually occur between the barrier islands and the swash platforms.

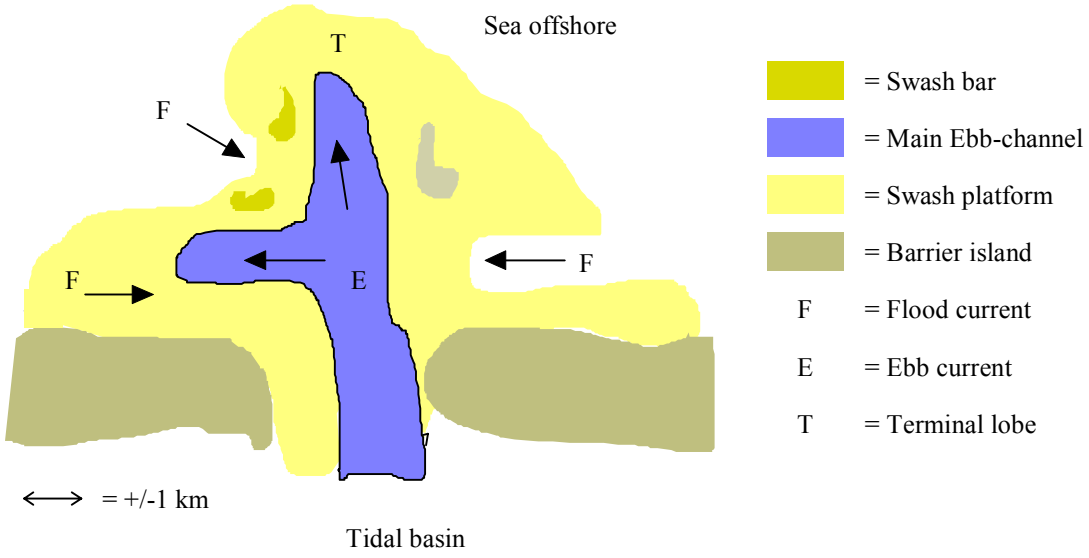

Figure 2-6 Ebb-tidal delta

The accumulated shape and volume of the ebb-tidal delta is modified by marine processes driven by for instance waves and longshore tide and wave driven currents. These processes lead to complex sediment transport patterns.

Empirical correlation geometry and forcings ebb-tidal delta

Studies have been carried out by Walton and Adams (Walton and Adams, 1976) and Sha and van der Berg (Sha and van der Berg, 1993) which were aimed on the macro-scale relation between the morphology and forcings like tide and waves. First these studies will be explained, as these are of interest for long-term behavioural modelling. Hereafter, the underlying process-based phenomena will be explained.

In studies by Walton and Adams (1976) it was concluded that a strong relation exists between the volume of sand stored in the ebb shoals of an inlet and the tidal prism. They further demonstrated that with increasing onshore directed wave energy the outer delta shoal volume tends to become smaller. The other way around, the volume will be larger in the case of low onshore directed wave energy and large tidal forcings. Walton and Adams also developed a calculation method for the volume of the ebb-tidal delta that appears to be very suitable for comparisons between inlets. According to this definition, the volume of the ebb-tidal delta is equal to the (net) volume of sand above a reference coastline (see figure 2.7). This coastline equals the coastline which should be present without an inlet. This definition is also used in Asmita (see chapter 3).

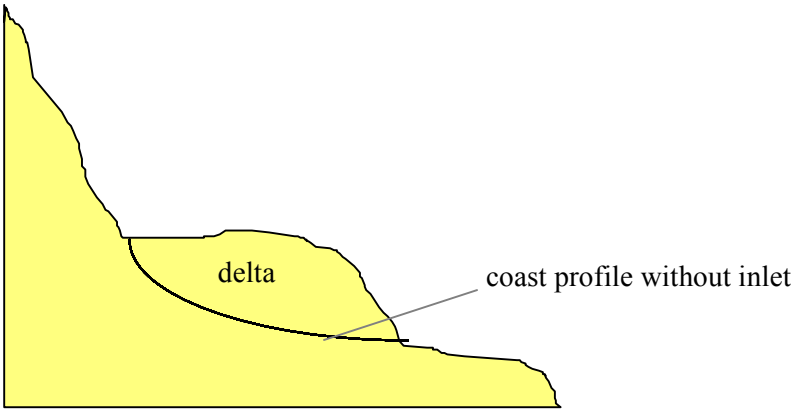

Figure 2-7 Cross-section of delta relative to coast profile without inlet

Studies by Sha and and Van den Berg (1993) described the relation between the variation in ebb-tidal delta geometry and the local variations in both wave climate and tidal regimes. For this study, they used tidal inlets in the south-western part of the Netherlands and the western Wadden Sea as study material.

Beside the tidal range and the wave direction, the interaction between offshore and inshore tidal currents play a role in the geometry of the ebb-tidal delta. Along the coast of the Wadden islands the velocity of the tidal currents along the coast reaches its maximum around the mid-tide water level. At the same time the tidal discharge through an inlet is at its maximum. High tidal slack water occurs almost simultaneously within the inlet throat and the adjacent offshore area. The same counts for low tidal slack water. The interaction of inlet tidal currents with offshore tidal currents during flood and during ebb under such a tidal regime is illustrated in figure 2.8. In this figure the tidal current approaches from the west (left part of the figures). During floods, tidal currents approach the inlet from the left side of the inlet; during ebb, tidal currents are also concentrated on the left part of the ebb-tidal delta.

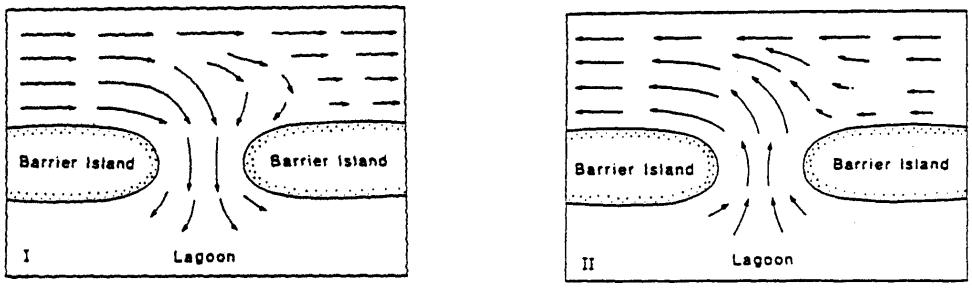

Figure 2-8 Interaction longshore tidal wave and inlet tidal currents, I:Midflood, II:Midebb

In this figure, only the effect of tidal currents is illustrated. As shown in figure 2.8, the interaction between inshore an offshore tidal currents in this area enhances a bending of the ebb channels tot the left side of the deltas, thus to a westerly direction. The bending of the channel and the corresponding shape of the ebb-tidal delta, is influenced by the variation of

the tidal range along the coast and by waves. Regarding these variations, Sha and Van den Berg gave a classification for the geometry of ebb-tidal delta's presented in figure 2.9.

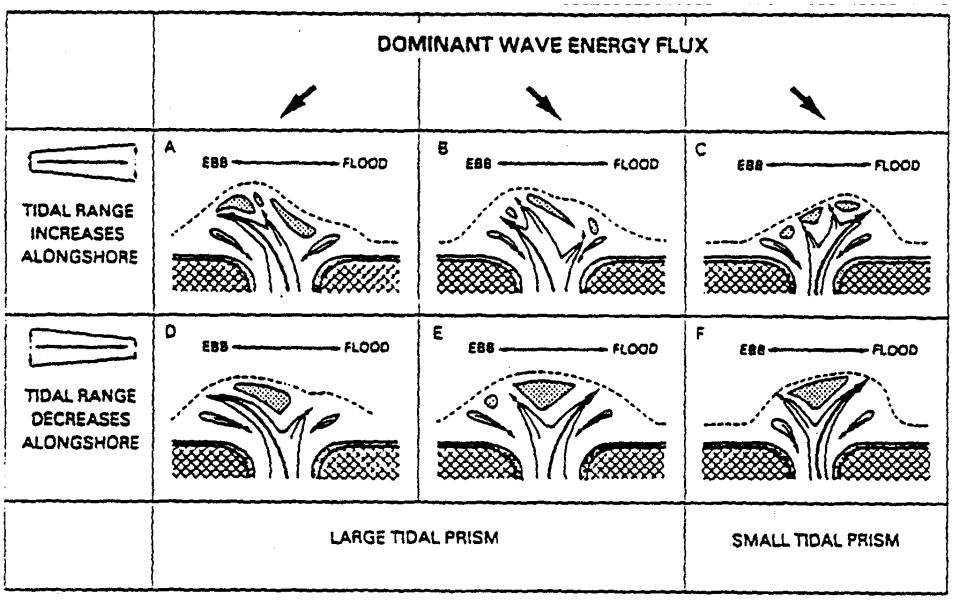

Figure 2-9 The geometry of ebb-tidal deltas under different tide and wave regimes (Sha and Van den Berg, 1993).

In this figure is illustrated that an increase in tidal range in the direction of the tidal wave propagation along the coast gives a stronger asymmetry. A decrease in tidal range leads to a somewhat restrained asymmetry. Furthermore, the waves tend to push a way the main ebb channel in the main wave direction at deep water. The actual geometry of the ebb-tidal delta is determined by combination of the effects as demonstrated in figure 2.9.

Along the Wadden coast, the common wave direction is from the west. As the position of the barrier islands varies, the angle of wave approach and influence varies as well. The changes in offshore wave energy along the Wadden coast are small compared to differences in tidal prism between the inlets, therefore the magnitude of the tidal prism mainly determines the variation in overall shape of the ebb-tidal deltas. Inlets with a large tidal prism show up-drift asymmetrical ebb-deltas and inlets with a small tidal prism have down-drift asymmetrical ebb-tidal deltas (Sha 1990). The tidal range increases from Den Helder towards the German islands. Given this information, the geometry of the deltas of the western Wadden Sea can be characterised as in figure 2.9.

The ebb-tidal delta of Marsdiep is an example of what falls between figure 2.9A and 2.9B: waves approach to the coast perpendicularly and a negligible net longshore drift is produced. The asymmetrical geometry of the ebb-tidal delta in this case is dominated by the interaction of onshore and offshore tidal currents. Figure 2.9B and 2.9C, waves produce a net longshore drift pushing the ebb-tidal delta system to the downdrift direction, opposite to the direction due to the interaction of inshore and offshore tidal currents. In that case, the direction of the asymmetrical geometry of the ebb-tidal deltas is determined by the relative importance of tidal currents to wave energy flux. Inlets like the Vlie and the Borndiep have a tidal prism which is relatively important compared to the longshore drift, hence the main ebb channel is directed to the updrift direction (figure 2.9B). Inlets with a relative small

influence of the tidal prism compared to the longshore drift have a main ebb-channel to the downdrift direction (figure 2.9C), e.g. the Nordeneyer Seegat, German coast). Figures 2.9D, E and F refer to a phase difference of inshore and offshore tidal currents of a quarter of a tidal period, as is the case in the south-west of the Netherlands.

Sediment transport in ebb-tidal delta

Some background information will be given on the process-based phenomena in the ebb-tidal delta, which provide basis for the empirical relations between the morphology (the geometry) and the hydrodynamics (tide).

Because waves approach the coast under an angle, they generate wave-induced currents in the breakerzone. These currents transport a lot of sediment, which is partly by-passed over the ebb-tidal delta. Also a considerable part of the sediment enters the tidal basin with the flood current. After a while, or directly at the gorge of the inlet, this sediment is transported out of the basin by the ebb current. The ebb current transports large volumes of sediment through the gorge of a tidal inlet. At the inlet's seaward-mouth, the velocity rapidly decreases and the sediment is deposited. The larger the tidal prism, the larger the extension of the delta offshore.

The waves counterbalance this extension. Along the extended delta, the angle of wave approach varies. Because of this, gradients in the wave driven long-shore transport occur along the delta. As a consequence, erosion on the terminal lobe of the delta occurs. the delta is "swept" out by the waves. This effect is strengthened by the fact that on the shallow parts, the currents are directed in the wave direction. Thus on the shoals, the sediment transport is dominated by waves and are directed onshore.

So a higher tidal regime causes a larger extension of the delta, while the waves restrain this extension.

As the delta does not only consist of a extended lump of sand, but of a serie shoals and channels, another mechanism of transport is important in the delta, the sediment bypassing. The part of the sediment which is transported over the delta is called sediment by-passing. Sediment by-passing is defined as the process which allows material after a short interruption, caused by an inlet, channel, breakwater or other littoral barrier, to become part again of the normal longshore zone a short distance downdrift from the littoral barrier (see figure 2.10). In the upper part of the figure, the wave currents around the shoals in the delta, together with the tidal currents are reflected. Here, is illustrated that the (wave induced) longshore transport approaches the inlet from the west (left). Then, on the shallow parts the wave driven currents dominate, while in the deeper channels, the tidal flow currents dominate. This results in a zig-zag pattern of the bypassing flow. At the down-drift side of the delta, the normal littoral transport continues towards the east (right).

In the down part of figure 2.7, the sediment transport as a consequence of these currents are shown. Sediment enters the ebb-tidal delta and due to sediment transport in downdrift direction between the channels and shoals, the channels migrate over the inlet. The time for a shoal to cross the inlet may take about 40 years. The cyclic movements in the shoals lead to

accretion on the down drift side and erosion on the updrift side of the barriers. Because of this, the island slowly migrate eastwards.

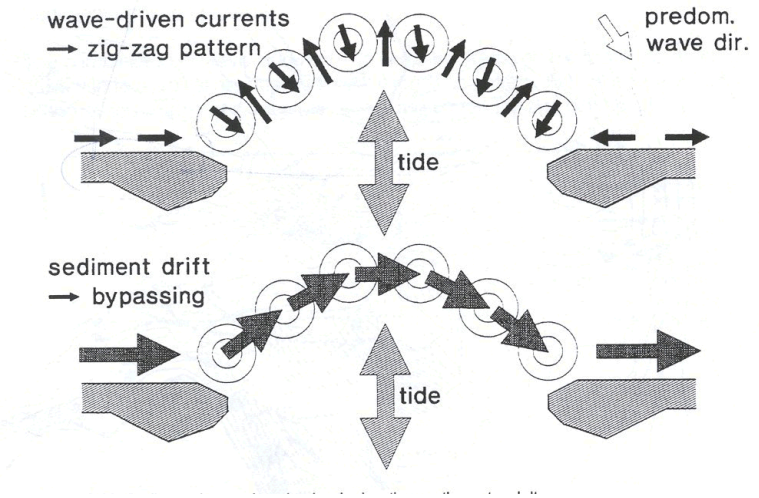

Figure 2-10 Sediment bypassing (De Vriend et al, 1999)

Summarised, the stability, size and shape of the ebb-tidal delta is controlled by a combination of the ‘sweeping‘ effect due to the wave driven longshore drift, and the in-and outgoing transport due to the tidal flow. Besides, sediment bypassing plays a role in the long term development of the geometry of the delta..

2.4.2 Tidal basin: channels and flats

The Wadden Sea is an example of a series of short tidal basins, which means that the length of the basin is relatively small compared to the tidal wave length in this area. The tidal wave is reflected and has a standing character. Because the tidal influence is strong and the wave influence is relatively weak, the flood delta which could be present just inside the basin is not really developed (the ebb-tidal delta, in contrary, is). Tidal basins can be characterised by a branched system of channels and an intertidal area, which are identified as flats.

The flats are defined as the area which dries during low water and inundates during high water. Hence, all areas between MHW and MLW. A further distinction can be made between high flats between MHW and MSL and the low flats between MSL and MLW. In figure 2.11 a cross-section is presented of a tidal inlet, where the flats can be recognised. The height of the tidal flats of the Dutch Wadden Sea range between MSL and MHW -0.3 m. On the watersheds between the basins, the bed levels roughly vary around MHW -1 m.

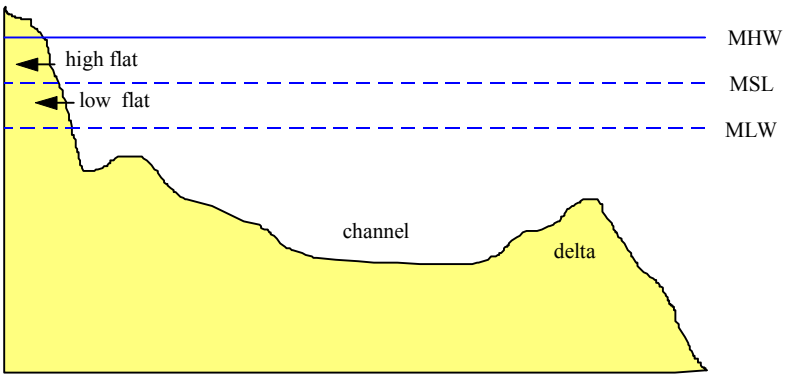

Figure 2-11 Cross-section inlet

Eysink (1993) found that, the presence of tidal flats depends on the tidal range and the basin area. In the case of a larger basin, a relative smaller (relative to the basin surface) flat area can be found. This is because local current and wave effects, due to larger fetches, could prevent the extension of tidal flats. Furthermore, a larger tidal range generally increases the height of tidal flats. The derived equilibrium relation of Eysink is discussed in section 3.4.

Channels are usually defined as the wet area below MLW. Channels transport considerable amounts of water and sediment. During flood, water enters the inlet, which brings a large amount of sediment. A part of this sediment may be deposited in the channels or at the flats. A part is transported out of the basin during ebb. Near the gorge, the channel cross-section is largest, away from the gorge, the cross-section of the channel becomes smaller as they have to process a smaller tidal volume. Given this information the equilibrium relation that Eysink (1993) found between the cross-sectional area and the tidal volume in a channel, is very plausible. From this relation, an equilibrium relation was derived between the volume of the channel, and the tidal volume, see also section 3.5.

In this section, we have discussed the elements of a tidal inlet, and the influence of different forcings on the morphology of these elements. Besides these forcings, the inlet is sometimes subjected to human interventions. This will be discussed in the subsequent section.

2.5 Closure Zuiderzee: human intervention on macro-scale

Human interventions like a closure of a part of a tidal basin can have a major impact on the morphology. A change in morphology implies a change in local tidal currents and waves (section 2.3.2). Other examples of human interferences are sand mining, large scale dredging and land reclamation. These interventions are scaled on macro-scale (see chapter 1).

The effect on the response of elements of a tidal system, caused by human interventions, are of special interest in the present study, especially the closure of the Zuiderzee. This closure will be used as a case to calibrate Asmita and to obtain more insight into morphological processes which occurred due to closure. Therefore a brief overview will be presented in this section.

Background of the construction of the Afsluitdijk

Hendric Stevin suggested already in 1667 that a closure of the Zuiderzee would diminish the inundation danger in large parts of the Netherlands. In his time this plan was considered infeasible. Many plans have been developed since. Even plans were drawn up to reclaim the Zuiderzee and the total Wadden Sea. Reclaiming the Zuiderzee was an attractive option, but the main reason for building the Afsluitdijk was a better protection against storm floods. After a long list of ideas and indicative plans, engineer C. Lely came up with the first serious feasible plan in 1881. Four years later, he was appointed as minister of Public Works and Transport, but still no agreement could be made on the design and construction of the Afsluitdijk. It was not until 1913 that Lely became minister again and the plan for closure and reclaiming of the Zuiderzee was approved. Probably the main reasons for this approval, were food scarcity after the first World War (closure would be an essential step towards massive land reclamation for agricultural purposes) and the great storm-flood in 1916. Finally, the Afsluitdijk was built in five years and it was completed in 1932. (Rijkswaterstaat 200 jaar)

Predictions

The Afsluitdijk was designed such that the effects on the water movement and the tidal amplitude were as little as possible. At that time, knowledge about hydrodynamic and especially morphological effects of a closure was limited. However, the calculations made at that time already predicted considerable increase of the tidal range and an increase of the flow velocities in inlets.

Despite the investigations carried out by the Staatscommissie, still many uncertainties arise regarding behaviour of tidal inlets and future morphological changes. Therefore, this closure is an interesting case for this study. About 8 digitised maps are available, which contain depth measurements in the period 1925-1998. These maps represent the long term morphological development and will be used in further analysis. These bathymetric maps will be used to obtain insight into morphological processes and for modelling purposes in the following chapters.

2.6 Summarise

In this chapter we discussed the genesis of the Wadden Sea on mega-scale. Historic geological evolution shows that since the beginning of the Holocene sea level started rising due to melting ice caps. The sea level rise decreased from more than eighty centimetres a century to the present sea level rise of approximately 17 centimetres per century. As a consequence, the Wadden islands and Wadden Sea with an intertidal area slowly developed.

The Wadden area consists of a chain of tidal inlets. At the scale of interest, macro-scale, a tidal inlet consists of three major elements: the ebb-tidal delta, the channel and flat. These elements are mainly subjected to forcings like tide and waves. Empirical relations are found between the shape and size of these elements and these forcings. These relations are derived at macro-scale. Based on similar relations, the behaviour orientated model Asmita is formulated, which will be discussed in the subsequent chapter.

Human Interventions could have a large influence on the morphological development of a tidal inlet. In 1932, the Zuiderzee was closed. The Staatscommissie Zuiderzee (1926) calculated possible future behaviour at that time. Nowadays, still uncertainties are present regarding future morphological changes. Therefore, this closure is an interesting case to calibrate Asmita.

3 Asmita

3.1 Introduction

As pointed out in chapter 2, the Asmita (Aggregated Scale Morphological Interaction between a Tidal inlet and the Adjacent coast, Stive and Wang 1996) model will be used to improve the insight into the morphological behaviour of tidal inlets and to analyse the consequences of the closure of the Zuiderzee. In this chapter, the concept of Asmita will be explained.

3.2 Asmita schematisation

The Asmita approach can be considered as an aggregation on the one hand and an extension on the other hand of the Estmorf model (Wang and Karssen, 1992). Aggregated concerns the fact that the system elements are characterised by one state variable (viz. a total wet or dry volume). Extension concerns the possible incorporation for the ebb-tidal delta and directly adjacent coast.

A tidal inlet system is considered consisting of three major morphological elements; the tidal flats, tidal channels and the ebb-tidal delta. (The coast can also be defined as element, but this is not considered in this study). Besides these elements, an outside world can be defined for which an overall equilibrium state can be defined. This outside world comprises the coastal zone surrounding the ebb-tidal delta, which acts as a boundary for the system. An important hypotheses is that the outside world is able to provide sand which is demanded by the ebb-tidal delta and basin, unconditionally. The morphological development of the tidal inlet does not influence the outside world.

The degree of schematisation is determined by that element of the system which yields the lower boundary to the relevant spatial scale. This concerns typically the ebb-tidal delta, for which there is presently no other option than to consider its volume as an integral state variable, implying that the ebb-tidal delta is modelled as a single element. Therefore, the same level of schematisation is used for all the elements in the system. This way, the following basic elements are included in the model. (figure 3.1).

1. the ebb-tidal delta
2. the total intertidal flat area in the basin
3. the total channel volume in the basin

Each of these elements is described by one variable representing its morphological state:

Delta: Volume sediment above a fictitious sea bottom, which would be there if there was no inlet (sand volume in m^3)

Flats: Volume of the tidal flat between MLW en MHW (sand volume in m^3)

Channel: Total channel volume below MLW (water volume in m^3)

Each of these elements is influenced primarily by the basin related tidal flows and secondarily by wave related hydrodynamics. It is assumed that long term residual sediment exchange occurs between the tidal flat and the channel in the basin, between the channel in the basin and the ebb-tidal delta and between the ebb-tidal delta and the adjacent boundaries, the outside world. This can be schematised as follows (see also figure 2.5)

Empirical relations between the equilibrium volume of an element and the tidal prism or tidal range are derived on basis of field data (Eysink and Biegel, 1992).

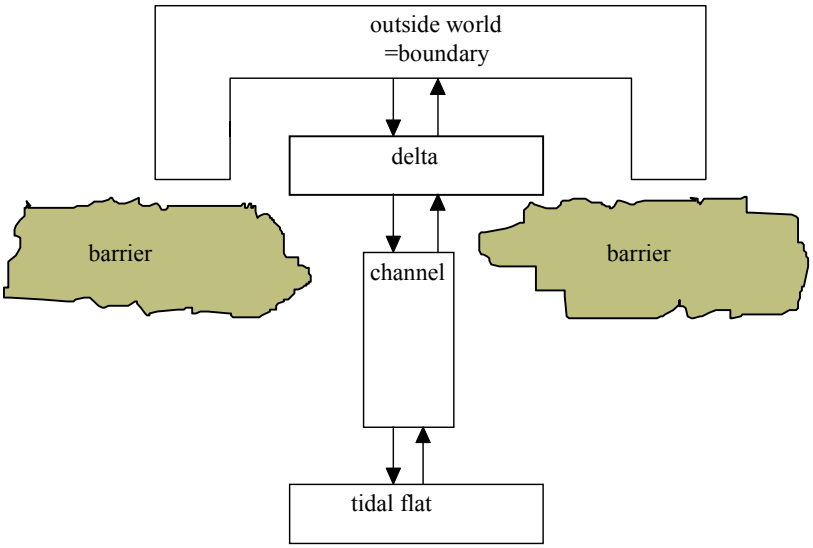

Figure 3-1 Schematisation elements and exchange in Asmita

The evolution of the elements towards a state of equilibrium can be described on an aggregated scale, based on the following principles:

- The most important principle is that all elements tend to evolve towards an equilibrium state, which can be defined for all elements.
- When an element is out of equilibrium, a need or surplus of sediment is created, which depends on the disturbance of the element.
- Whether this need or surplus actually results in sedimentation or erosion depends on the availability of sediment, which in turn depends on the need of the adjacent elements.

In Asmita this behaviour orientated approach is elaborated as follows:
Evolution towards an equilibrium state is only possible by exchange of sediment between the elements. This is realised by the in- and outgoing tidal prism. There are two forms of sediment exchange; within an element and between two elements. Within an element, the rate of sedimentation or erosion is proportional to the difference between the actual sediment concentration and the equilibrium concentration of that element. The latter depends on deviation from the equilibrium state of the element.

Between the elements, sediment exchange takes place depending on the difference in sediment concentration. Sediment transport will always take place from a high concentration towards a relatively lower concentration. When an element tends to export sediment, a high

concentration will be present because of the sediment which comes in suspension. This sediment could be transported towards another element with a lower concentration. In that element, sediment will settle, or will be transported to the next element (with an even lower concentration) which depends on the mutual will to import or export sediment.

So, all exchange is realised by the in- and outgoing tidal currents which bring sediment in suspension (higher concentration), or cause sedimentation (lower concentration), dependent on the need, and thus disturbance, in the elements.

The exchange between the delta and the outside world is, in contradiction to the other elements, not only determined by the prism. There, the waves play an important role (see section 2.4). The wave driven longshore current determines the availability of sediment for the delta, and hence in the end, for the entire inlet. This sediment, which is supplied by the boundary of the system, is represented in Asmita by the overall equilibrium concentration, which is present in the 'outside world'.

With this schematisation, the actual state of an element is related to its morphological change at a certain moment. This can be translated to a mathematical model which can be solved numerically according to the following scheme.

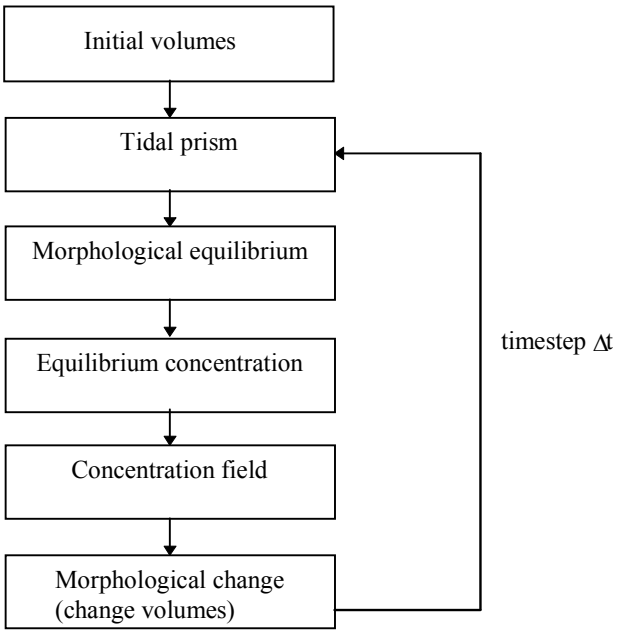

Figure 3-2 Scheme Asmita

In the following sections, a more detailed formulation of Asmita will be explained, based on this scheme.

3.3 Tidal prism

The tidal range and tidal prism should be determined in order to calculate equilibrium values. These values are dependent on the bathymetry. If the size of the tidal basin is assumed to be small compared to the tidal wave length (which, in the case of the Wadden

Sea is a correct assumption), spatial variation of the water level in the basin can be neglected and the tidal prism can thus be calculated from:

$$P = H \cdot A_b - V_f \tag{3.1}$$

where P is the tidal prism, A_b equals the total basin area and H is the tidal range. Furthermore, the channels and flats are schematised by depth-averaged surfaces and average heights/depths. This is explained in figure 3.3, where the cross-section of a tidal basin is schematised as used in Asmita.

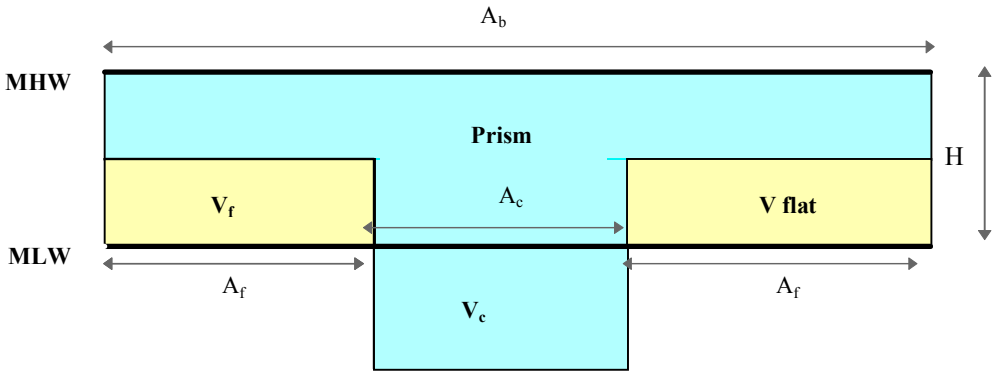

Figure 3-3 Schematisation cross-section tidal basin

P = tidal prism; wet volume between MLW and MHW (m3)
V_f = the volume of the tidal flat between MLW en MHW (m3)
V_c = the total channel volume under MLW (m3)
A_b = average basin area (m2)
A_f = average flat area (m2)
A_c = average channel area (m2)
H = tidal range, difference between MHW and MLW (m)

3.4 Morphological equilibrium

Empirical relations have been developed (a.o. Eysink 1991) between the geometric morphological parameters and characteristic hydraulic parameters. These relations describe the empirical relation between the prism and the wet/dry volume of the morphological elements. The tidal prism appeared to be an important hydraulic parameter in these relations.

For all elements an equilibrium relation holds between the volume of the element and the tidal prism, or tidal range:

$$V_e = f(P) \text{ or } V_e = f(H, A_b) \tag{3.2}$$

An empirical relation is found between the volumes of the delta and the channel and the tidal prism. The flat volume is related to the tidal range and the basin area. The relations

used in the present study are derived from literature (Eysink 1991). They are discussed below.

Channel

The following relation holds between the volume of the channel and the tidal prism:

$$V_{ce} = \alpha_c \cdot P^{1.55} \tag{3.3}$$

with:
V_{ce} = Equilibrium volume of channel, below MLW (m^3)
α_c = equilibrium coefficient, for the Wadden Sea amounts to: 16e-6 ($(m^3)^{-0.55}$)

Tidal flats

The quantity of flat area relative to the basin area (A_f/A_b) depends on the size of the basin. Renger and Partensky found the following relation for the German Bight.

$$\frac{A_f}{A_b} = 1 - 2.5 \cdot 10^{-2} \cdot A_b^{0.5} \tag{3.4}$$

Thus a large basin has a relative small flat area compared to a small basin. This is caused by, among other things, wind that plays a large role in a large basin, compared to small basins, which results in a smaller flat area.

The height of the tidal flats is related to the tidal range: the average height of the flats relative to MLW is α_{fe}*H. Eysink (1991) derived an empirical relation between the basin area and the coefficient α_{fe} for the Wadden Sea tidal basins.

$$\alpha_{fe} = 0.41 - 0.24 \cdot 10^{-9} \cdot A_b \tag{3.5}$$

The volume of the tidal flats is defined as the product of area and height above MLW. Thus, the following relation can be derived:

$$V_f = \alpha_{fe} \cdot \left(\frac{A_f}{A_b} \right) \cdot A_b \cdot H \tag{3.6}$$

In Asmita the time-averaged surface area of channels and flats are used. This means that relation 3.4 is not taken into account. In this case a time-invariant flat area is used in the equilibrium relations, thus the relation reduces to:

$$V_f = \alpha_{fe} \cdot A_f \cdot H \tag{3.7}$$

In these equations the following symbols were used:
A_b = area of tidal basin at MHW (m^2)

A_f = area of tidal flats measured at MLW (m^2)
H = mean tidal range (m)
V_f = volume of flats above MLW (m^3)
α_{fe} = empirical coefficient for the average tidal flat level (-)

Ebb-tidal delta

For the sand volume in the ebb-tidal delta, the relation of Walton and Adams (1976) is used for a rough wave-climate and corrected for average tide (see figure 3.4). It reads:

$$V_d = 63.3 \cdot 10^{-4} P^{1.23} \tag{3.8}$$

V_d= Volume of sand in ebb-tidal delta (m3)

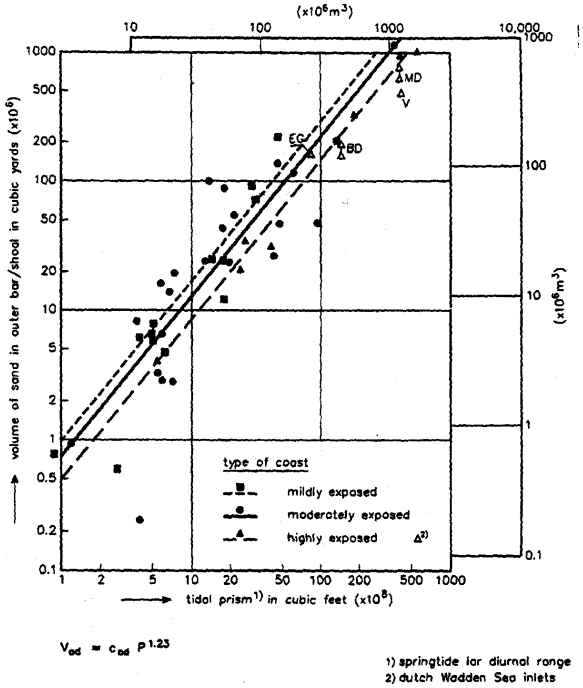

Figure 3-4 Equilibrium relation ebb-tidal delta

3.5 Equilibrium concentration and concentration field

A key element in the Asmita modelling concept is the equilibrium concentration. The constant concentration which is present, in the case all the elements are in equilibrium, is called the overall equilibrium concentration c_E. For each element in the system a local equilibrium sediment concentration c_e is defined such that it is equal to c_E ($c_e = c_E$) if the element is in morphological equilibrium, larger than c_E when a tendency to erode exists ($c_e > c_E$), e.g. the volume of the ebb-tidal delta is larger than the equilibrium value, and smaller than c_E if tendency to accrete exists ($c_e < c_E$).

The local equilibrium concentration depends on the actual volume V and the equilibrium volume V_e. To represent this behaviour a simple power relation is used for the equilibrium concentrations. For the channel element this means:

$$c_{ce} = c_E \cdot \left(\frac{V_{ce}}{V_c} \right)^n \tag{3.8}$$

For the tidal flat and the ebb-tidal delta this relation is inverted, as then the dry volume is considered. For the flat it holds that:

$$c_{fe} = c_E \cdot \left(\frac{V_f}{V_{fe}} \right)^n \tag{3.9}$$

and for the ebb-tidal delta:

$$c_{de} = c_E \cdot \left(\frac{V_d}{V_{de}} \right)^n \tag{3.10}$$

where:
c_E = overall equilibrium concentration (-)
c_{ce} = equilibrium concentration channel (-)
c_{fe} = equilibrium concentration flat (-)
c_{de} = equilibrium concentration ebb-tidal delta (-)
n = commonly taken as 2 (with a third power for the sediment transport as a non-linear function of the mean velocity) (-).

This adjusted equilibrium concentrations, compared to the equilibrium concentration outside, represent the need of elements as discussed in section 3.2.

3.6 Morphological change

Morphological changes occur when the local sediment concentration deviates from the local equilibrium sediment concentration. The local sediment concentration generally tends towards the equilibrium value corresponding to the element at hand. Erosion occurs when the sediment concentration is smaller than the equilibrium value ($c<c_e$) and sedimentation occurs if it is larger than its equilibrium value ($c>c_e$). For the channel element this reads:

$$\frac{dV_c}{dt} = w_s \cdot A_c \cdot \left(c_{ce} - c_c \right) \tag{3.11}$$

Again, for the dry volumes the equation changes, in this case to:

$$\frac{dV_f}{dt} = w_s \cdot A_f \cdot \left(c_f - c_{fe}\right) \tag{3.12}$$

$$\frac{dV_d}{dt} = w_s \cdot A_d \cdot \left(c_d - c_{de}\right) \tag{3.13}$$

w_s = vertical exchange coefficient (m/s)
A_c = horizontal area of the channel element (m^2)
A_f = horizontal area of the flats (m^2)
A_d = horizontal area of the ebb-tidal delta (m^2)
c_f = actual sediment concentration flat (-)
c_c = actual sediment concentration channel (-)
c_d = actual sediment concentration delta (-)

The actual morphological change of the elements (dV/dt) depends on the availability of the sediment, which is governed by the transport between the elements This transport across the boundaries of an element can be derived from the mass-balance in the water phase, for example for the channel element it reads that :

$$T = w_s \cdot A_c \cdot \left(c_{ce} - c_c\right) \tag{3.14}$$

T = (time-averaged) residual horizontal exchange with adjacent elements (m^3/s)

This diffusive exchange represents the long-term residual transport, which is related to the difference between the actual concentrations of the elements. For the exchange between the channel and the flats, for example, it reads that:

$$T = \delta_{fc} \cdot \left(c_c - c_f\right) \tag{3.15}$$

A mass-balance can be formulated for each element, where the morphological change equals the residual exchange with the adjacent elements. The mass-balance is written down in a manner that an increase volume of all different elements is considered. This means an increase in water-volume and an increase in sand-volume for, respectively the channel the flats and the delta.

For the flats this reads:

$$w_s \cdot A_f \cdot \left(c_f - c_{fe}\right) = \delta_{fc} \cdot \left(c_c - c_f\right) \tag{3.16}$$

For the channel

$$w_s \cdot A_c \cdot (c_{ce} - c_c) = \delta_{fc} \cdot (c_c - c_f) + \delta_{dc} \cdot (c_c - c_d) \tag{3.17}$$

For the delta

$$w_s \cdot A_d \cdot (c_d - c_{de}) = \delta_{do} \cdot (c_E - c_d) + \delta_{dc} \cdot (c_c - c_d) \tag{3.18}$$

where:
δ_{fc} = diffusion coefficient representing the residual transport capacity between the flat and channel (m^3/s)
δ_{dc} = diffusion coefficient representing the residual transport capacity between the delta and channel (m^3/s)
δ_{do} = diffusion coefficient representing the residual transport capacity between the delta and the outside world (the boundary). (m^3/s)

In figure 3.6, the sediment balance is illustrated. The arrows indicate a positive transport which corresponds to an increase of the volumes of the elements. Note that the channel comprises wet volume, whereas the flat and delta dry volume.

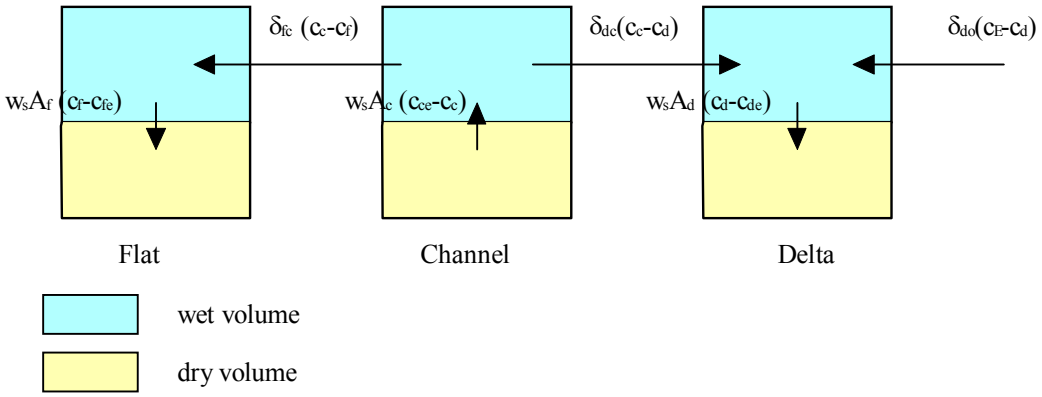

Figure 3-5 Sediment balance tidal inlet, represented by transport within and between elements

Based on this sediment balance, the morphological change for each element can be calculated during a certain period.

3.7 Input parameters in Asmita

To calculate the morphological change of the elements in Asmita the following parameters must be given as input in Asmita.

Diffusion coefficients (δ_{do}, δ_{dc}, δ_{fc})

Generally, asymmetry of the tide leads (if tide dominates), to a non-zero tide-residual transport of sediment. At the scale of aggregation considered in Asmita, this net effect is described as a diffusion type phenomenon. The diffusion coefficients represent the tide-residual exchange capacity between two elements. Buisman(1997) used values ranging from 500 m^3/s to 1500 m^3/s for the Zoutkamperlaag.

Overall equilibrium concentration in the outside world (c_E)

For three elements, the outside world represents the coastal and offshore regions around the delta area. The concentration which is present here, is mainly determined by longshore transport. In Asmita, it is assumed that initially, this concentration is found in all elements. Its magnitude can be derived by estimating the sediment transport caused by waves. Annually this is about 1 to 2 million m^3 along the Dutch coast. According to Van Goor (2001) this leads to a range of the concentration from 1.2e-4 to 2.4e-4. Buisman (1997) used 2e-4.

Vertical exchange coefficient (w_{sf}, w_{sc}, w_{sd})

This parameter represents the net vertical exchange per unit area, per second. This must not be confused with the fall velocity, although it has the same dimension! In Asmita, this parameter describes the long-term residual erosion or sedimentation. This means that the vertical exchange is the long-term residual effect of all kind of processes, which cause erosion or sedimentation. For the delta, for example the vertical exchange is influenced by the waves, which can stir up a lot of sediment. At the flats the wave climate is much calmer than at the delta and therefore the vertical exchange may be faster than at the delta. But on the other hand, sediment particles nearby the flat are usually finer than at sea, which decreases the vertical exchange compared to the other parts of the inlet. Buisman(1997) used values ranging from 1e-5 to 1e-4 m/s.

Geometric parameters (A_c,V_{c0}, A_f, V_{f0}, A_d, V_{d0})

Areas and volumes of the distinguished elements are part of the initial conditions in an Asmita application.

Equilibrium relations

Equilibrium relations (see section 3.5) are required to determine the equilibrium state, to which the elements tend to develop. These relations are discussed in section 3.4 for the Wadden inlets. However, for each inlet the empirical equilibrium coefficients could differ due to changes in size and shape. Therefore, these coefficients should be calibrated with the equilibrium state of the particular inlet.

Tidal range (H)

With this value, the tidal prism and hence, equilibrium volumes of the elements are calculated. The change in flat volume results in a change in prism, according to equation 3.1.

n-parameter

This parameters is used in the definition of the local equilibrium concentration. It is based on a sediment transport formula, which gives a non-linear relation between sediment transport and mean velocity. For this value 2 is used in previous studies (Buisman, 1997 and Van Goor, 2001), which is in compliance with a third power for the sediment transport formula.

Time-step and number of time-steps (dt and nt)

Besides the discussed input parameters, also the time-step and the number of time-steps must be given as input in advance. No problems have been found regarding the stability of the model and the used time-step. The number of time-steps is related to the period of interest. The period of interest in turn depends on the period which covers the morphological development till the equilibrium state. By trial and error, this period will become clear during tests.

3.8 Approach calibration Asmita for closure Zuiderzee

As we could see in the previous section, information on several parameters is needed to simulate the morphological behaviour of an inlet with Asmita. From section 2.5, it became clear that the available data on the closure of the Zuiderzee are limited (8 maps of bed topography covering 65 years).

Calibrating Asmita with a sparse data-set requires a proper estimation of the input parameters. Depending on the available data, only a limit number of input parameters should be used as calibration parameters, which means that they will be varied till an acceptable calibration of Asmita is realised. Parameters not included in the calibration process, must be estimated on other grounds, such as experience with similar inlet systems.

To achieve the desired calibration, a good understanding of the morphological behaviour of tidal inlets is needed. Moreover, insight is required into the impact of variations of the input parameters.

In the following chapter, a linearised approximation of Asmita will be elaborated, which helps to obtain insight into morphological behaviour of tidal inlets and the calibration of Asmita.

4 Linear approximation of Asmita

4.1 Introduction

In this chapter a simplified approximation of Asmita will be derived in order to obtain more insight into the morphological behaviour of tidal inlets and related time-scales and to come to a proper calibration of Asmita.

The morphological time-scale turns out to be an important parameter in the morphological development. These cannot directly be deduced from Asmita, but these can be derived after linearising the basic equations.

It is not improbable that this simplification has a negative influence on the predictive capability of Asmita, when applied beyond the point around which linearisation has been carried out. However, it is expected that the advantages of a simplification counterbalance this negative effect by providing more information on the morphological behaviour, in particular with respect to time-scales.

4.2 Morphological time-scale and Asmita

A characteristic of the morphological development is the morphological time-scale. The morphological time-scale is related to the initial adaptation-capacity. This means that it expresses the way the element *initially* reacts when placed in an out of equilibrium state. In the model Morres, developed by Eysink (1992), the adaptation towards equilibrium is assumed to take place asymptotically. This means that the morphological development has an exponential character, just like many other processes in nature. The evolution of a disturbance is given by:

$$(V - V_e) = (V_0 - V_e) \cdot e^{\left(\frac{-t}{\tau}\right)} \tag{4.1}$$

where:
t = time after imposition of a disturbance
V_0 = initial volume
V_e = equilibrium volume
V = actual volume, function of time
τ = morphological time-scale, for which applies:

$$\tau = \left| \frac{V_0 - V_e}{dV_0} \right| \tag{4.2}$$

dV_0= initial adaptation-rate

Just as in Asmita, the basic principle is that all elements (delta, channel, flats) attempt to reach some equilibrium state. This is realised by an asymptotic (or exponential) evolution towards equilibrium. This is shown graphically in figure 4.1

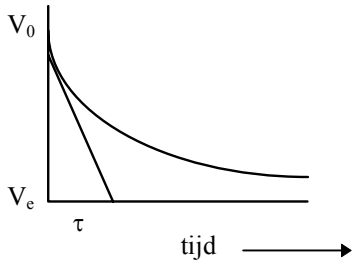

Figure 4-1 Morphological time-scale

An advantage of relation 4.1 is that it is simple and clear. The morphological time-scale is directly related to the morphological development. Only three parameters are required; the initial situation, the equilibrium state and the characteristic time of adaptation or morphological time-scale of an element.

A disadvantage of the approach given in equation 4.1 is that elements are modelled independently of one another. This means that interaction between elements is not taken into account explicitly. Only estimates of time-scales based on field data, may include implicitly effects of interaction between elements.

To deal with this, an extension of equation 4.1 has been developed that includes such interaction and that at the same time hardly compromises the simplicity and transparency of equation 4.1. To achieve this, it has been chosen in the present study to linearise the Asmita equation around the equilibrium volumes.This could help understanding the fundamental morphological behaviour of tidal inlets and hence it aids the calibration of Asmita.

We defined the tidal inlet as a system consisting of three elements. This implies that the linearisation of Asmita is also desired for three elements. However, deriving this linearised approach for a set of three dependent differential equations is rather complex. Therefore, this linear approximation is derived in different stages, for one, two and three elements, respectively.

4.3 Deriving linear approximation Asmita

4.3.1 One element

First a system with one element is considered, for example the channel (see figure 3.1) and a boundary with a constant equilibrium concentration c_E. Following the steps as discussed in chapter 3, the morphological change is expressed as a function of the volume of the element.

The mass-balance equation reads:

$$w_s \cdot A_c \cdot (c_{ce} - c_c) = \delta_{co} \cdot (c_c - c_E) \tag{4.3}$$

From this equation the actual concentration c_c can be determined:

$$c_c = \frac{\delta_{co} \cdot c_E + w_s \cdot A_c \cdot c_e}{\delta_{co} + w_s \cdot A_c} \tag{4.4}$$

When c_c together with c_{ce} (equation 3.9) are substituted into the equation for morphological change:

$$\frac{dV_c}{dt} = w_s \cdot A_c \cdot (c_{ce} - c_c) \tag{4.5}$$

the following equation can be obtained:

$$\frac{dV_c}{dt} = \frac{\delta_{co} \cdot w_s \cdot A_c \cdot c_E}{\delta_{co} + w_s \cdot A_c} \left[\left(\frac{V_{ce}}{V_c} \right)^n - 1 \right] \tag{4.6}$$

This is a non-linear equation between morphological change (dV/dt) and V. It can be simplified by linearising it around $V_c=V_{ce}$. If we use a Taylor series expansion for this purpose and neglect terms of second and higher order, it follows that:

$$\frac{dV'}{dt} = -\frac{w_s \cdot A_c \cdot \delta_{co} \cdot c_E \cdot n}{(\delta_{co} + w_s \cdot A_c) \cdot V_{ce}} \cdot V' \tag{4.7}$$

with $V'=V_c-V_{ce}$ = disturbance

The solution of this equation is:

$$V' = V_0' \cdot exp(\frac{-t}{\tau}) \tag{4.8}$$

V_0'=initial disturbance $V_{c0}-V_{ce}$

where

$$\tau = \frac{1}{c_E \cdot n} \left(\frac{V_{ce}}{w_s \cdot A_c} + \frac{V_{ce}}{\delta_{co}} \right) \tag{4.9}$$

From this linearisation it becomes clear that the morphological behaviour has an exponential character, where τ is the morphological time-scale of the system. In this case the system consists of one element only and therefore this is the morphological time-scale of the element as well. Equation 4.8 shows that every disturbance V' is damped out with an exponential process. For one element, the morphological time-scale of the element is independent of the initial disturbance.

The time-scale can be seen as a combination of two time-scales; a time-scale corresponding to the dispersive or horizontal sediment transport and a time-scale of sedimentation, related to the vertical exchange:

$$\tau = \frac{1}{c_E \cdot n} \cdot (T_s + T_d) \tag{4.10}$$

$$T_s = \frac{V_{ce}}{w_s \cdot A_c} \tag{4.11}$$

$$T_d = \frac{V_{ce}}{\delta_{co}} \tag{4.12}$$

T_s: Time-scale for sedimentation
T_d: Time-scale for dispersive transport

The time-scale τ is inversely proportional to the concentration at the boundary c_E,. And, if the diffusive transport between the channel and the outside world, δ_{co}, increases the time-scale will decrease. Fokkink (1996) derived similar time-scales for Estmorf. He defined the time-scale for each element as in equations 4.11 and 4.12.

The linearisation points out that it is possible to simplify the Asmita concept into a form with one important parameter: the morphological time-scale. This result provides opportunities to gain more insight into morphological behaviour and to come to better calibration of Asmita. Therefore, this type of linearisation will be elaborated for two and three elements as well.

4.3.2 Two elements

A similar linearisation is elaborated for two elements. (see for details appendix A). Hereafter, the channel and ebb-tidal delta are considered, see figure 3.1. The delta is connected to the open boundary. In the same way as illustrated for one element, the Asmita equations can be formulated for the delta element as:

$$\frac{dV_d}{dt} = A' \cdot \left(\frac{V_d}{V_{de}}\right)^n + B' \cdot \left(\frac{V_{ce}}{V_c}\right)^n + C' \tag{4.13}$$

and for the channel element as:

$$\frac{dV_c}{dt} = D'\cdot\left(\frac{V_d}{V_{de}}\right)^n + E'\cdot\left(\frac{V_{ce}}{V_c}\right)^n + F' \tag{4.14}$$

In the equations above, coefficients A', B', C', D', E' and F' all depend on geometric and exchange parameters of Asmita like $A_{d.}$, Ac, w_s, c_E, $\delta_{dc,}$ $\delta_{do.}$ The equilibrium condition, that dV/dt=0 when $V=V_e$, is guaranteed provided that it holds that:

$$A'+B'+C' = 0 \tag{4.15}$$

and

$$D'+E'+F' = 0 \tag{4.16}$$

With Taylor series expansion it is possible to linearise the set of differential equations 4.13 and 4.14 around the equilibrium-value $V=V_e$, in the same way as has been carried out in the previous section for one element. When the second and higher order terms are neglected, this results in:

$$\begin{bmatrix} \frac{dV_d'}{dt} \\ \frac{dV_c'}{dt} \end{bmatrix} = \begin{bmatrix} A & B \\ D & E \end{bmatrix} \cdot \begin{bmatrix} V_d' \\ V_c' \end{bmatrix} \tag{4.17}$$

where:
$V_d' = V_d - V_{de}$
$V_c' = V_c - V_{ce}$

In the above equation, the mutual dependency of the elements becomes clear. The reaction, or morphological development (dV/dt) of, for example, the channel, depends on the disturbance of both the channel and the delta. The coefficients A, B, D and E depend on A', B', D' and E' and hence on the parameters of Asmita. The solution of this differential equation is given by:

$$\begin{bmatrix} V_d' \\ V_c' \end{bmatrix} = C_1 \cdot \begin{bmatrix} Q_{11} \\ Q_{12} \end{bmatrix} \cdot e^{\lambda_1 \cdot t} + C_2 \cdot \begin{bmatrix} Q_{21} \\ Q_{22} \end{bmatrix} \cdot e^{\lambda_2 \cdot t} \tag{4.18}$$

where:
Q_1= eigenvector =$[Q_{11}\ Q_{12}]^T$
Q_2= eigenvector = $[Q_{11}\ Q_{12}]^T$

In which λ_1 and λ_2 are the eigenvalues of the 2x2 matrix in equation 4.17. Furthermore, as both eigenvalues are negative values (see appendix A), we are dealing with a dampening system as expected. The corresponding eigenvectors are Q_1 and Q_2 respectively. The constants C_1 and C_2 depend on the imposed disturbances. The result is that the

morphological behaviour is determined by two morphological time-scales, which are equal to the inverses of the eigenvalues (T_1= - $1/\lambda_1$ and T_2= - $1/\lambda_2$). These time-scales are time-scales of *the system* and they depend on geometric and exchange parameters (input Asmita).

The distinction between the sedimentation time-scale and the dispersive time-scale, as discussed for one element, cannot be recognised for a system consisting of one element (see appendix A).

So far, a model with two linearised equations has been derived, which approximates Asmita for small disturbances. Now, it is interesting to know what these system time-scales and eigenvectors stand for. This will be answered on the basis of the example of the Marsdiep inlet. This means that *order of magnitudes* of the geometric values of the Marsdiep inlet are taken as example, together with values for other parameters as used in previous studies. These values are presented in appendix B. It is emphasised that these values are indications of sizes and as such they provide rough quantitative insight into time-scales and rates of volume change.

With respect to further use of the linear equations for two elements, we choose the time-scales T1, T2 and the eigenvectors Q1 and Q2 as defined in appendix A. This means that: T1>T2 and if we standardise Q_{11}=Q_{12}=1 then Q_{12}<0 and Q_{22}>0.

4.3.3 System time-scales and responses in the case of two elements

To get an idea of how the system time-scales work in this set of linearised equations for two elements, the Marsdiep is used as an example. If we assume that this inlet is described sufficiently by distinguishing between the delta and channel, the following relation can be determined:

$$\begin{bmatrix} V_d' \\ V_c' \end{bmatrix} = C_1 \cdot \begin{bmatrix} 1 \\ -7.5 \end{bmatrix} \cdot e^{-\frac{t}{400}} + C_2 \cdot \begin{bmatrix} 1 \\ 0.5 \end{bmatrix} \cdot e^{-\frac{t}{25}} \tag{4.19}$$

The smallest time-scale (T2) is 25 years. This time-scale corresponds to an eigenvector where both components have the same sign. This means that both elements are too big or both are too small compared to their equilibrium volumes. When both elements are too big, the delta has sediment available and the channel demands sediment. Then, it is clear that the response connected with this eigenvector corresponds to the smallest time-scale as the elements can support each other by exchanging sediment.

The largest time-scale (T1) is 400 years. In the corresponding response, both components of the eigenvector have opposite signs. If, for example the delta wants to grow and the channel wants to diminish, sediment is needed for both elements. The elements cannot support each other. Sediment from outside is needed for both elements, which is attended with a large morphological time-scale.

The contribution of these two system time-scales to the morphological behaviour is not only governed by the eigenvectors, but it is described also by the constants C1 and C2. In figure 4.2 the effect of a variable C2 is shown on the morphological development of the two elements, given a constant C1 and in figure 4.3 the effect of a variable C1 is shown, given a constant C2. The volumetric values are purely indicative.

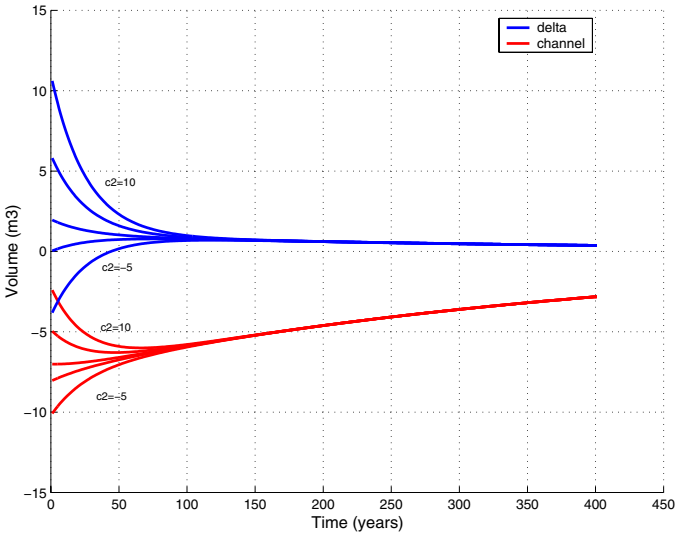

Figure 4-2 Effect of varying C2, with constant C1=1

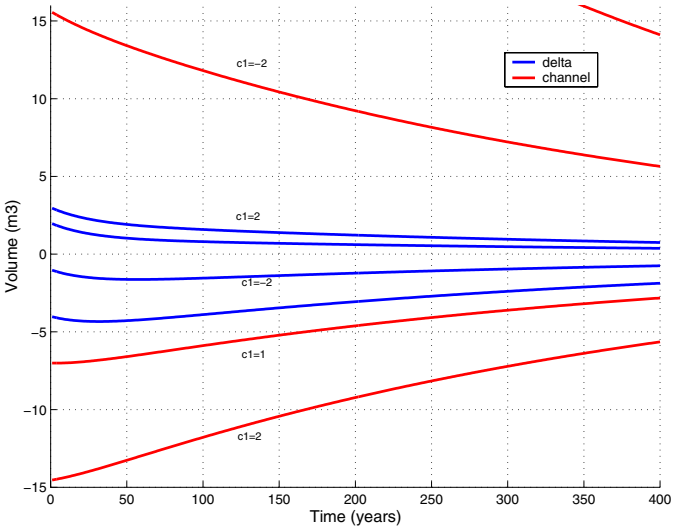

Figure 4-3 Effect of varying C1, with constant C2=1

From these figures, it becomes clear, that primarily the smallest time-scale (In this case T2), determines the initial development. The response with the smallest time-scale has damped out after a while and then, only the response with the largest time-scale remains. In figure 4.2 it can be seen that for a constant value of C2, both elements evolve in the same direction (both increasing or both decreasing) and from figure 4.3 it becomes clear that for a constant value of C1, both elements evolve in opposite directions, just as explained for the eigenvectors.

The actual value of the two constants, and thus the actual contribution of the two time-scales, is determined by the combination of the two initial disturbances of the volumes of the elements. Given these initial disturbances, the constants and thus the morphological development in time can be calculated from equation 4.19. With respect to the Marsdiep, these constants can be derived by, evaluating 4.19 at t=0:

$$C_1 = \left.\frac{0.5 \cdot V_d' - V_c'}{8}\right|_{t=0} \tag{4.20}$$

$$C_2 = \left.\frac{V_c' + 7.5 \cdot V_d'}{8}\right|_{t=0} \tag{4.21}$$

Summarising, it can concluded that in general, the morphological development of the elements of a tidal inlet is determined by a combination of the system time-scales, which depend on geometric parameters and the exchange coefficients of the system, ánd on the combination of disturbances. Hence, the interaction between the elements plays a large role in the morphological development of the elements. The development later on, when the response with the smaller system time-scale has damped out, is determined mainly by one system time-scale, in this example 400 years.

4.3.4 Three elements

As the linearised equations look useful to obtain insight into morphological interaction between elements and morphological time-scale, the linearisation has been elaborated also for three elements in the same way as described in section 4.3.3 for two elements. Apart from the delta and the channel, the flats are considered as well. The solution of the linearised differential equations has the form:

$$\begin{bmatrix} V_f' \\ V_c' \\ V_d' \end{bmatrix} = C_1 \cdot \begin{bmatrix} Q_{11} \\ Q_{12} \\ Q_{13} \end{bmatrix} \cdot e^{\frac{-t}{T1}} + C_2 \cdot \begin{bmatrix} Q_{21} \\ Q_{22} \\ Q_{23} \end{bmatrix} \cdot e^{\frac{-t}{T2}} + C_3 \cdot \begin{bmatrix} Q_{31} \\ Q_{32} \\ Q_{33} \end{bmatrix} \cdot e^{\frac{-t}{T3}} \tag{4.22}$$

Q_1= eigenvector= $(Q_{11}\ Q_{12}\ Q_{13})^T$
Q_2= eigenvector= $(Q_{21}\ Q_{22}\ Q_{23})^T$
Q_3= eigenvector= $(Q_{31}\ Q_{32}\ Q_{33})^T$

The solution consists of three eigenvectors (Q_1, Q_2 and Q_3) and three time-scales, which are dependent on system variables as δ_{dc}, w_s, $c_{E.}$, A_f and $V_{de.}$ The three time-scales can be seen as system time-scales corresponding to a response reflected by the eigenvectors. This equation indicates that an arbitrary combination of three disturbances is damped out by a combination of three exponential functions with three time-scales. As shown for two elements in section 4.3.4, the magnitude of the contribution (the values of the constants C1, C2 and C3) is determined by the eigenvectors and the values of disturbances. The Marsdiep (see appendix B) is used as an example, to get an idea on response characteristics.

For this inlet, it is found that:

$$\begin{bmatrix} V_f' \\ V_c' \\ V_d' \end{bmatrix} = C_1 \begin{bmatrix} -384 \\ -383 \\ 1 \end{bmatrix} \cdot e^{\frac{-t}{3}} + C_2 \cdot \begin{bmatrix} 0.11 \\ -7.5 \\ 1 \end{bmatrix} \cdot e^{\frac{-t}{412}} + C_3 \cdot \begin{bmatrix} -0.07 \\ 0.5 \\ 1 \end{bmatrix} \cdot e^{\frac{-t}{26}} \qquad (4.23)$$

The first term on the right hand side corresponds to the response where the exchange between flat and channel dominates. This is attended with the smallest system time-scale, which is approximately 3 years. Because of the relatively small flat volume in this example, this element hardly influences the morphological development of the system. As a consequence, this linear solution contains the same characteristics as the solution for two elements, where delta and channel were considered.

It must be emphasised again, that these values illustrate orders of magnitudes for the Marsdiep. As these values depend on the system, they do not hold for other systems.

The linear approximation may be valuable to obtain more insight into the morphological behaviour and to estimate the parameters of Asmita. On the other hand, the linear approximation is not suitable as a predicting model like Asmita. It has been derived to describe the morphological development around the equilibrium volume. This means that there is a limitation on the validity of the linear approach. Moreover, in the case of three elements, 15 parameters need to be estimated. These parameters do not have a direct physical meaning, which makes estimating them difficult. Thus for predicting future equilibrium situations, the linear approximation does not seem appropriate, which will also be discussed in section 4.5, where the validity is concerned. In the following section we will discuss the use of the linear approximation.

4.3.5 Use of linearised equations

So far, we derived the linear approximation of Asmita and analysed the meaning of the eigenvectors and eigenvalues. We concluded that the linearised equations describe the fundamental morphological behaviour of a tidal system in reaction to an imposed disturbance, with a combination of system time-scales. These system time-scales depend on geometric parameters and on the exchange coefficients of the system. They form characteristics of a tidal system.

The linear approximation is derived for the morphological development around the equilibrium volume. This means that there is a limitation to the validity of the linear approach. Moreover, in the case of three elements, 15 parameters need to be estimated. These parameters do not have a direct physical meaning, which makes estimating them difficult. This makes the approximation not appropriate to be used as replacement of the original formulation of Asmita.

Despite the limitations as mentioned above, it can be stated that we have already derived some interesting information on the morphological development, based on system time-scales. There are opportunities to use the linearisation to obtain further insight into this

behaviour, which can help the calibration of Asmita. Obtaining this insight will be carried out with the following complementary approaches.

Theoretical application linear approximation

First we will apply the linear approximation to enlarge the theoretical understanding of the morphological behaviour of tidal inlets (see section 4.4). This means that we will theoretically discuss the morphological time-scale of an element and the character of the morphological behaviour, based on the linear approximation. This will be done at a simple scale of interaction, namely for two elements.

Assessment validity linear approximation

Applying the linearised equation to obtain insight into morphological behaviour and to obtain insight into the input parameters of Asmita, requires insight into the limits of the validity of the approximation. It is analysed how we can express the error made by linearising Asmita and how we should interpretate the use of linearised equations in relation to this error (section 4.5).

Using linear approximation for calibration Asmita

Subsequently, the linear approximation is linked to a fictitious data-set in order to assess the possible use of the linearised equations, and especially the system time-scales, for calibrating Asmita.
1. To validate the linearisation, we want to know whether the system time-scales, found from Asmita parameters, can be derived from the data. This would confirm that we can use system-time-scales to characterise the morphological development of a tidal system. (section 4.6)
2. Deciding which parameters in Asmita should be varied during calibration and how they should be varied, requires insight into the influence of these parameters on the morphological development. To gain this, a sensitivity analysis is carried out (section 4.7).

The above three approaches will be elaborated successively in the following sections.

4.4 Theoretical application of the linear approximation

In this section we will apply the linear approximation for a tidal system with two elements to enlarge the theoretical understanding of its morphological behaviour. First the morphological time-scale of an element will be considered and the specific factors that affect this time-scale. Subsequently, the morphological behaviour in time will be discussed.

4.4.1 Morphological time-scale of an individual element

We have seen in the previous sections that the behaviour of an element partly depends on system characteristics and partly on the imposed combination of disturbances. The morphological time-scale of an element turns out not suitable as general characteristic of an element as it depends on the disturbances. Yet, it is interesting to find an expression for the

morphological time-scales of individual elements, as these reflect properties of the response to a disturbance easily identified from observations. In this section we will derive an analytical expression for the time-scale of an element, based on the linearised equations.
The morphological time-scale of an element is equal to the ratio of the disturbance (V') and the initial adaptation rate (dV'/dt at t=0) (see also figure 4.1):

$$\tau_{element} = -\frac{V'}{\left.\frac{dV'}{dt}\right|_{t=0}} \tag{4.24}$$

The initial adaptation rate can be found by differentiating equation 4.18 and evaluating the result for t=0:

$$\left.\frac{dV_d'}{dt}\right|_{t=0} = -\frac{C_1 \cdot Q_{11}}{T_1} - \frac{C_2 \cdot Q_{21}}{T_2} \tag{4.25}$$

Note that T1 and T2 are the *system* time-scales as described in the previous section!

$$\left.\frac{dV_c'}{dt}\right|_{t=0} = -\frac{C_1 \cdot Q_{12}}{T_1} - \frac{C_2 \cdot Q_{22}}{T_2} \tag{4.26}$$

The constants C1 and C2 depend directly on the initial disturbances (equations 4.20 and 4.21), hence in the end, the morphological time-scale of an element is dependent on the combination of disturbances and eigen vectors and time-scales.

As a conclusion it can be stated that the applied linearisation of Asmita equations can be used to arrive at simple analytical expressions for time-scales of individual elements. However, it should be remembered that the linearised equations only represent the same results as Asmita in the case of small disturbances. This will be elaborated in section 4.5.

In the next section the influence of various factors on the above defined time-scale is analysed.

4.4.2 Factors that influence the interaction between elements

In the previous section we derived an expression for the morphological time-scale of individual elements, corresponding to the initial morphological response to a disturbance. In more detail, we are interested in the factors that increase or decrease the time-scale of elements.

Eysink and Biegel (1992-1993) especially investigated the effect on flats with respect to sea level rise. According to Eysink (1992), the flat elements generally react the fastest, as here the relative disturbance is the largest. However, as we consider initial disturbances, it is

likely that factors like the proximity of the outside world and absolute size of the disturbance also play an important role.

In this section, the influence on time-scales of the following aspects will be analysed:
- magnitude disturbances
- the relative disturbances
- proximity of the outside world that supplies sediment

The actual morphological behaviour of the elements is determined by a combination of these three aspects. Three tests have been carried out to determine the influence of these aspects. In each test V_e is used as a measure for the size of the element. The delta and channel are considered in these tests.

1. Tests with 2 elements which have the same size (V_{ce}=V_{de}= $1*10^8$ m3).
2. Tests with 2 elements with order of magnitudes of Marsdiep as used before (V_{ce}=$23.9*10^8$ m3,V_{de}=$6*10^8$ m3).
3. Tests with 2 elements with reversed sizes of Marsdiep (V_{ce}= $6*10^8$ m3 V_{de}=$24*10^8$ m3). Then the influence of the outside world becomes clear.

With these tests the relation between the time-scales and the disturbance for each element is analysed qualitatively. The change of these relations due to a change of (relative) disturbances and proximity of the outside world will be analysed as well.

Test 1 showed that the size of the absolute disturbance has the following influence:
- an enlargement of an absolute disturbance in one element increases the time-scale of this element, and at the same time it will decrease the time-scale of the other element.

This is derived as follows. From figure 4.4 it can be seen that, given a certain disturbance for the channel (suppose V_c'=1e7 m^3), a relation exists between the time-scale of the elements and the disturbance in the delta. This relation shows that the time-scale of the channel decreases, and the time-scale of the delta increases with an increasing disturbance in the delta. The same becomes clear if we increase the disturbance in the channel. This is illustrated by the translation of the relations (between time-scale and disturbance in the delta) for both elements, which is illustrated by the arrows. Naturally, the actual values depend on the system parameters, but in general figure 4.4 shows the character (increasing/decreasing) of the relation between the time-scale of an element and the disturbances in each element. Similar relations are shown in the two other tests.

We can confirm that this conclusion holds in general, if we use the general form of the linearised equations. When we substitute 4.20 and 4.21 into 4.25 and 4.26, and subsequently susbsitute 4.25 and 4.26 into 4.24, then the time-scale of an element can be expressed directly as function of the disturbance. This is elaborated in appendix A3.

The conclusion is rather logic. Given an increasing disturbance in the channel, the delta can loose sediment to decrease towards equilibrium more easily as the channel needs this sediment to decrease as well. However the channel has to cope with a increased disturbance

which is attended with a slower reaction than in the case of a smaller disturbance in this element.

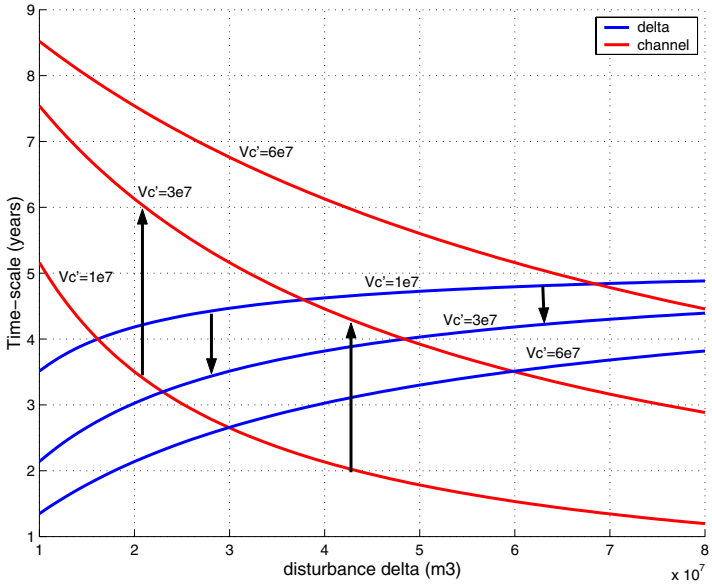

Figure 4-4 Time-scales of elements for different disturbances

Test 1 and test 2 showed the influence of the relative disturbance :

- a relative larger disturbance (compared to the relative disturbance in the other element) will decrease the time-scale of that element, compared to the other element

The effect of the relative disturbance becomes clear if figure 4.4 and 4.5 are compared. In figure 4.4, the relation between disturbances and time-scales are presented in the case of two elements with the same size ($1*10^8 m^3$). In the second test we increased the size of the delta with a factor 24 and we increased the size of the delta with factor 6. Similar relations as in figure 4.4. are presented in figure 4.5.

From figure 4.5 becomes clear that both the time-scales of the delta and channel increased, compared to the results in the first test. This implies that an increase in the magnitude of the element increases the time-scale of that element. Furthermore, figure 4.5 shows that the increase of the time-scales of the channel are much larger than those for the delta. When we express this in the relative disturbance (V'/V_e), it means that the time-scale of an element decreases when the relative disturbance is larger (smaller element).

Considering the two conclusions from test 1 and test 2, it can be stated that both the size of the element and the size of the disturbance in the element determines the time-scale of that particular element. They have opposite effects.

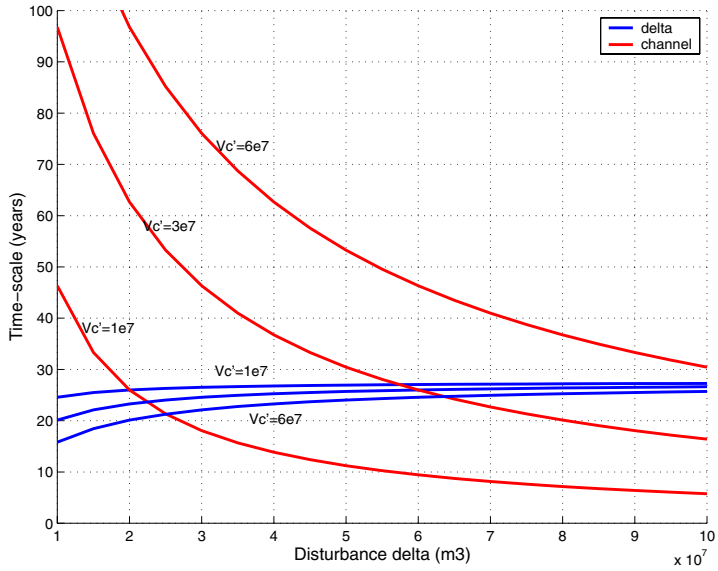

Figure 4-5 Time-scales of elements for different disturbances

Finally, also the proximity of a sediment supplier like the outside world, plays an important role. Comparing time-scales from tests 2 and 3 for equal disturbances, showed the following:

- The closer an element is to the outside world, the smaller its time-scale will be.

This can be observed from figures 4.5 and 4.6.

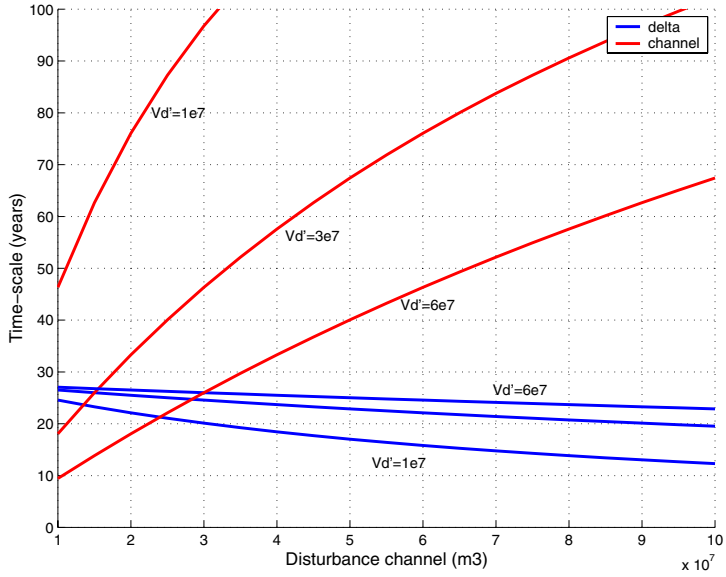

Figure 4-6 Time scales of elements for different disturbances

The only difference between test 2 and test 3 is that the sizes of the elements have been switched, so that without the influence of the outside world, the time-scales for the delta given in figure 4.5 should correspond with the time-scales for the channel in figure 4.6, provided that equal disturbances are imposed in both elements. The same holds for the results of the channel given in figure 4.5 which should correspond to the time-scales of the

delta in figure 4.6. However, this seems not to be true: the time-scales of the channel in figure 4.5 are larger than the time-scales of the delta in 4.6. In the same way, the time-scales of the channel in 4.6 are larger than the time-scales of the delta in 4.5.

A similar conclusion can be drawn from test 1. In test 1 the elements are of the same size, so imposing two equal disturbances should result in two equal time-scales if the outside world did not have any influence. However, it turns out that in that case the time-scale of the channel is larger than that of the delta. So the proximity of the outside world surely influences the time-scale. The reason behind the fact that an element closer to the outside world has a smaller time-scale, is that sediment is more readily available, which is not the case for the channel. In Asmita there is no limit to the supply from the outside.

Summarising, the time-scale is determined by factors like absolute disturbances, relative disturbances and the proximity of the outside world. The morphological behaviour of an element is determined by a combination of these three aspects. It is not possible to conclude which aspect will dominate as this depends on the system and the magnitude of the disturbances.

4.4.3 Character of the morphological behaviour in time

In the previous section the time-scale of an individual element and the factors influencing this time-scale have been analysed. Another aspect we would like investigate is the feasibility to characterise morphological behaviour of the elements in time with the linear equations. Again this will be elaborated for two elements: delta and channel.

If elements are given sufficient time to respond to a disturbance, they will always evolve towards an equilibrium state. This evolution is not necessarily a monotonous one. Depending on the combination of the disturbances, the initial response of an element may be away from its equilibrium (this type of behaviour is referred to in the present report with the term ‘bump’). It is also possible that an element overshoots its equilibrium. These two deviating situations are illustrated in figure 4.7.

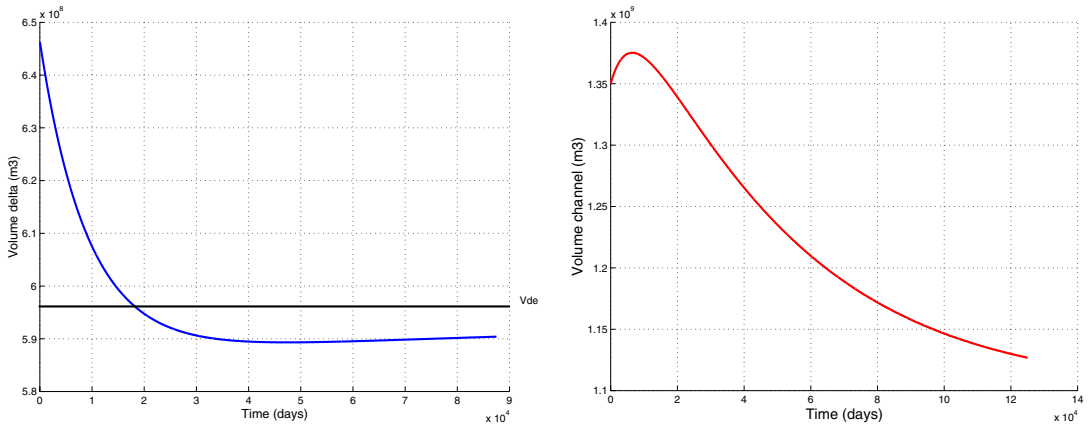

Figure 4-7 Examples of possible morphological development; left: overshoot, right: bump

Considering these two possible behaviours we will explain in this section:

- How we can simply derive from the linear equations, which situation is likely to occur, given an imposed disturbance
- What the physical process is behind this kind of behaviour.

Based on the linear approximation and for given disturbances, it can be derived whether an overshoot, or a so-called bump, will occur and in which element.

As indicated in section 4.3.3, the signs of C1 and C2, together with the signs of the components of the eigenvectors, indicate the direction (increasing or decreasing volume) of the response. In section 4.3.2 was mentioned that we choose the time-scales T1, T2 and the eigenvectors Q1 and Q2 as defined in appendix A. This means that: T1>T2 and when we standardise $Q_{11}=Q_{12}=1$ then $Q_{12}<0$ and $Q_{22}>0$. Hence, we can conclude that the signs of the components of the eigenvectors, are independent of the system characteristics.

Then, both C1 and C2 determine the initial response (increasing or decreasing volume), and only C1 determines the response on long-run. The values of C1 and C2 can be derived for a system, given the disturbances, similar to equations 4.20 and 4.21.

The signs of the constants, together with the signs of the disturbances determine the character of the morphological behaviour. Considering the delta, for example, if the disturbance in the delta is positive (V>Ve, the delta will decrease) and the sign of C1 is negative, which indicates an increasing response on long-run, then the result is that the delta overshoots its equilibrium. Different signs for C1, C2, V_d-V_{de} and V_c-V_{ce} result in eight possible situations for morphological behaviour, which are elaborated in appendix C. The figures in the appendix are meant to indicate types of morphological development and numbers must be disregarded.

The given characters for corresponding conditions hold for systems where a smaller and a larger system time-scale can be distinguished, and hence only C1 (together with the sign of the component of the eigenvector) indicates the response on the long-run. Then, all presented characters are unambiguous for the given conditions (signs of C1, C2, V-Ve), except for the bumps. This is because the occurrence of a bump depends on the dominance of C1 relative to C2. If C2 dominates initially over C1, then a bump will be visible. If C1 dominates initially, then a bump does not occur. Furthermore, the actual size of overshoots and bumps depends on the situation.

We can also conclude from the combinations of morphological behaviour for two elements (see appendix C) that for an arbitrary system and arbitrary disturbances (at least) *one* of the elements will evolve monotonously towards equilibrium and *the other* element will overshoot or possibly move away from its equilibrium (which results in a bump). These 8 possible characters are described in table 4.1.

Situation	Disturbances	Constants	Channel	Delta
1	$V_c>V_{ce}$, $V_d<V_{de}$	C1<0, C2<0	monotone/bump	monotone
2	$V_c>V_{ce}$, $V_d<V_{de}$	C1<0, C2>0	monotone	monotone/bump
3	$V_c>V_{ce}$, $V_d>V_{de}$	C1<0, C2>0	monotone	overshoot
4	$V_c>V_{ce}$, $V_d>V_{de}$	C1>0, C2>0	overshoot	monotone
5	$V_c<V_{ce}$, $V_d>V_{de}$	C1>0, C2>0	monotone/bump	monotone
6	$V_c<V_{ce}$, $V_d>V_{de}$	C1>0, C2<0	monotone	monotone/bump
7	$V_c<V_{ce}$, $V_d<V_{de}$	C1>0, C2<0	monotone	overshoot
8	$V_c<V_{ce}$, $V_d<V_{de}$	C1<0, C2<0	overshoot	monotone

Table 4.1 Different types of morphological behaviour (see appendix C)

So far, we described the 8 possible characters of the morphological development for two elements in general. Subsequently, we use the Marsdiep as an example to illustrate how we can create an overview for the expected morphological behaviour for a specific tidal system. For the linear approximation of the Marsdiep holds:

$$\begin{bmatrix} V_d' \\ V_c' \end{bmatrix} = C_1 \cdot \begin{bmatrix} 1 \\ -7.5 \end{bmatrix} \cdot e^{-\frac{t}{400}} + C_2 \cdot \begin{bmatrix} 1 \\ 0.5 \end{bmatrix} \cdot e^{-\frac{t}{25}} \tag{4.27}$$

Evaluating this equation for t=0 gives (see also 4.20 and 4.21):

$$C_1 = \frac{0.5 \cdot V_d' - V_c'}{8} \tag{4.28}$$

$$C_2 = \frac{V_c' + 7.5 \cdot V_d'}{8} \tag{4.29}$$

In figure 4.8 equations 4.28 and 4.29 are plotted for C1=0 and C2=0. In this figure, the 8 combinations of the signs of C1, C2, V_d-V_{de}, V_c-V_{ce} can be identified. For a certain combination of disturbances, the signs of these four variables can be derived, and hence, the corresponding character of morphological behaviour, as presented in appendix C.

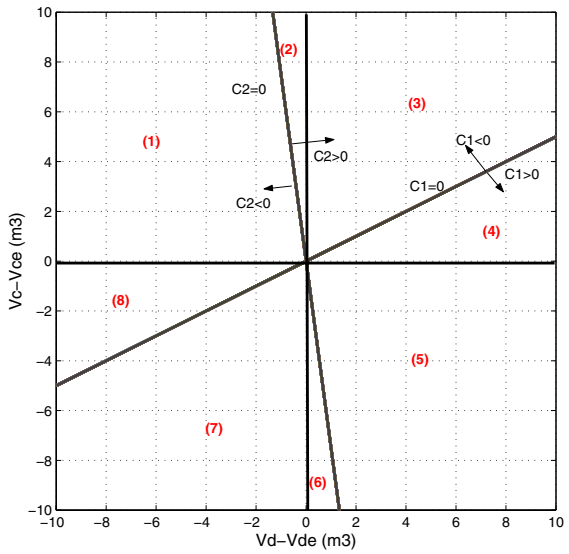

Figure 4-8 Different types of morphological behaviour regarding Marsdiep (for eight situations, numbers correspond with appendix C)

From appendix C, we can see that an overshoot will occur in one of the elements in the case of two positive disturbances (V_c>V_{ce} and V_d>V_{de}) will occur. An example for this could be a closure of part of a small basin compared to the tidal wave length. For a better understanding of this kind of behaviour we will explain the case that an overshoot occurs in the delta (situation (3))

We have computed the time-scales for different combinations of disturbances and we concluded that it is likely that the overshoot occurs in the morphological development of the element with the smallest time-scale. The corresponding behaviour can be explained in terms of demand and supply of sediment, in the same way as formulated in Asmita. In situation (3), the delta, as reflected by the smallest time-scale, reacts the fastest and will reach equilibrium first. This is accomplished by transporting sediment to the outside world and to the channel. The channel uses this sediment to decrease its volume as well. At the moment that equilibrium is reached in the delta, the channel still demands sediment to decrease. This is because the channel reacted slower and did not reach equilibrium yet. The sand needed for further decrease of the channel will be supplied by the delta, which therefore continues eroding. In this case, the overshoot will occur in the delta development. Because the delta erodes, the outside world will start supplying sand to the delta. Then both elements will tend to equilibrium. Sediment transport in the system continues as long as this equilibrium is not reached yet for one of the elements.

Hence, the overshoot will occur in the element with the shortest time-sale. Which element this is, depends on the disturbances. In the previous section (4.4.2) we stated that the following factors influence the time-scale of an element:
- magnitude disturbance (compared to other element)
- relative disturbance (V'/V_e, compared to other element)
- proximity of outside world

4.4.4 Conclusion theoretical application linear approximation

In the sections 4.4.1-4.4.3 we applied the linearised equations to analyse the morphological time-scale of an element, where it concerns the initial response to a disturbance, and to characterise the morphological behaviour of elements. It turned out that the applied linearisation of Asmita equations can be used to arrive at simple analytical expressions for time-scales of individual elements. Furthermore, we concluded that factors like absolute disturbance, relative magnitude disturbance and proximity of outside world play a role in the interaction between the elements as follows:

- an enlargement of an absolute disturbance in one element increases the time-scale of this element, and at the same time it will decrease the time-scale in the other element.
- a relatively larger disturbance (compared to the relative disturbance in the other element) will decrease the time-scale of that element, compared to the other element
- The closer an element is to the outside world, the smaller its time-scale will be.

Finally, we can use the linearised equations to predict the characteristics of the behaviour of the elements, for different combinations of disturbances in a system, on the condition that the magnitudes of the time-scales differ substantially. The characterisation indicates that for arbitrary disturbances (at least) one of the elements will evolve monotonously towards equilibrium and the other element will overshoot or possibly move away from its equilibrium (the latter depends on the initial dominance of the two time-scales). Whether an overshoot or bump occurs depends on the disturbances. An overshoot in the development of one of the elements is expected in the case of two positive disturbances ($V_c > V_{ce}$ and $V_d > V_{de}$). This overshoot is likely to occur in the element that has the smallest time-scale.

4.5 Validity of linearised equations

The linearised equations were derived around equilibrium. This means that in the case of relatively small (compared to volumes) disturbances, the linear approximation gives a good representation of Asmita. However, the approximation becomes less accurate when larger disturbances are considered. We concluded in section 4.3.4 that the linearised equations are not suitable to serve as a prediction model.

On the other hand, we can conclude that linearised equations are very suitable to characterise the morphological behaviour and time-scales for comparatively small disturbances. For the latter purpose, it is desirable to value the linear approximation and to get an idea of the validity of the linear approximation. This will dealt with in this section, by comparing the linearised equations with the actual differential equations of Asmita, and providing a possibility to assess the deviations between these two.

The differential equations (as discussed in chapter 3) of Asmita have the form:

$$\begin{bmatrix} \frac{dV_f}{dt} \\ \frac{dV_c}{dt} \\ \frac{dV_d}{dt} \end{bmatrix} = \begin{bmatrix} A & B & C \\ D & E & F \\ G & H & I \end{bmatrix} \cdot \begin{bmatrix} \left(\frac{V_f}{V_{fe}}\right)^n \\ \left(\frac{V_{ce}}{V_c}\right)^n \\ \left(\frac{V_d}{V_{de}}\right)^n \end{bmatrix} + \begin{bmatrix} R1 \\ R2 \\ R3 \end{bmatrix} \tag{4.30}$$

The linear approximation, which is valid close to equilibrium reads:

$$\begin{bmatrix} \frac{dV_f}{dt} \\ \frac{dV_c}{dt} \\ \frac{dV_d}{dt} \end{bmatrix} = \begin{bmatrix} P & Q & R \\ S & T & U \\ X & Y & Z \end{bmatrix} \cdot \begin{bmatrix} V_f - V_{fe} \\ V_c - V_{ce} \\ V_d - V_{de} \end{bmatrix} \tag{4.31}$$

The deviation between original and approximation is given by:

$$\left.\frac{d\overline{V}}{dt}\right|_{ASMITA} - \left.\frac{d\overline{V}}{dt}\right|_{LINEARISED} \tag{4.32}$$

where

$\overline{V}$ = volume-vector $(V_f, V_c, V_d)^T$

This error will be zero at equilibrium state and will increase with increasing disturbance from equilibrium. Apart from the effect of a potential bump, the maximum deviation from the original formulation of Asmita will occur at t=0 as here the deviation of equilibrium is at its maximum. One way to define this maximum error at t=0 is to express it in a deviation in time-scale of the element at t=0.

The deviation in time-scale can be expressed for each element as (see equation 4.24 for definition time-scale of element):

$$\Delta\tau_{element} = \left(\frac{1}{\left.\frac{dV}{dt}\right|_{ASMITA}} - \frac{1}{\left.\frac{dV}{dt}\right|_{LINEAR}} \right) \cdot (V - V_e) \tag{4.33}$$

This deviation in time-scale varies with the imposed combination of disturbances. For every disturbance, the actual time-scales of the elements are different as well. Therefore, the deviation in time-scales is made relative to the actual time-scale of the element:

$$linearisation\_error = \frac{\Delta\tau_{element}}{\tau_{element}} \tag{4.34}$$

So, the maximum error made by using the linear approximation of Asmita can be expressed as a relative deviation in time-scale for each element, which depends on the disturbances. The time-scale is calculated with the linear equations (see equations 4.24).

The combination of the disturbances in the elements are taken relative to the volumes of the elements according to:

$$relative\_disturbance = \frac{V - V_e}{V_e} \cdot 100\% \tag{4.35}$$

In the following figure we can see the maximum linearisation errors for several combinations of relative disturbances. In order to calculated the time-scales, the system characteristics of the Marsdiep were used (see appendix B).

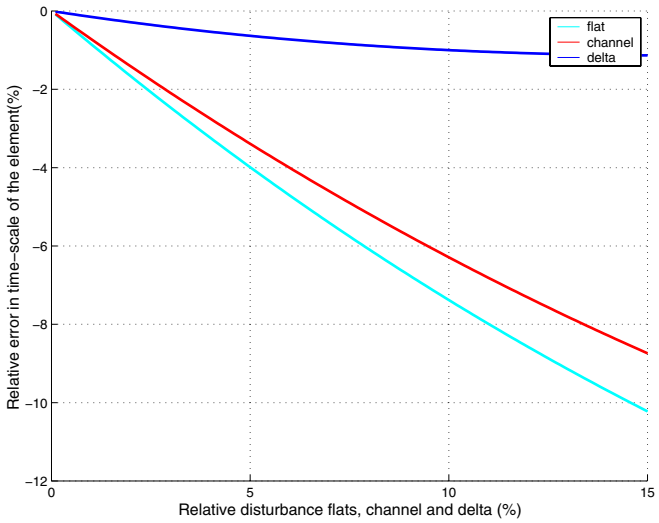

Figure 4-9 Relative error in time-scale element as a function of relative disturbance

In this example, it becomes clear that an increase in disturbance corresponds with an increase in error, as explained before. If, for example, the relative disturbance in the three elements equal 15%, then the relative error in time-scales equals at most 11%. A figure like 4.9 provides possibilities to decide whether it is acceptable to use the linearisation for the previous (in section 4.4) discussed purposes for a particular situation.

Concluding, we can state that if we use the linear approximation to determine the time-scales of elements from section 4.4.1, we should bare in mind that in the case of disturbances the time-scales will deviate from the results of Asmita. Despite the deviation, we assume that the linearised equations characterise the morphological behaviour (see section 4.4.2 and 4.4.3) in the same way as Asmita. In other words, for rough estimations of time-scales and for qualitative analyses, it is appropriate to use the linearised equations.

4.6 Deriving system time-scales from data

4.6.1 Calibration process

In this section we will derive a procedure to estimate the system time-scales directly from field data. This would validate the system time-scales, which we can use to characterise the morphological development of a tidal system.

The time-scales which result from the linearised equations (e.g. 3, 25 and 400 years for Marsdiep), are determined with estimated values for geometry and exchange parameters. Whether this information results in correct time-scales could be validated if we could derive these time-scales directly from field data. To achieve this, we will calibrate the linearised equations on observations. In this test, fictitious Asmita results, based on Marsdiep input (see appendix B) will be used as observations instead of the real field data. This has two advantages:

- it is prevented that we are faced with problems related to sparsity of available data
- the system time-scales found from Asmita parameters can be used as a check for the fitted time-scales

The intended calibration concerns fitting the linear approximation to a set of fictitious field data in a Least Squares sense. All 15 parameters mentioned in the right hand side of equation 4.22 are varied in this procedure. Results of an Asmita computation with respect to the morphological development of a Marsdiep-like inlet over a period of 68 years are used as fictitious field data. This forms an imitation of real field data, be it with a larger resolution in time.

When, the system time-scales which are found from the calibration correspond to those calculated from Asmita parameters, we can conclude that deriving system time-scales is theoretically possible. Yet, utility in practical applications with sparsely available field data has yet to be proven in that case.

4.6.2 Results optimising system time-scales

The calibration has been performed numerically, with 3, 413 and 25 years as first estimates for the system time-scales. After a long iteration process (approx. 200 steps) for several different imposed disturbances, it turned out that the same time-scales 3 and 25 years were found as optimum combinations for system time-scales. Also with different initial values, for example 20, 20 and 20 years, the same values 3 and 25 were found. However, the time-scale 413 years did not result directly from the iteration. This is probably because the observations cover a period of 68 years, which may be insufficient to identify the comparatively large time-scale. This time-scale could possibly be derived if a longer period would be considered.

In the following figure the calibration results of one example of imposed disturbances are shown. Actually, similar results were obtained for other disturbances, which means that only the two smaller time-scales were found.

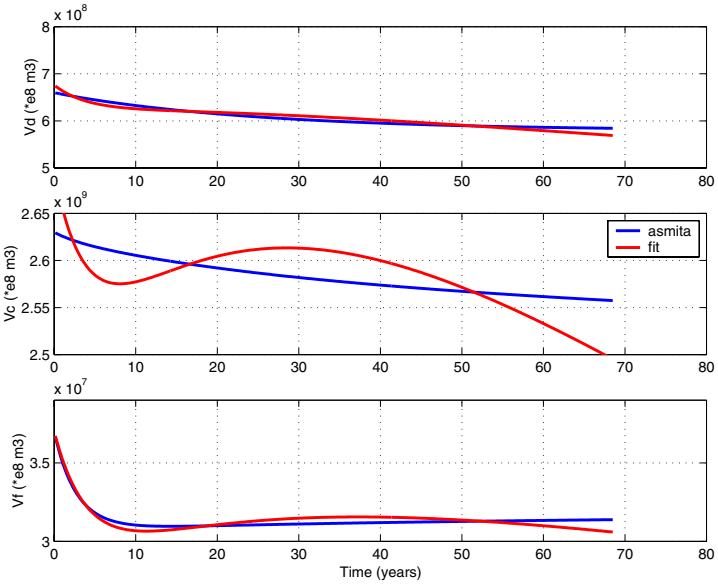

disturbances (10% of Ve)
delta: 6e7 m3
channel: 2.4e8 m3
flat: 0.3 e7 m3

Figure 4-10 Fit linear approximation to Asmita results over 68 years.

In the figure above, it can be seen that the fitted system time-scales yield a reasonable representation of the Asmita results for the flat and delta. Only the development of the channel, gives a clear deviation. Apparently, the channel development on a time-span of 68 years is already governed by the larger time-scale, which cannot be derived from data covering only 68 years.

Considering a calibration with a smaller period (with the same disturbances and same input in Asmita), results in a more accurate fit for all elements, also for the channel (see figure 4.11). Apparently, a better fit is possible for the channel, as the larger time-scale is relatively unimportant in the first 34 years. Furthermore, the error turns out to be smaller in the case of smaller disturbances. This is logical as the linearised equations were derived near equilibrium values, hence for small disturbances.

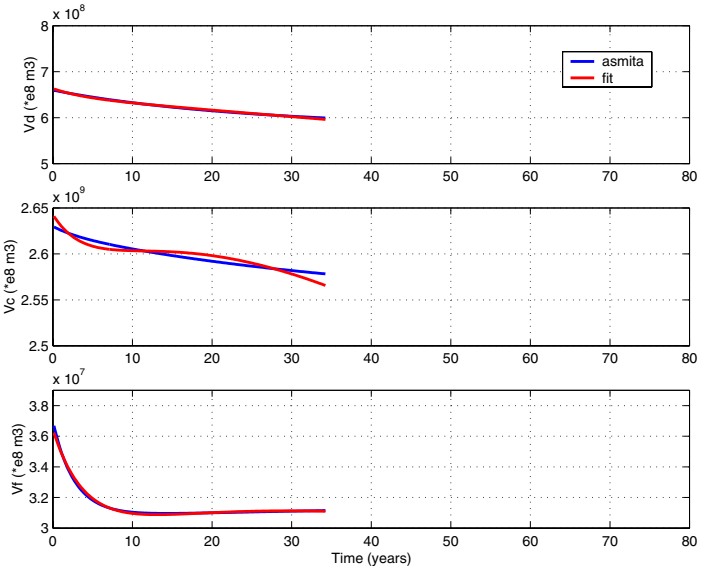

disturbances (10% of Ve)
delta: 6e7 m3
channel: 2.4e8 m3
flat: 0.3 e7 m3

Figure 4-11 Fit linear solution to Asmita results over 34 years

Comparing eigenvectors derived from Asmita parameters with those obtained from calibration, shows that they are not almost equal. In the linear approximation, the components of the eigenvectors are mathematically related. In the fit, these components have turned into a set of more or less mutually independent 'fit' factors. Apparently, system time-scales could be derived in the calibration for larger disturbances, but then with other proportions than based on the linear approximation.

4.6.3 Conclusion calibration of linear approximation

From the calibration of the linear approximation on Asmita results, we conclude that system time-scales, which were derived analytically, can be derived from data-observations, on the condition that the observation period is of the same order as the system time-scales. This is concluded from the finding that with an observation period of 68 years, the larger time-scale (413 years) cannot be recognised, simply because insufficient data are available to cover this scale. It looks as if, in the example of the Marsdiep, the channel development is governed by this larger time-scale.

The linearised equations were derived around equilibrium, but we found that also for larger disturbances the system time-scales, which were found from Asmita parameters, could be derived from observations. It turned out that the corresponding eigenvectors resulting from the fit, are not equal to those found in the linear approximation. Nevertheless, we can conclude that system time-scales may be appropriate to characterise the morphological behaviour of a tidal system regardless of the magnitude of the disturbances.

In this analysis we used Asmita output as fictitious observations, together about 500 data-points. In the case of the closure of the Zuiderzee, we have a rather sparse data-set (8 data-points per element). This means that it is not possible to calibrate all 15 parameters as we have done in this section. We have to limit the number of degrees of freedom by estimating some parameters in a different way than by calibration. Unfortunately, eigenvectors do not qualify for such an alternative estimation, as:

- We concluded in this section that in the case of larger disturbances the analytical eigenvectors are not the same as the calibrated 'eigenvectors'. This means that we cannot base our estimations on the analytical solution.
- We cannot estimate these parameters based on other knowledge, as these parameters do not have a physical meaning

As a result, sufficient reduction of the number of degrees of freedom is not possible, so that we cannot derive the system time-scales from the available data of the closure of the Zuiderzee.

4.7 Sensitivity analysis on system time-scales

4.7.1 Approach Sensitivity analysis

In this chapter we have seen that the system time-scales form characteristics of the morphological development of a tidal system. These system time-scales are directly related to the input parameters, and could help the calibration of Asmita.

When calibrating Asmita, information on input parameters is desired with respect to two aspects:

1. Calibrating Asmita requires insight into the actual influence of these parameters on the morphological development. This means that we would like to know which parameters we should vary in what direction to obtain the desired calibration.
2. We want to know which parameters in Asmita have a relatively large influence, compared to the other input parameters. Then, we can decide which parameters can be estimated roughly and could be fixed during the calibration. However, parameters which have a large influence should be used as calibration parameter, or should be investigated in more detail, for example by means of field-investigations.

For these purposes, the sensitivity of the system time-scales to Asmita input parameters will be analysed.

So far, the linear approximation has been used in an example for the Marsdiep. For this, values are assumed for the input parameters of Asmita. For the order of magnitude of the geometric parameters, values for Marsdiep of 1934 have been used. In this year, there was no equilibrium, but the data were used anyway to get an idea of the system and the interaction based on the linear approximation. For other parameters we used values based on previous studies. (see appendix D).

To find out what the sensitivity of the system time-scales are for a variation of these parameters, a sensitivity analysis is carried for each parameter separately, keeping the other parameters constant.

In table 4.2 the ranges are given within which the various parameters are varied in the sensitivity analysis. For the geometric parameters a deviation of 20%, relative to the central value, is used. For the other parameters, ranges were used from previous investigations (Buisman, 1997 and Van Goor, 2001) as discussed in section 3.7. The n parameter, with a value of 2, originates from the sediment transport formula (where the sediment transport is related to the velocity as discussed in section). Different transport formulas exist, where the n-parameter can roughly vary between 2 and 4.

Parameters	central values	unit	range
δ_{dc}	1000	m3/s	500-2000
δ_{co}	1000	m3/s	500-2000
δ_{fc}	1000	m3/s	500-2000
c_E	2e-4	-	1.2-2.4e-4
w_s	1e-4	m/s	1e-5-1e-4
V_{de}	5.96e8	m3	4.7-7.2e8
V_{ce}	23.9e8	m3	19-29e8
V_{fe}	0.34e8	m3	0.25-0.5e8
A_d	1.31e8	m2	1.05-1.6e8
A_c	5.61e8	m2	4.43-6.73e8
A_f	1.31e8	m2	1.08-1.62e8
n	2	-	2-4

Table 4.2 Ranges used in sensitivity analysis.

Estimated time-scales based on central values (see table 4.2) for input of Asmita:
T1 = 2.85 years,
T2 = 412.7 years,
T3 = 25.7 years
The results of the sensitivity analysis can be found in appendices D1 till D12. In the following description of the results reference is made to the system time-scales T1,T2 and T3 as defined above. Regarding the sensitivity of the different input parameters for the system time-scales, the following conclusions can be made:

4.7.2 Diffusion coefficients

The diffusion coefficients represent the sediment exchange capacity between adjacent elements. The larger the exchange coefficient, the larger the sediment exchange, and hence the larger the amount of available sediment. This corresponds to a decrease of the time-scale. So, for all system time-scales it holds that, the larger the exchange coefficient, the smaller the system time-scale. To which extent the system time-scales vary, as a consequence of variation in the three exchange coefficients is shown in appendices D1 to D3.

δ_{dc} and δ_{co}: these parameters do not influence the smallest time-scale T1 but the other two time-scales are sensitive to a variation of these two exchange coefficients.
δ_{fc}: The other way around, this parameter does not influence T2 and T3 (412 and 25 years), but does have an impact on T1.

The influence of the various exchange coefficients corresponds to the interactions as discussed for three elements in section 4.3, namely that the T1 is related to the exchange

between the flats and the channel and the time-scales T2 and T3 are related to the exchange between the channel and the delta, and between the delta and the outside world.

4.7.3 Equilibrium concentration

As discussed in chapter 3 the concentration in the outside world, c_E, is present in all the elements of the inlet initially and, again when equilibrium is reached. The larger the equilibrium concentration, the smaller the system time-scales. This is because the concentration difference between the elements become larger, which is attended with a faster transport across boundaries of elements. The concentration has a large influence on all three system time-scales. The influence of the equilibrium concentration on the different elements can be found in appendix D4. System time-scales are inversely proportional to the equilibrium concentration.

4.7.4 Vertical exchange coefficients

The vertical exchange parameters determine how quickly the incoming sediment can settle, or counterwise, how quickly sediment can erode. It is quite logic that this parameter influences the system time-scales. The three vertical exchange coefficients (one for each element) are varied simultaneously, in contradiction to for example the diffusion coefficients. The larger the vertical exchange, the smaller the system time-scales, see appendix D5.

4.7.5 Equilibrium volumes

The equilibrium volumes of the elements are a measure for the size of the system when it is in equilibrium. Larger equilibrium volumes, implies a larger system. A larger system needs more time to adjust. This goes with larger system time-scales. This is shown from the sensitivity tests as well. Also it results that the three equilibrium volumes all have their impact on one time-scale, which is different for all elements. The equilibrium volume of the delta has the largest influence on the T3 (26 years), the equilibrium volume of the channel mainly influences the T2 (413 years) and the equilibrium volume of the flat has relatively the largest influence on the smallest time-scale (3 years), (see also table 4.3 and appendices D6 to D8). The mentioned relations between the equilibrium volume and the system time-scales are linear relations.

4.7.6 Areas of elements

The area does not seem to have a noticable influence on the system time-scales. This does not seem logical, as the areas are directly related to the volumes of the elements, which do have a significant influence. The reason for this is that it is not possible to vary these parameters independently as volume and area are directly related to each other. Concluding from the sensitivity analysis, no large error will be made by assuming a constant area (see appendices D9 to D11).

4.7.7 n-parameter

The larger the n-parameter, the smaller the time-scales are. This can be explained from the fact that the sediment transport (with constant prism) increases in the case of an increasing n-parameter. As a consequence, more sediment will be available. In the linear approximation of Asmita, the relation between the system time-scale and this parameter is inversely proportional, just as the equilibrium concentration in the outside world is (see appendix D12).

4.7.8 Conclusion Sensitivity analysis

The results, which are presented in appendices D1 to D12 are summarised in table 4.3. The extreme values of the system time-scales are presented, in the case of variation of *one* of the parameters between the ranges as indicated in table 4.3, with constant values for the other parameters.

	T1min	**T1max**	**T2min**	**T2max**	**T3min**	**T3max**
δ_{dc}	2.86	2.86	**325**	**600**	18	34
δ_{co}	2.86	2.86	**300**	**640**	19	32
δ_{fc}	1.8	5.5	412	413	26	25
c_E	2.4	4.8	**345**	**687**	21.5	43
w_s	2.87	5	413	443	26	58
V_{de}	2.87	2.87	406	419	20	32
V_{ce}	2.86	2.88	**335**	**490**	25.5	26
V_{fe}	2.2	4.2	411	415	26	26
A_d	2.87	2.87	412.7	412.7	25.2	26.5
A_c	2.86	2.88	412	413.5	25.7	25.8
A_f	2.85	2.91	412.7	412.7	25.7	25.7
n	1.4	2.85	**200**	**412**	13	25.7

Table 4.3: Results sensitivity analysis

central-values:
T1 = 2.86 year
T2 = 412.7 years
T3 = 25.7 years

The values in table 4.3 give the sensitivities of the variation in individual model parameters. These sensitivities are derived for the Marsdiep. Other inlets with other sizes of element, will yield different results. We can use the results from table 4.3 for the two purposes with respect to the calibration of Asmita as mentioned in the beginning of this section:

1. What is the effect of variation of the different input parameters
2. Which parameters have a relatively large influence on the morphological development of the elements, compared to other input parameters

ad 1) Table 4.3, and the corresponding relations in appendix D are useful to give more insight into the actual influence of the variation of the parameters for the calibration. Calibrating Asmita for different stages of the morphological development is related to the sensitivity of the parameters for the different system time-scales. If, for example the initial development requires a better fit, then we can derive that it is useful to vary the vertical exchange coefficient as this parameter especially influences the smaller time-scales T1 and T3. The relations in appendix D indicate the effect of increasing or decreasing parameters. The number of calibration parameters is limited by the amount of available data. In the case of a large data-set, it is possible to use more parameters in the calibration, then in the case of a small data-set. Hence, the specified results are especially useful in the case of a large data-set compared to the number of input parameters.

ad 2) However, in the case of sparse data set, only few parameters can be varied in the calibration. Then we have to decide which parameters have the relative largest influence on the morphological development. This means that we consider the sensitivity of the largest time-scale, which determines the overall morphological development. This system time-scale is sensitive for the coefficients expressing the exchange between channel and delta, and between the delta and the outside world, the equilibrium concentration, the n-parameter and the equilibrium volume of the channel. It is be recommended to fix the n-parameter and to assume that the adapted sediment transport formula gives an appropriate description of reality. Then, the morphological system time-scales and hence development are sensitive for equilibrium volumes, diffusion coefficients and equilibrium concentration. These parameters should be used in the calibration, or require further investigation into the possible values.

4.8 Conclusion use of linear approximation

In this chapter the Asmita equations were linearised to obtain more insight into morphological interaction and time-scales, in order to come to a proper calibration of Asmita for the closure of the Zuiderzee. First we analysed the linearised equations to enlarge the theoretical understanding of the morphological behaviour of tidal inlets. Besides, we analysed the use of the linearisation for the calibration of Asmita. With respect to these investigations, the following conclusions are drawn:

- From the linear approximation we concluded that the morphological development of the elements of a tidal inlet can be described by a combination of system time-scales, which depend on geometric parameters and the exchange coefficients of the system.

- The linear approximation is not appropriate to be used as replacement of the original formulation of Asmita, because of the limited validity and the fact that 15 parameters without a direct physical meaning, need to be estimated. From analysis of the validity of the linearised equations, we concluded that for rough quantitative estimates and for qualitative analysis of morphological behaviour, the linearised equations are appropriate.

- The linear approximation gives a simple analytical expression for the time-scale of an element. Furthermore, we concluded that factors like absolute disturbance, relative disturbance and the proximity of the outside world influence the interaction and time-scales of the elements.

- The linearised equations turned out to be useful to predict the characteristic behaviour of the elements, given a certain combination of disturbances imposed on a system. In particular, it can be demonstrated that in some situations an element does not evolve monotonously towards its equilibrium state, but first overshoots its equilibrium or initially moves away.

- Using the linearised equations, it may be possible to derive system time-scales from observations on the condition that:
  1) the period of interest is such that all time-scales can be recognised
  2) the number of data points is large compared to the number of degrees of freedom.

- From a sensitivity analysis applied to the Marsdiep inlet, we conclude that a variation in equilibrium volumes, diffusion coefficients and equilibrium concentration has the largest influence on the overall morphological development as formulated in Asmita. These parameters should be used in the calibration, or require further investigation into the possible values. Furthermore, a sensitivity analysis provides the opportunity to obtain more insight into the specific influence of the different input parameters on different time-spans (related to the different system time-scales). This is especially useful in the case of calibration on an extensive data-set, compared to the number of input parameters.

5 Analysing data regarding closure Zuiderzee

5.1 Introduction

The aim of the present study is to calibrate Asmita to the morphological development of the Wadden inlets since the closure of the Zuiderzee and to obtain more insight into the morphological behaviour of tidal inlets.

Directly related to this objective, we have two reasons to analyse the data regarding the closure of the Zuiderzee:

1. Enlarging the insight into large-scale morphological processes of tidal inlets. Due to the closure of the Zuiderzee, the tidal basin transformed from a large basin (compared to the tidal wave) into a small basin. This will affect the character of the tide, and hence the morphological development.
2. Obtaining volumetric information for the calibration of Asmita:
    - Volumetric data of the inlets which were affected by the closure (1933-1998)
    - Instantaneous change in tidal volume due to the closure (in order to predict equilibrium situations of the elements, based on equilibrium relations (section 3.4))

To achieve these two goals, we have the following data at our disposal:

- Measurements and calculations of the tidal pattern before and after closure, by the Staatscommissie Zuiderzee (1926)
- Digitised maps of bed topography from 1925 to 1998, based on measurements by the Adviesdienst Hoorn and complementing JARKUS measurements after 1962.
- Volumetric data, from Eysink and Biegel (1992) for the inlets of the western Wadden Sea from 1925 to 1985.

We have seen in the chapters 2 and 3 that the tidal volume is the main forcing behind the morphological development of tidal inlets. Therefore, we will first discuss the changes in tidal pattern and the related changes in tidal volume (section 5.2). Then, we will consider the available digitised maps to analyse the large-scale changes in bathymetry (section 5.3). Subsequently, we will obtain volumetric data, based on studies by Eysink and Biegel (1992), which we can use for calibration purposes. For recent years, some additional volumes will be computed (section 5.4). The trends in the volumetric data will be analysed and checked for consistency (section 5.5). Finally an error analysis will be elaborated for the total calibration process, to make an inventory of the errors introduced from both the data-point of view and the model point of view (section 5.6).

It is of great importance to keep in mind that we are considering the long-term or macro-scale (see chapter 1). This means that the morphological elements delta, channel and flats are analysed and not every small shoal or gully. In the same way the tide will be analysed: the change of pattern is of interest and not the local changes. Furthermore we are interested in the period since the closure till an equilibrium state is reached. This means that we consider a period of at least 70 years.

5.2 Changes tidal volume

5.2.1 Introduction

In the previous chapters, we discussed that the morphological development is directly related to the tidal volume of a tidal inlet. Equilibrium relations were derived from field data (section 3.4), which describe the relation between the volume of elements and the tidal volume. So, to obtain more insight into the (expected) morphological development of the tidal inlets due to the closure of the Zuiderzee, it is essential to obtain more information on the changes in tidal volume.

Due to the closure of the Zuiderzee, the character of the basins behind the western Wadden islands has changed considerably. Before the closure, the length of the basin was in the same order as the tidal wave length, so that the water level along the basin could vary considerably. After the closure, only a small ($L_{basin} << L_{tide}$) basin remained where the water level along the basin hardly changes. As a consequence, the tidal motion in the basin changed.

In the previous chapters we used the term tidal prism (volume in the basin between MHW and MLW at high water) to quantify the amount of water which enters the inlet during a tidal period. This prism is directly proportional to the tidal volume only for basins which are small compared to the tidal wave length and that does not apply for a large basin like the Zuiderzee basin before closure. Then the water slice between MHW and MLW does not equal the amount of water which enters the inlet during a tidal period, because of the spatial water level variation within the basin. Therefore, we will use the term tidal volume instead of tidal prism, to define the quantity of water which enters the inlet during one tidal period.

This tidal volume depends on the tidal range and the size of the basin. These factors will be analysed for the conditions before and after closure by relating the available tidal data to a simple theoretical consideration. In this respect we will also discuss the investigations of the Staatscommissie Zuiderzee (1926).

5.2.2 Theory tidal wave

We consider a tidal wave in a long straight prismatic channel. For a simple description of the water levels and related currents, two equations can be used; the mass-balance and the equation of motion (see amongst others Battjes (1996)). If we assume that friction and advection are small compared to inertia, and the tidal amplitude is small compared to the water depth, then reads for the mass-balance:

$$\frac{\partial \eta}{\partial t} + \frac{\partial q}{\partial x} = 0 \qquad (5.1)$$

and for the equation of motion:

$$\frac{\partial q}{\partial t} = -gh\frac{\partial \eta}{\partial x} \tag{5.2}$$

where
q = discharge per unit width of channel (m2/s)
η = surface level elevation (m)
h = average water depth (m)

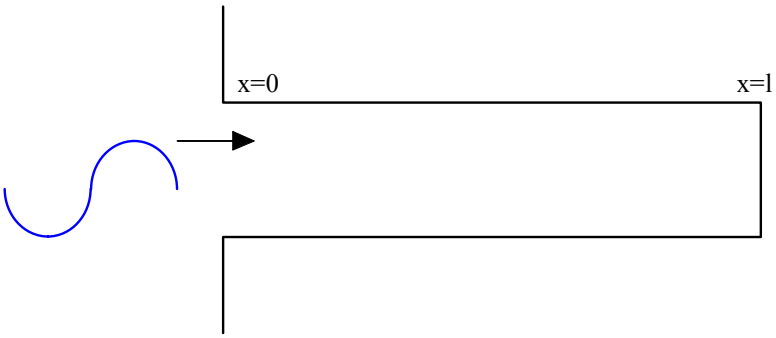

Figure 5-1 Channel with open and closed boundary

Subsequently, a tidal wave in a channel with an open boundary and a closed boundary is considered (figure 5.1). We are interested in the changes of the water level η and related discharge *q* along the channel as function of time. In order to derive an expression for these two variables, we need two boundary conditions. At the sea side (open boundary), the water level variation at sea, and the second (at the closed boundary) comprises the discharge at the closed boundary which equals zero, hence:

open boundary (x=0): $\eta(0,t) = a \cdot \sin \omega t$ (5.3)

closed boundary (x=l): $q(l,t) = 0$ (5.4)

with these two conditions we can solve equation 5.1 and 5.2:

$$\eta(x,t) = a \cdot \frac{\cos k(l-x)}{\cos kl} \cdot \sin \omega t \tag{5.5}$$

where
ω = angular frequency tidal wave (=2π/T) (rad/s)
k = ω/c= phase difference per unit length measured in the direction of propagation of the tidal wave (rad/m)
a = amplitude tidal wave (m)
l = length channel (m

substituting this equation into (5.1) results in:

$$q(x,t) = \frac{a\omega \sin k(l-x)}{k \cos kl} \cos \omega t \qquad (5.6)$$

In equation 5.5 the formulation of a standing wave can be recognised. At an arbitrary position in the basin x, the water level fluctuates with a sinusoidal pattern, and the corresponding amplitude depends on the position x, according to:

$$A(x) = \frac{a}{\cos kl} \cdot \cos k(l-x) \qquad (5.7)$$

This means that nodes (minima) in water level occur in the channel where cos k(l-x) equals zero, and anti-nodes (maxima) occur where |cosk(l-x)| equals one. From equation 5.6 it can be derived that at nodes in water level the discharge is at its maximum, while at the position of anti-nodes in water level the discharge equals zero (as holds at the closed boundary). The phases between two successive nodes in water level are the same, and are opposite to the phases adjacent to these nodes. This means, as illustrated in figure 5.2, that the change in water level is realised by a periodic exchange of water. Transport of water takes place only between two successive nodes in discharge, and hence two anti-nodes in water level. This means that in the case of a basin with a length of half the tidal wave length, all exchange of water will take place within the basin (without friction!).

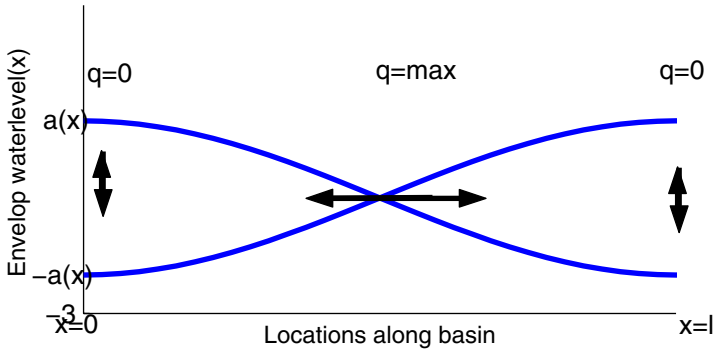

Figure 5-2 Envelop standing wave pattern and exchange of water in a channel

The standing wave pattern actually is a sum of two oppositely propagating waves: the incoming tidal wave and the seaward propagating wave, which has been reflected at the closed boundary.

So far, the friction has been neglected. If we take into account friction, the equation of motion becomes:

$$\frac{\partial q}{\partial t} = -gh\frac{\partial \eta}{\partial x} - fq \qquad (5.8)$$

where:
f = friction coefficient

If the two variables h en q are solved, based on equations (5.1) and (5.8), a damping term is introduced in expressions for the water level variation and discharge. Due to the friction the tidal wave looses energy and the amplitude slowly decreases as the wave enters the channel. Also the reflected wave is subjected to friction. This means that from sea (open boundary) towards the closed boundary the tidal amplitude decreases and the corresponding phase slackens. As a consequence, anti-nodes in the water level do not coincide with nodes in the discharge, as was illustrated in figure 5.2. The tidal wave has the character of a propagating tidal wave near the open boundary, and a standing character near the closed boundary.

In this section we have discussed the basis of the theory of a tidal wave in a channel. In the subsequent section, we will link this theory to field data on the closure of the Zuiderzee.

5.2.3 Tidal wave before and after the closure of the Zuiderzee

Investigations by Staatscommissie Zuiderzee

The Staatscommissie Zuiderzee was given the assignment in 1918 to investigate the consequences of a closure of the Zuiderzee with respect to expected water levels and wave-run up during storms (see Staatscommissie Zuiderzee, 1926). To achieve this, it was necessary to analyse the tidal changes as well. At that time, no mathematical methods existed yet to describe the tidal motion in shallow basins. The only way to describe this phenomenon was based on observations. Yet, in order to make predictions of the tide which would be present after closure, mathematical descriptions were necessary. The chairman of the Staatscommissie Zuiderzee, Lorentz, developed a useful calculation method. He developed the now-known equation of motion with linearised friction, as discussed in the previous section and used this equation together with a mass-balance to compute the water levels and depth-averaged currents.

The Zuiderzee area was schematised in a network of prismatic channels. The tide at sea was schematised to one main component, M_2, which functioned as the boundary condition. Then, for several locations in the Zuiderzee, it became possible to calculate the water level variation and corresponding currents with the above mentioned method. This method required a substantial amount of calculations, without the use of any computer! To validate the method, measurements were carried out in the Zuiderzee area around 1920. Using the harmonic method, the M_2 component could be derived from the observations. With the developed mathematical method, it turned out to be possible to reproduce the tidal motion, which was present before closure. Hence, this method was assumed to be suitable to predict the tide in the Wadden Sea area after closure.

Based on the computations, the Staatscommissie Zuiderzee assessed two alternative locations for the position of the Afsluitdijk (the name of the closure dam). They already predicted the increase in tidal range and currents for all alternatives, but they assessed which alternative would minimise the changes in tide and currents. The Afsluitdijk was situated near a former anti-node in the water level to minimise the consequences (a new anti-node at the spot of a former anti-node). In the previous section we concluded that due to friction, an

anti-node in water level does not coincide with a node in discharge. This implies that changes in tide, and consequently in morphology are inevitable. Hereafter, we will describe the tide before and after closure, based on the measurements of the Staatscommissie Zuiderzee and previously discussed theory.

Tidal wave before closure

The Zuiderzee before closure in 1932, formed one comparatively large tidal basin that was connected to the North Sea via the Marsdiep and Vlie inlets (see also appendix E1). In order to schematise the overall (change in) tidal pattern, we have schematised the Zuiderzee and corresponding Wadden area in one straight prismatic channel with a length of approximately 130 kilometres from sea to Nijkerk. In the northern part of this channel, roughly between the inlets and the island of Urk, the average depth amounts to approximately 3.5 m. In the southern part, between Urk and Nijkerk, an average depth of approximately 2 m is attained in the schematisation. The length of the tidal wave in the Zuiderzee area is related to the averaged depth in the area:

$$L_{tide} = c \cdot T_{tide} \tag{5.9}$$

with

$$c_p = \sqrt{g \cdot h} \tag{5.10}$$

where
L_{tide}= tidal wave length (m)
c_p = propagation velocity tidal wave (m/s)
T_{tide}= tidal wave period (s) (12h25min = 44700 s)
g = gravitational acceleration (9.81m/s^2)
h = average depth (m)

This means that the average tidal wave length in the Zuiderzee area approximates 200 to 260 km, and hence that the length of the basin approximates half the tidal wave length. We concluded that due to the friction the observed wave pattern can be described only partly by a standing wave. However, the observed envelop of the wave pattern before closure can roughly be schematised as follows:

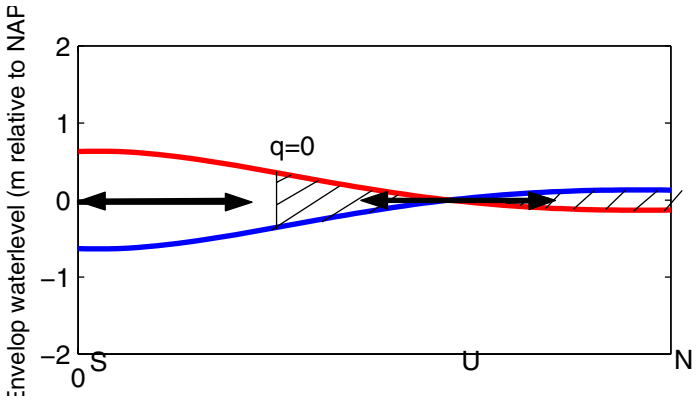

S= Sea
U=Urk
N= Nijkerk

Figure 5-3 Schematised envelop tidal wave before closure

These results were obtained from measurements and calculations of the Staatscommissie. Only the damped water level variation is shown in this figure and not the phase differences.

In the theory, we have seen that the exchange with sea takes place in the area from the gorge of the inlet till the location where the first node in discharge occurs. The anti-node in water level was situated near the present Afsluitdijk, (due to the dominating friction this is not visible from figure 5.3) but the node in discharge was probably situated somewhere between the present Afsluitdijk and the former Urk. This means that most part of the former Zuiderzee did not take part in the exchange with sea. Water level changes in the back part of the basin were realised by exchange of water within the back part of the Zuiderzee. This is an important aspect when considering the change in tidal volume.

Tidal wave after closure

By constructing the Afsluitdijk, the size of the basin was reduced with approximately 3700 km^2. After the construction of the closure dam, the length of the tidal basin from sea to the Afsluitdijk was reduced to approximately 25 kilometres. This means that the remaining basin is small compared to the tidal wave length, (this effect is strengthened by the fact that the average depth and hence, the tidal wave length increased somewhat).

Due to the construction of the Afsluitdijk, the tidal wave is already reflected at the dam. Both the incoming and reflected wave are less subjected to friction and keep more energy, compared to the situation before closure. As a consequence, the generated tidal ranges increased in the Wadden Sea area. While, the tidal range decreased from sea towards Nijkerk before closure, the tidal range now increases towards the Afsluitdijk. Based on the calculations of the Staatscommissie Zuiderzee (table 5.1), the more or less standing wave after closure can be schematised as:

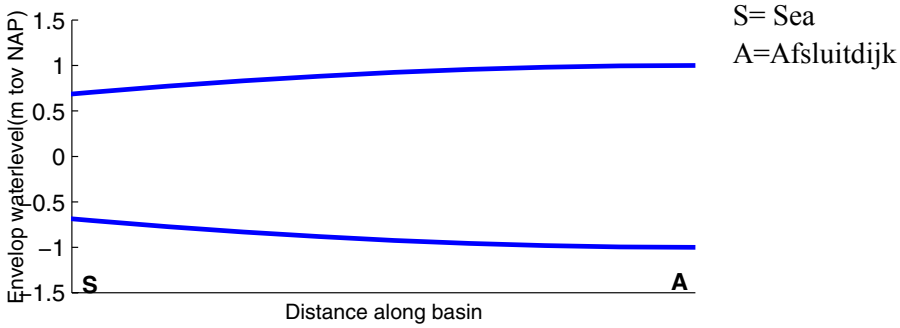

Figure 5-4 Schematisation envelop tidal wave after closure

In table 5.1 the tidal ranges before and after closure are presented derived from the investigations of the Staatscommissie. The tidal ranges before closure have been measured and validated with computations and the tidal ranges after closure are based on computations only. The locations are successive according to the propagation of the tidal wave from sea towards Nijkerk (see appendix E1).

Location (province)	Tidal range		
	before closure (cm)	after closure (cm)	increase (%)
Den Helder (NH)	106	128	21
Oudeschild (Texel, NH)	86	136	58
Den Oever (NH)	74	146	97
Kornwerderzand (Friesland)	84	156	86
Harlingen (Friesland)	114	158	38
Vlie (gorge inlet)	142	162	14
Stavoren (Friesland)	42	-	
Enkhuizen (NH)	24	-	
Urk (Zuiderzee)	14	-	
Nijkerk (Gelderland)	28	-	

Table 5.1: Tidal range before and after closure (Staatscommissie Zuiderzee, 1926)

5.2.4 Change in tidal volume

So far, we analysed the change in tidal pattern due to the closure. Subsequently, we are interested in the change in tidal volume. The tidal volume is a combination of the tidal range and the related storage area of the basin. With respect to the storage area, we have seen in the previous section that before closure a significant part of the Zuiderzee did not take part in the exchange with sea. Hence, the actual reduction in tidal basin area is much smaller than we would expect considering the area of the former Zuiderzee. The tidal range increased compared with the situation before closure. The summed effect of the changes in tidal range and storage area on the tidal volume is calculated, based on the computations of the Staatscommissie.

The Staatscommissie calculated the amplitudes of the discharge in the throat of the inlet, before and after closure, based on equation 5.8. From these amplitudes we can calculate the tidal volume, by integrating the sinusoidal tidal discharge over an ebb or flood period (in the case of a sinusoidal tidal wave it holds: tidal volume=ebb volume=flood volume). This yields:

$$V_g = \frac{2 \cdot Q}{\omega} \tag{5.11}$$

where

V_g = tidal volume (m3)

Q = amplitude M_2 discharge through inlet gorge (m3/s)

ω = angular frequency of tide ($=2\pi/T= 1.4*10^{-4}$ rad/s)

This results in the following tidal volumes before and after closure:

Inlet	Before closure		After closure		Increase
	Amplitude M_2 (*1000 m^3/s)	Tidal volume (*10^6 m^3)	Amplitude M_2 (*1000 m^3/s)	Tidal volume (*10^6 m^3)	(%)
Marsdiep	50	712	64	907	26
Eierl.gat	8.7	124	9.4	134	8
Vlie	53	757	60	857	13
Borndiep	17	243	18	257	6

Table 5.2: Change in tidal volume (values Amplitudes from Staatscommissie Zuiderzee,1926)

Table 5.2 points out that for all inlets an increase in tidal volume occurred. Especially the tidal volume in the throat of the Marsdiep and the Vlie inlets increased. The effect of the closure on the tidal volume in Eierlandse gat and Borndiep is less significant.

Furthermore, in the years after the closure the tidal volume increased some more. This is confirmed by recent measurements in the gorge of the Marsdiep carried out by NIOZ (Ridderinkhof, 2000). Based on these measurements a harmonic analysis was carried out as well. This investigation shows that the amplitude of discharge of the M_2 component has increased to 68.6*10^3 m^3/s in 1998, which implies a tidal volume of 980 million m^3. The reason for the fact that the tidal volume increased over the past 66 years is probably due to the rising sea level. The rising sea level increases the storage area somewhat and decreases the bottom friction, which increases the tidal range and hence the tidal volume. This holds for basins where the throat of the inlet is large enough for significant tidal intrusion into the basin.

5.2.5 Conclusion tide analysis

The tidal volume in all four western Wadden inlets increased due to the closure of the Zuiderzee, though significant changes occurred only in the Vlie and Marsdiep inlets. The character of the tidal wave along the basin changed from a more propagating character in the former Zuiderzee, into a more standing character after closure. While before closure the tidal range decreased from sea towards the closed boundary, the tidal range after closure increased from sea towards the Afsluitdijk. The change from a relatively large into a small basin makes the closure totally different than the closure of part of a smaller basin like the Lauwerszee, where the character of the tidal wave remained the same after the closure.

The increase of the tidal volume will effect the morphological development of the inlets. The resulting large-scale changes in bathymetry are analysed in the subsequent section, based on the digitised maps of bed topography.

5.3 Analysis of maps of bed topography 1933-1998

5.3.1 Introduction

In this section we analyse the available digitised maps of the western Wadden Sea. They concern the period between the closure of the Zuiderzee and 1998. The analysis aims at obtaining insight into the large-scale morphological effects of the closure. This means that large-scale bathymetric changes (changes in depth) are considered of the four western Wadden inlets (see figure 1.1). Inlets where significant changes occurred are the most useful for the calibration of Asmita.

5.3.2 Available digitised maps

For a better understanding of the changed situation of the inlets since the closure, the available digitised maps are analysed of the inlets of the Western Wadden Sea (provided by RIKZ). These maps are based on field campaigns that have been carried out by the Adviesdienst Hoorn and the Dienst Hydrografie since 1933, complemented by JARKUS measurements (Jaarlijkse Kust metingen) that have been carried out since 1962. (For a more detailed description of the measurements, see Rakhorst, (2000)).

The digitised maps consist of a grid, where, based on the available measurements, the average depth per grid-cell is determined. The accuracy of the measurements (determining x-, y- and z-co-ordinates) increased during the years, due to the more advanced observation techniques. Related to this accuracy, the grid dimension of the maps have been chosen. For the maps till 1985 a grid was set up (by the Adviesdienst Hoorn) consisting of cells of 250 by 250 metres. For each cell the average depth was determined. Cell values are based on at least 20 observations. Regarding the digitised maps after 1985, a finer grid is applied, where depth measurements are gathered in grid-cells of 20 by 20 metres. All measurements are relative to NAP.

For the presentation of the digitised maps, we used the graphic presentation program Arc View. In appendices E3 and E4 the maps are presented and the difference in grid size is clearly visible. We are particularly interested in the changes in elements which are distinguished in Asmita, namely delta, channel and flats. The latter two are defined relative to mean low water. Therefore, the legend is chosen in such way that the area above MLW is indicated in yellow (flats), and the area below MLW is indicated in blue (channel). Mean low water is estimated at NAP -1 m for the entire considered area.

In the subsequent section the digitised maps are analysed and the observed large-scale morphological changes in the elements are described. In appendix E2 an overview is given of the different channels of the Wadden Sea, which are used in the following description.

5.3.3 Bathymetric changes in Marsdiep and Vlie inlets

Bathymetric changes in Marsdiep and Vlie basins

The Marsdiep basin is part of the inlet between Texel and the mainland of Noord-Holland, while the Vlie basin is part of the inlet that is situated between Vlieland and Terschelling, see also figure 1.1. Names of the channels are presented in appendix E2.

Before closure the propagation of the flood currents was mainly directed towards the south. There were three main channels connected with the Zuiderzee: the Amsteldiep (part of Marsdiep inlet), the Vlieter (part of Marsdiep inlet) and the Middelgronden (part of Vlie inlet). Hardly any exchange took place through the 'short-cut' channels Scheurrak and the Doove Balg.

After the closure the three main channels were cut off and lost their function. The currents in these channels decellerated and sediment was able to settle down. This can be seen on the maps: from the map of 1933 these three channels can still be recognised, but after 1950, considerable sedimentation has occurred in these channels nearby the present Afsluitdijk (appendix E3). After the closure, the water entering the Marsdiep inlet is diverted via the Doove Balg. In this channel the currents increased considerably. As a consequence, the Doove Balg channel has eroded. When we compare the maps of 1933 and 1998, this change in significance of the Doove Balg can be seen. It looks as if the Doove Balg and the parallel situated Boontjes, which are part of the Marsdiep basin, extended towards the Vlie basin. This means that the Marsdiep basin increased at the cost of the Vlie basin. This is visible, if we consider the maps in figure 5.5 and 5.6:

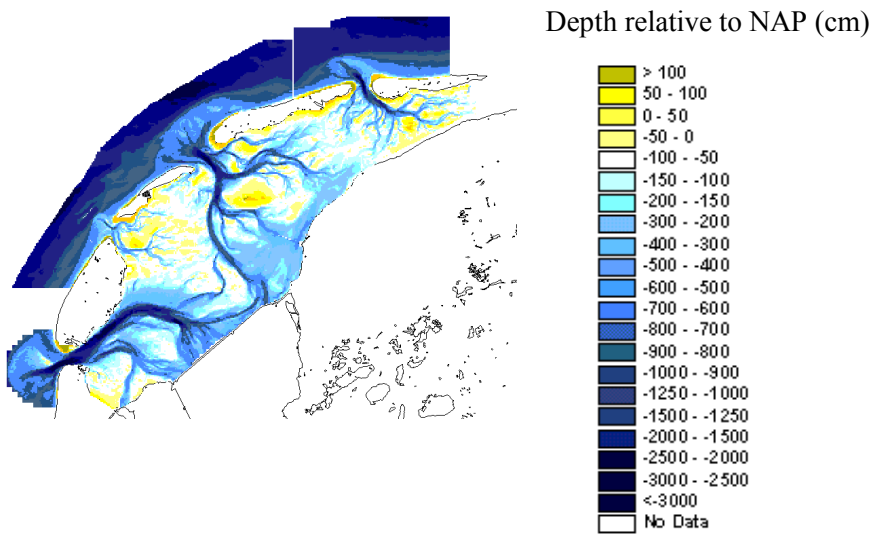

Figure 5-5 Map bed topography 1933 (see appendix E3)

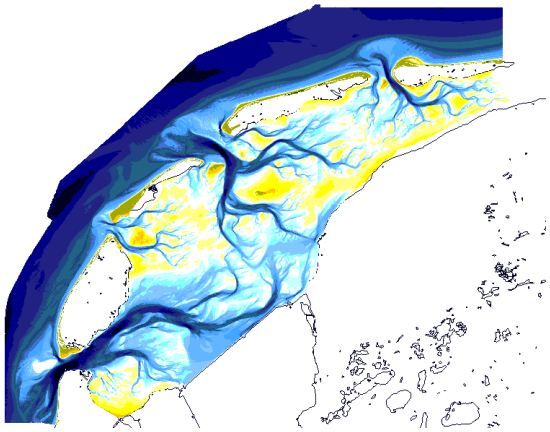

Figure 5-6 Map bed topography 1998 (see appendix E3)

The situation particularly changed near the former watershed between the Vlie and the Marsdiep basins. This watershed is totally different from the common ones. Normally a watershed occurs where two flood currents meet behind a barrier island and the oppositely directed flood currents are compensated. At the watershed, the currents decelerate considerably and sediment settles (see section 2.3.2). Therefore, watersheds can be recognised easily from bathymetric maps as these areas are the most shallow parts that separate two basin areas.

Between the Vlie and the Marsdiep basins the watershed has never been well-developed, which means that channels cross the intertidal area. Before closure the currents from the Zuidoostrak and the Doove Balg joined and entered the Zuiderzee, and hence, the development of a clear watershed was not possible (figure 5.5). After the closure, the situation changed: the direction and the magnitude of the currents in the area between the Vlie and Marsdiep basin decreased as the flood currents from these two basins partly compensated one another. As a consequence, sediment was able to settle in this area. This becomes clear from the maps: the area between the Vlie and Marsdiep basin has become shallower. Possibly, this area will become shallower in the future. However, there are different factors which could prevent the development of well-developed watershed:

- Under dominating western wind directions, a large fetch in the Marsdiep basin could cause drift currents which can prevent sediment from settling.
- The currents entering the Vlie and Marsdiep basin are not able to compensate each other completely as they are directed perpendicular instead of opposite.
- Circulation currents are present between the Zuidoostrak, the Doove Balg and Scheurrak, which could prevent sediment from settling.

As a consequence of the underdeveloped watershed between the Vlie and Marsdiep basins, transport of water takes place over the semi-boundary of the basins. This means that part of the water that enters the Marsdiep basin, leaves the Wadden Sea via the Vlie gorge, and vice versa. This leads to complex current patterns, and as a consequence to a complex morphological behaviour.

Finally, the area close to the Frisian Coast, which belongs to the Vlie basin decreased in depth. Since the closure, this area slowly developed into an intertidal area.

Bathymetric changes in Marsdiep and Vlie deltas

If we consider the ebb-tidal deltas of the Vlie and Marsdiep inlets (see appendix E4), two changes can be identified for both inlets. These comprise the changed orientation of the main ebb-channel and the regression of the ebb-tidal delta.

First we will consider the changed orientation of the ebb-tidal delta. Before closure and directly after closure, the main ebb-channel of both deltas had a more or less central position in the deltas. Since the closure, the main ebb-channel moved in south-westerly direction. An explanation for this is probably the changed interaction between the tidal currents along the coast and through the inlet as explained in section 2.4.1. Before closure, a phase difference between these two currents was present. As a consequence, the geometry of the delta was more similar to the geometry of the inlets of the south-west of the Netherlands. At present the basin is much smaller, which means the maximum ebb-flow out of the inlet coincides with the maximum (southward) ebb-flow along the shore. As a consequence the ebb-channel more tends to the south (see also figure 2.8 and 2.9). The Arrows illustrate extension in 1933 (red) and 1998(yellow).

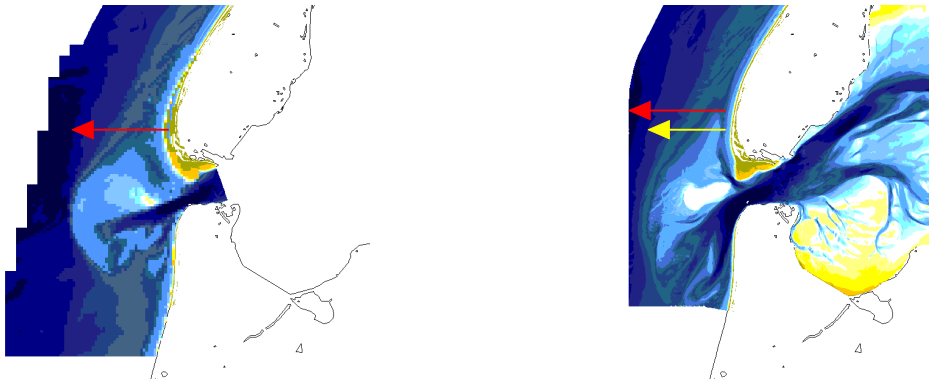

Figure 5-7 Retreat of Texel delta, 1933 (left) and 1998 (right).

A second aspect we can derive from the maps is that the ebb-tidal deltas retreated somewhat. This might be due to:

- Retreat of the coastal profile.

The coast adjacent to the delta is subjected to erosion, among others due to the sea level rise and the demand of the tidal inlet. This could cause the delta to retreat.

- Decrease of the delta

It could be that the actual size of the delta also decreases in order to deliver sand to the tidal basin.

Which of these factors dominates cannot be concluded from the bathymetric maps. This will be a point of attention in the analysis of the volumes (section 5.5) and the analysis of the coastal regression in chapter 6.

5.3.4 Bathymetric changes in Eierlandse gat and Borndiep inlets

The Eierlandse gat is a relatively small inlet situated between Texel and Vlieland. The Borndiep inlet is situated between Terschelling and Ameland and is also called the Amerlander zeegat. (see also figure 1.1).

In contradiction to the Marsdiep and Vlie inlets, these inlets were not connected directly (by channels) to the former Zuiderzee before the closure. Furthermore, due to the well-developed watersheds between these inlets and the Vlie and Marsdiep basins, the Eierlandse gat and Borndiep were not significantly affected by the changes in the Vlie and Marsdiep inlets. As a consequence, the large-scale effect of the closure on the bathymetry is hardly observable in these inlets.

5.3.5 Conclusion map analysis

Summarising, it can be stated that since the closure the channel pattern changed, particularly in the Vlie and the Marsdiep inlets. Channels, which were connected to the former Zuiderzee lost their function and as a consequence accretion occurred near the Afsluitdijk. Other channels, like the Doove Balg needed to increase in width, which is accomplished by erosion. The watershed area between the Vlie and Marsdiep basins has become more shallow. A well-developed watershed like the one behind Terschelling, or surrounding the Eierlandse gat will probably not develop, because of the perpendicularly orientation of the channels, and due to the drift currents under western wind directions. The deltas of Marsdiep and Vlie inlets, retreated a little towards the coast after the closure. It is not clear from the maps, whether the delta decreased or the coastal erosion dominates. This will be analysed in the next chapter. Furthermore, the main ebb-channel moved in south-westerly direction. This is probably the result of the changed interaction between the long-shore tidal currents and the tidal currents through the inlet.

Regarding the Eierlandse gat and Borndiep inlets, hardly any large-scale morphological changes could be observed from the maps.

5.4 Obtaining volumetric data of elements for calibration

5.4.1 Introduction

In the previous section, the large-scale changes in the bathymetry of the inlets of the western Wadden Sea were analysed and insight into the related processes was obtained. For the calibration of Asmita we are especially interested in volumetric and area data of those elements (flat, channel and delta) where significant changes occurred.

Based on the analysis of the tide and bathymetry, we can conclude that the changes in tidal volume and the large-scale changes in bathymetry are relatively small in the Eierlandse gat and Borndiep inlets. Most of the change occurred in the Marsdiep and the Vlie inlets, which were directly connected with the former Zuiderzee. Therefore the Marsdiep and the Vlie inlet will be used for further calibration purposes.

Biegel (Eysink and Biegel, 1992) carried out an extensive investigation in the inlets of the Western Wadden Sea and computed characteristics of the elements, e.g. volumes, areas. For this they used the digitised maps, which were discussed in the previous section. Digitised maps from 1933 to 1985 were available at that moment.

We will discuss the data of Biegel that we will use for the calibration and will extend this data set with volumes of recent years.

5.4.2 Volumetric data computed by Biegel

Biegel (Eysink and Biegel (1992)) computed, based on the digitised maps of the Western Wadden Sea, integral volumes and areas (among other characteristics) of the channel, flat and delta with respect to the western Wadden inlets for the period 1933-1985.

Volumetric data of delta

Biegel computed the delta volumes according to the Walton and Adams method (1976) (see section 3.4.1). This means that the delta equals the net dry volume seaward compared to a reference coastal profile. As reference coastal profile, the coast adjacent to the deltas was used. This profile was determined to a height of NAP +1 m. For all volumetric calculations the adjacent coastal profile of 1972 is used as reference. For the Marsdiep also calculations were made with the coastal profile of 1925 as a reference (see appendix F1-F2).

Volumetric data of channel and flat

Biegel (1991-1993) divided the Wadden Sea into different basins. The seaward boundary is determined by the presence of a cross-section at which generally a discharge measurement has been done or which is located at the smallest distance between two islands. Boundaries between basins are digitised from maps or from computer display following the highest points between channels. In this way a morphological watershed is estimated. An example of these boundaries, as determined by Biegel, is illustrated in appendix E5.

The integral wet volumes between the watersheds, relative to MLW and relative to MHW, make it possible to calculate the volumes of the channel and flat, in the same way as the definition used in Asmita (see figure 3.1).

Biegel made computations for the volumes of the basins, with variable and invariable boundaries of the basin and with variable and invariable tide (MLW and MHW) as reference over the years (see appendix F3-F6). Subsequent, we will discuss the boundaries that will be used for calibration purposes.

1. Boundaries basin
From the maps it became clear that the watershed, and hence the size of the basins are changing in time. In the Asmita formulation, the sediment demand of the elements depends on the deviation from the equilibrium state. So, in order to assess the actual demand of the elements, the actual, time-varying, boundaries are considered.

A disadvantage, is that the sediment balance in Asmita may be disturbed. In the case of varying boundaries the volumetric data of the channel could show an increase, which is not the result of sediment transport. With respect to the calibration of Asmita to the closure of the Zuiderzee, the latter effect is being neglected. In this case, it is considered more important to analyse the actual magnitude of elements, as this is relevant for the insight into the interaction between elements.

2. Boundaries in water level
After the closure an instantaneous increase in tidal range occurred. After the closure till the present, the tidal range has increased somewhat as well, which implies a decreasing MLW level and an increasing MHW level. This is probably the result of the sea level rise and the corresponding decreasing effect of the bottom-friction. In the present study we neglect the morphological effect of the increasing tidal range and use the computations with invariable water levels. However, we do take into account the rising sea level itself. This means that the volumes of the flat and channel are corrected for the rising sea level. This will be elaborated in section 5.5.

Summarising, for further calibration purposes the computed data of Biegel (1993) is used regarding the Marsdiep, the Vlie inlets (see appendix F1, F2, F7.1 and F8.1). Regarding the basin data, calculations for actual (time-varying) boundaries and a time-invariant tide are chosen. The effect of sea level rise will be taken into account in interpreting the data.

5.4.3 Extension volumetric data-set

Volumetric data till 1985 have been computed by Biegel. There are opportunities to extend this data set, based on recent digitised maps and recent field investigations. This is desired in order to improve the accuracy of the calibration of Asmita.

Extension volumetric data delta

From studies by Marion (1999) and Mulder (1999) recent information could be derived on sedimentation and erosion of the deltas. Based on these data and the volumetric data of Biegel, we estimated the volumes of 1992 for the Vlie and in 1992 and 1998 for the Marsdiep delta (see appendix F1 and F2).

Extension volumetric data of channel and flat

Comparing the calculated basin-data of Biegel and the available digitised maps, volumes are lacking for 1965, 1992 and 1998. Hence, we determined the volumes of the flat and channel of the Marsdiep and Vlie inlets in the years 1965, 1992 and 1998. This will extend the data-set from 5 data points, to 8 points. The basin boundaries are determined in the same way as Biegel did (see previous section). The wet volumes were calculated relative to MLW and to MHW. As discussed in the previous section, a fixed tide is used as reference.

From these integral volumes, the tidal prisms and flat volumes could be determined according to the following equations (see also figure 4.3):

$$P = V_{mhw} - V_{mlw} \tag{5.12}$$

and

$$V_f = \left(A_{mhw} * H\right) - P \tag{5.13}$$

The additionally calculated volumes of the channel and flat, together with the volumetric data of Biegel, are presented in appendix F7.1 and F8.1.

5.5 Analysis volumetric data-set of the elements

5.5.1 Introduction

In the previous section we collected a volumetric data-set for channel, flat and delta of the Marsdiep and Vlie inlets. This data-set will be used for the calibration of Asmita. Prior to the calibration, we will analyse the trend in the volumes, shown by the data-sets, and check whether these comply with expectations that are based both on equilibrium relations and the observed trends in development in tide and bed topography as discussed in sections 5.2 and 5.3.

First we will apply a correction for the channel and flat regarding sea level rise. As discussed before, we want to filter the effect of the closure and therefore we will define the volumes of the channel and flat relative to the actual water level.

5.5.2 Adjustment channel and flat volume for sea level rise

It is assumed that at this moment, the system can keep up with the present sea level rise (see Van Goor(2001) and Eysink and Biegel (1992). This means that the bottom is rising at the same level as the sea level rise (17 cm/century). As long as we calculate the volumes relative to the actual water level, the elements do not change in volume as a result of the sea level rise.

Because we have a volumetric data-set relative to a fixed reference (MSL in 1925), we will apply a correction for the flats and the channel. This means that a reduction of the flat volume is applied and an increase of the channel volume. The yearly adjustment amounts to the element area times the sea level rise per year. The volumetric data of channel and flat relative to the actual water level is presented in appendix F7.2 and F8.2.

Regarding the delta element, the changes due to sea level rise are discussed in the subsequent chapter, as this concerns a different type of adjustment.

5.5.3 Trend in volumetric data of elements

In appendix E6 the volumetric data-points, including the adjustment of channel and flat for sea level rise for the Marsdiep and the Vlie are presented in graphs. In this section the observed trends will be discussed and explained.

Observed trend

The following trends in the data covering the period 1933 to 1998 can be observed:

- Marsdiep flat: the flat volume does not show a clear trend. This is because of the relative very small flat volume (1% of wet volume below MHW)
- Marsdiep channel: a decrease in the volumes below MLW occurred (5%)
- Marsdiep delta: the volume of the delta shows a decrease of 25% in the period between 1933 and 1981.
- Vlie flat: the flat volume increased (46%)
- Vlie channel: a decrease in the volume below MLW can be seen (11%)
- Vlie delta: the delta volume decreased with 15% after 1933 till 1981.

The increase in flat volume is consistent with the equilibrium relations, which also hold for large basins (see section 3.4). The reduction of basin causes an increase in flat volume. For the Vlie inlet, this increase is considerable. This is partly because of the further decrease in basin area after the closure. For the Marsdiep basin the computations are too inaccurate to show a clear trend.

Despite the increase in tidal volume, which occurred directly after closure (see section 5.2), the volumes of both the channels and the delta of the Marsdiep and Vlie inlets have decreased. This is in contradiction to the expectations, based on the equilibrium relation between the volumes of these elements and the tidal volume (see section 3.4). In the following section we will explain the reason for this behaviour, which at first appears contradictional.

Explanation trend in volumetric data of channel

In section 5.2 we concluded that in the case of a large basin, the term prism is not appropriate. As a consequence, the equilibrium relation between prism and volume (like equation 3.3) does not hold for Marsdiep and Vlie for the period prior to the closure. Therefore, in order to explain the decrease in channel volume, we will concentrate on the relation between cross-section of the channel and tidal volume, which does hold for both large and small basins. This relation yields:

$$A_{cross} = c_g \cdot V_g \qquad (5.14)$$

V_g = tidal volume (m3)
c_g = coefficient (m-1)
A_{cross} = cross-section channel (m2)

This relation illustrates that in the equilibrium situation, the cross-section of a channel in the basin is proportional to the tidal volume which passes this cross-section. Furthermore, the tidal volume and corresponding cross-section of the channel decreases from a maximum in the inlet (I) to zero, as shown in figure 5.8. For large basins, this boundary (C) is the location where the first (from sea) node in discharge occurs (see section 5.2) and for small basins, (C) is the closed boundary.

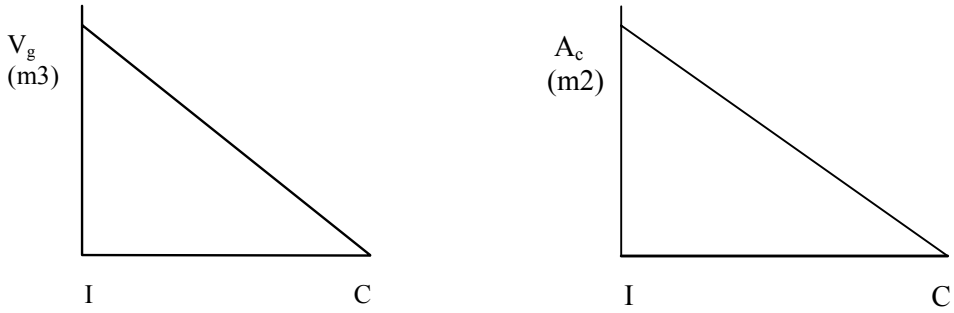

Figure 5-8 a) Tidal volume along channel, b) Cross-section channel along channel

I= Inlet throat
C= Closed boundary/ first node in discharge

The volume of the channel equals the cross-sectional area integrated over the length of the channel, hence the integrated surface in figure 5.8b indicates the volume of the channel. In other words, the change in tidal volume and related cross-section along the basin, indicates the change in channel volume which is expected in the case of the closure of the Zuiderzee.

We can schematise the tidal volume along the basin before and after closure roughly as follows :

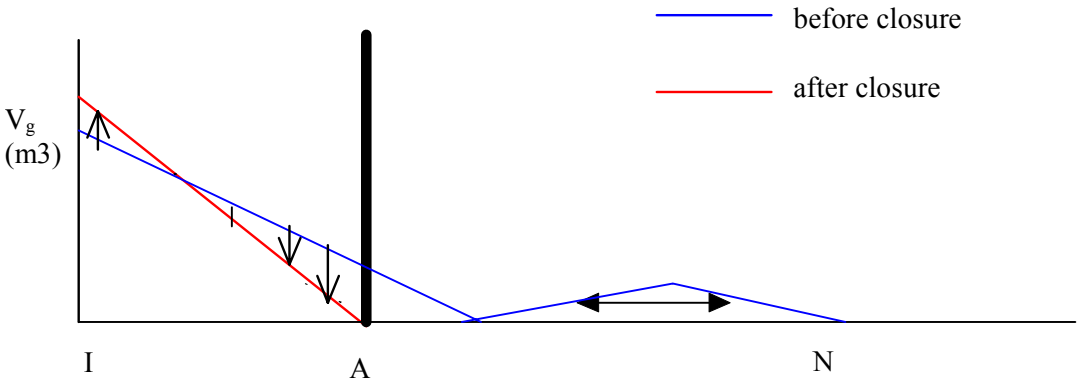

Figure 5-9 Change tidal volume/cross-section along basin length

I= Inlet throat
A= Afsluitdijk
N= Nijkerk

In this figure also the internal exchange within the back part of the basin is illustrated. The node in discharge, or the transition between this ‘internal’ exchange and the tidal volume from sea, is not as sharp as indicated in figure 5.9, but will probably show an overlap. This node occurred somewhere between Urk and the present Afsluitdijk.

By means of figure 5.9, it is possible to explain the fact that the tidal volume increased and the channel volume decreased. As a consequence of the closure, the tidal volume, which enters the inlet, increased. However, the tidal volume which passes the channels in the back has decreased. This is because the tidal volume decreases (to zero) towards the boundary. As a consequence, the related cross-section in the back of the basin is too large compared to its equilibrium and will hence accrete, while near the throat the cross-section of the channel is too small compared to its equilibrium and will erode (this is indicated with the arrows in figure 5.9). The accretion of the channels in the back was also derived from the maps of bed topography (section 5.3). The fact that the cross-section near the throat of the inlets increased is described by Gerritsen (1990).

So, part of the channel in the back accretes and part of the channel near the throat of the inlet erodes. Apparently, the sedimentation dominates the erosion, as the volumetric data of the channel show a decrease.

Explanation trend in volumetric data of delta

The tidal volume increased due to the closure and the delta volumes show a decrease. Based on the equilibrium relations we expect an increase of the delta. In section 5.3 we explained that two factors could cause this decrease: the coastal regression and the decrease of the delta itself. Hence, it could be that the delta itself is growing, but that this effect is dominated by the regression of the coast. Computing all volumes relative to the actual coastal profile (and not a fixed profile) would illustrate the net effect. This can be shown considering the two calculations of Biegel (1992). Biegel computed for the Marsdiep, the volumes relative to the coastal profile of 1925 and relative to that of 1972. From appendix E6.2, it becomes clear that the actual volume of the delta in 1972 shows a slight increase relative to the actual volume of 1925.

The National Institute for Coastal and Marine Management (RIKZ) is investigating the determination of the volumes of the Marsdiep delta relative to the actual (time-varying) coastal profile (march 2001) and therefore, recent data calculations are not available yet.

In the calibration of Asmita (see section 6.3), an adjustment will be made for the coastal regression, which influences the size of the delta according to the Walton and Adams (1976) definition.

5.5.4 Conclusion analysis of volumetric data-set

Summarised, the decreases of the channel and the delta of Vlie and Marsdiep can be explained as follows:

- Part of the channel in the back accretes and part of the channel near the throat of the inlet erodes. This is related to the changes in tidal volume (induced by the closure) that passes the channel along the basin. From the decreasing trend in the volumetric data, it becomes clear that the accretion dominates the erosion.
- The delta volumes of Vlie and Marsdiep show a decrease, this could be caused by neglecting coastal regression. This effect should also be taken into account in the calibration of Asmita and is investigated in the subsequent chapter.

5.6 Error analysis in the case of calibration of Asmita to data

5.6.1 Introduction

In the subsequent chapter, Asmita will be calibrated to the obtained set of volumetric data for the closure of the Zuiderzee. Both the use of data and the model may introduce errors, which affects the validity of the calibration. Therefore, a schematisation is made of the steps which are made during the total calibration process, which concerns data-analysis and modelling. Every step possibly introduces errors. These errors will mainly be assessed qualitatively and if possible also quantitatively. At the end of this chapter we will have gained insight into relevancy of the errors.

5.6.2 Overview errors

The following steps and related errors can be identified in the total calibration process for the closure of the Zuiderzee:

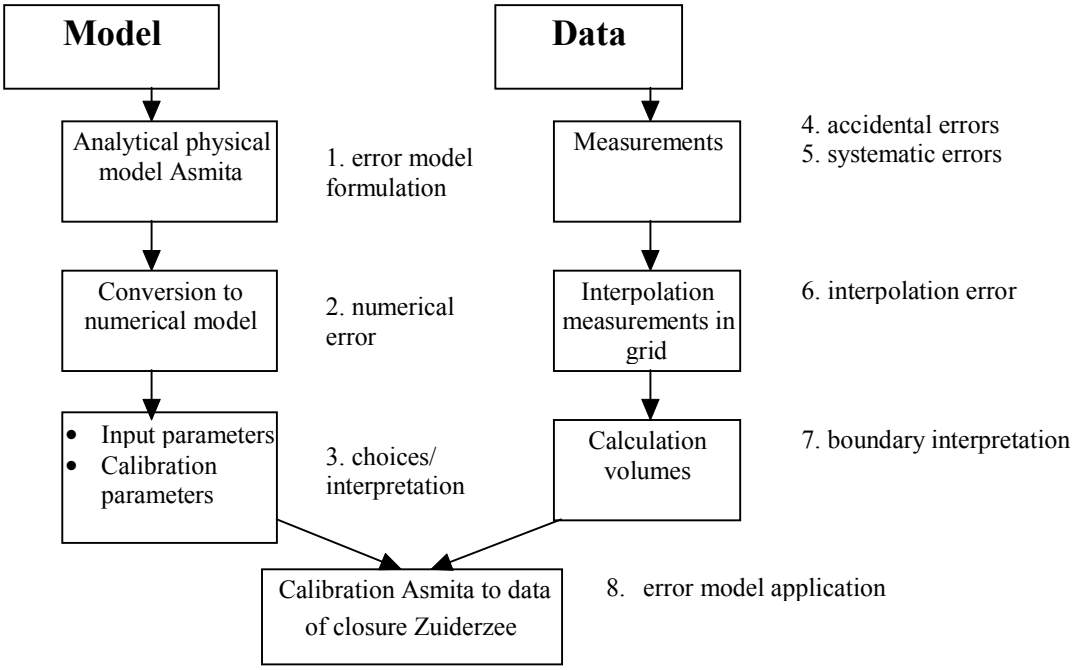

Figure 5-10 Overview total calibration process and related (numbered) errors

In the following paragraphs some specifications will be given on these errors. Then it will be discussed whether these errors are significant or not.

1. error model formulation

Asmita is a behaviour oriented model, based on the sediment exchange between morphological elements. This concept has proven to be a useful tool to describe the adaptation process of different elements towards equilibrium state in the case of the Friesche Zeegat (Buisman 1997). Therefore, this model is assumed to give a good, description of the

adaptation process in the case of an instantaneous interference like the closure of the Zuiderzee.

2. numerical error

In the case of a conversion of an analytical model into a numerical model, errors could arise both due to discretisation. In Asmita, only a discretisation in time is made. As long as we consider a small time-step compared to the period of interest, this error is not expected to be significant in the calibration process.

3. choices and interpretation input and calibration parameters

In the subsequent chapter an attempt is made to describe the morphological development of the elements of the Vlie and Marsdiep inlets with Asmita. For this, choices should be made to estimate input parameters. Some parameters will be assumed to be constant, while others will be varied during the calibration. The consequence is that the resulting calibration may be the most likely result, but not naturally the only or correct result.

4. random errors in measurements

A deviation in the depth measurements could occur as a consequence of inaccurate measurements. Especially the measurements in the period 1925-1940 are not so accurate as the facilities were not so advanced as at present. According to Rakhorst (draft, 2000) an occasional error of 25 cm could be made. Nowadays the random error is about 10 cm or less. If this deviation of 25 cm would be present over the entire area, a large deviation in volume would occur (namely 0.25 m*6.75*10^8 m^2=1.7*10^8 m3, order 10%). Yet, this error should be assessed as *maximum* and as *random* error.

We assume that this random error is normally distributed with zero mean and that the mentioned 25 centimetres corresponds to half the width of a 95% confidence interval. In that case the standard deviation σ_m of the random error in an individual depth measurement amounts to 12.75 cm (see figure 5.11).

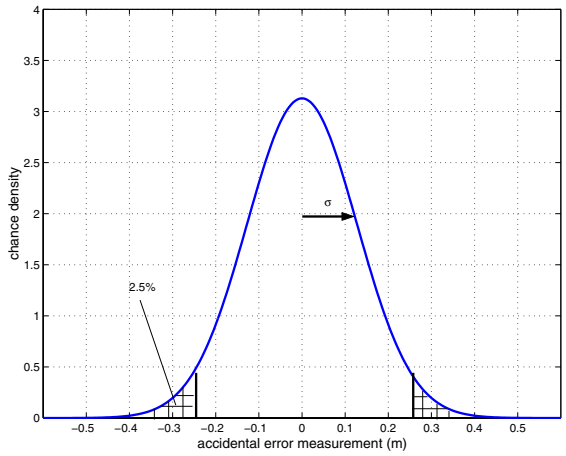

Figure 5-11 Probability density function for random deviation in measurements

In this figure the chance of exceedence is illustrated by the marked surface.

Computations of volumes are based on bathymetric maps on a grid with a mesh size of 250*250 m. The contribution to the volume of each grid cell is taken as the product of the cell area and the deviation between the cell-averaged bottom level and the concerned reference (e.g. MLW). The mentioned 25 centimetres and hence σ_m, concerns this cell-averaged level. Assuming that all these levels are statistically independent, the standard deviation σ_{vtot} of the entire volume of an element extending over m cells becomes:

$$\sigma_{vtot} = \frac{\sigma_v}{\sqrt{m}} \cdot m = \frac{7970}{\sqrt{6500}} \cdot 6500 = 6.4 \cdot 10^5 m^3$$

Thus, the standard deviation of the random error in measurements is only $6.4*10^5$ m^3 for the entire basin and can be neglected compared to the volumes (order 10^8 m^3). This illustrates that an, at first glance large error (25 cm), can turn out to be insignificant compared to the total basin volume.

5. systematic errors in measurements

Marion (1999) concluded that a systematic error was made in the measurements which were carried out in 1972 in a part of the Marsdiep basin. According to Rakhorst (2000), systematic errors are present in the 1965 registration of reference levels.

Unfortunately, no quantitative information is present for these systematic errors. Due to lack on information, these errors are not taken into account.

6. interpolation error

Besides the error in boundaries also the transformation of the depth measurements into a grid could lead to errors in volume calculation. Within and between these grid cells values of depth measurements are interpolated, which could cause deviation from the actual depth, and hence deviation in volume. Yet we assume that, in the same way as illustrated for the random errors, these deviations are not significant because of the averaging over many depth measurements per basin.

7. boundary identification

- Identification boundaries basin.

The watersheds form the system boundaries. Due to inaccuracies in the identification of these boundaries from the digitised maps, errors could occur in the calculated volumes. Especially the flat volume is sensitive for deviations as the boundaries mainly comprise intertidal area.

- Identification boundaries delta

For the delta the situation is more complex. This has to do with the way the delta volume is defined. Volumes of the delta are calculated relative to a reference coastal profile. This method is very sensitive for different interpretations of reference coast. This is confirmed by

Smittenberg (1999) who compared the sedimentation/erosion in the delta calculated by Eysink and Biegel (1992) with the ANW reports of the Adviestdienst Hoorn (Rakhorst, draft 2000). The difference in calculation method and boundaries is considerable. So, the actual volume of the delta contains deviations/uncertainties. The method to determine the reference coast (which would be present without inlet) and the determination of the actual definition of the boundaries of the delta consumes a lot of time and needs to be investigated properly.

This error is regarded as a very sensitive factor for deviation in the data.

8. application error of Asmita

Besides the mentioned errors, it could also be that other processes than the closure of the Zuiderzee play an important role on the long-run, which are not taken into account in the model formulation of Asmita. This could lead to disturbances in calibration results. Processes such as:

- transport across boundaries (see section 5.3)
- increasing tidal range in time (see section 5.4)
- sea level rise
- (artificial) interferences

The first process is due to the underdeveloped watershed between the Vlie and the Marsdiep basins. This process will probably lead to a somewhat different morphological behaviour than what Asmita predicts as this model works with element boundaries. This effect is not taken into account in the present study.

The influence of the increase tidal range will not be taken into account in the present study neither. However, the effect of the rising sea level will be taken into account, with respect to the changing boundaries (see chapter 6).

Artificial interferences like sand- and shell-mining and dredging of harbours took place in the period 1933-1998. Besides, sandwaves were present in the Vlie and Marsdiep basin (Rakhorst, 2000). These interferences are not taken into account in the model formulation as they do not include morphological effects due to closure. According to Smittenberg (1999) these interferences lead to a deviation of approximately $0.02*10^8$ m3 over the whole period 1933-1981. This is negligible compared to the volumes of the Marsdiep and the Vlie (order 10^8 m^3).

5.6.3 Conclusion Error analysis

An overview of the possible errors have been presented in a flow chart of the total calibration process. Errors from both the model point of view and from the data point of view have been distinguished. These errors are discussed and some considerations have been given on the significance of these errors.

Errors which are considered significant for the calibration process and data analysis, are errors due to boundary interpretation of the elements and due to estimates of model parameters.

5.7 Conclusion

Analysis of the tide and digitised maps of bed topography point out that inlets of Vlie and Marsdiep are suitable for calibration purposes as in these inlets significant changes have occurred in both the hydrodynamics and morphology.

The character of the tidal wave along the basin changed from a more propagating character in the former Zuiderzee, into a more standing character after closure. Before closure the tidal range decreased from sea towards the closed boundary, the tidal range after closure increased from sea towards the Afsluitdijk. As a result, the tidal volume in these inlets increased instantaneously due to the closure of the Zuiderzee. The change from a relatively large into a small basin makes the closure totally different than the closure of part of a smaller basin as the Lauwerszee, where the character of the tidal wave remained the same after the closure.

Large-scale bathymetric changes occurred in the Vlie and Marsdiep inlets. Channels, which were connected to the former Zuiderzee lost their function and as a consequence accretion occurred near the Afsluitdijk. Other channels, like the Doove Balg needed to increase in width, which is accomplished by erosion. The watershed area between the Vlie and Marsdiep basins has become more shallow. The deltas of Marsdiep and Vlie inlets, retreated a little towards the coast after the closure. Furthermore, the main ebb-channel moved in south-western direction. This is probably the result of the changed interaction between the long-shore tidal currents and the tidal currents through the inlet.

Analysing the volumetric data indicated that regarding the Vlie inlet the volume of the flats shows an increase due to the reduction in area (trend in flats of Marsdiep is inaccurate and not clear). The volume of the channel of both inlets is decreasing as the sedimentation in the back of the basin is larger than the erosion near the throat of the inlets. The delta volumes of Vlie and Marsdiep show a decrease, this could be caused by coastal regression. As this coastal regression influences the size of the delta, this effect should also be taken into account in the calibration of Asmita. This is investigated in the subsequent chapter.

Error analysis of the total calibration process (concerning data and model aspects) showed that deviations in volume are especially sensitive to the boundary assessment. Furthermore, interpretation of the model parameters is considered as an important aspect regarding the calibration process.

6 Calibration Asmita for closure Zuiderzee

6.1 Introduction

Due to the closure of the Zuiderzee, the basins of Vlie and Marsdiep inlets transformed into a basin with a length which is small compared to the tidal wave length. Based on this, we expect that such tidal inlets have the same characteristic morphological development as other inlets, which we can find in the eastern part of the Wadden Sea. Assumed that this expectation is correct, we can describe the large-scale morphological development of these tidal inlet systems (consisting of channel, delta and flat). In this chapter we will try and simulate this morphological development with the behaviour orientated model Asmita. For this, estimates of the parameters in Asmita are necessary. Some parameters can be used as calibration parameters, while others are fixed during the calibration.

Especially the volumetric changes of the delta are of interest. This volume is determined relative to the coastal profile which would be present without an inlet. It is plausible that this fictitious profile is the actual coastal profile adjacent to the delta. Hence, changes in the coast play a role in the determining the volume of the delta.

Before the calibration, we will first discuss the expected character of the morphological behaviour and related time-scales, based on the linear approximation of Asmita. In chapter 4 we have analysed how we can use the linear approach to predict the character of the morphological behaviour of the elements. In this chapter we will specify this for the Marsdiep and Vlie inlets.

6.2 Morphological behaviour of elements and related time-scales

From chapter 4 we derived that the linearised model is suitable to analyse the morphological behaviour and time-scales. In this section we will apply this for the Marsdiep and Vlie inlet. We will first discuss the system time-scales which are likely to play a role in Marsdiep and Vlie inlets. Subsequently, the expected character of the morphological development will be described.

6.2.1 System time-scales Marsdiep and Vlie

In section 4.6.3 we have concluded that it is not possible to calibrate the system time-scales, based on the available field data. This means that the system time-scales cannot be estimated from field data. Yet, they can give a first rough insight into the morphological behaviour in the case of a disturbance. Besides, they can be used to compare the two inlets with respect to the morphological development due to disturbances.

Inlet	T1 (years)	T2 (years)	T3 (years)
Marsdiep	3	412	25
Vlie	10	253	15

Table 6.1: System time-scales based on rough estimates of input parameters Asmita

These time-scales were derived from the linear approximation in equation 4.30, where rough estimations are made regarding the geometric values and exchange parameters. Moreover rough estimations of the equilibrium sizes were made.

Considering the system time-scales, we can see that there are two smaller time-scales, and one longer time-scale. For both Vlie and Marsdiep, it holds that the intensities of the responses corresponding to the smallest two time-scales have reduced with some 85% or more after about half a century. Then, the largest time-scale will dominate the morphological development. The Vlie inlet is likely to reach its equilibrium state sooner than the Marsdiep inlet. This is indicated by the longest system time-scale which amounts 253 years and 412 years for the Vlie and the Marsdiep respectively. It must be emphasised that these time-scales are estimates as they are based on estimates of the parameters of Asmita.

In the following section, the expected morphological behaviour is explained for two elements (section 4.4.2). This is elaborated for the Marsdiep inlet only, as the flats in the Marsdiep hardly play an important role. This justifies the schematisation in two elements.

6.2.2 Expected character of morphological behaviour

If we consider the elements channel and delta in the Marsdiep, we concluded in chapter 5 that the delta is expected to grow to reach its equilibrium value ($V_d<V_{de}$) and the channel is expected to diminish ($V_c>V_{ce}$). This is caused by the strong increase of the tidal prism as a result of closure of part of the basin.

In chapter 4 (section 4.4.2), the morphological development and interaction of the elements in time was discussed. We derived a method to predict the expected character of the morphological behaviour, given a combination of disturbances. We concluded that in the case of a combination of a positive and negative disturbance, a bump in the morphological development of one of the elements can be expected.

We created an overview of this expected behaviour or the Marsdiep in figure 4.8. Based on rough estimated disturbances and input parameters, it can be expected that situation (1) occurs. This means that a bump may or may not occur in the development of the channel, depending on the relative importance of the responses with the two system time-scales. The delta will evolve monotonously towards its equilibrium state. This is illustrated in figure 6.1.

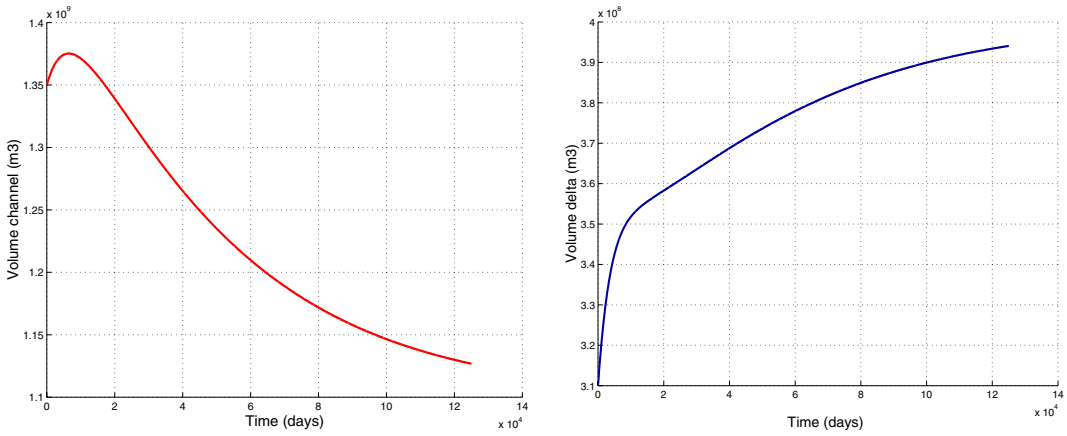

Figure 6-1 Example morphological behaviour

left: bump in morphological development of the channel, right: corresponding development in delta

In the case of the Marsdiep, the expected morphological behaviour of these two elements due to the closure can be explained physically as follows. Due to the closure the equilibrium situation, which was more or less present, was disturbed. In particular, the delta became smaller than its equilibrium volume and the channel became larger than its equilibrium. This means that, the delta needs to grow and the channel wants to decrease. Then, both the delta and the channel demand sediment to reach equilibrium. What exactly happens, depends on the disturbances in the two elements. The element with the 'strongest' demand, will receive sediment first. Based on the conclusions from figure 4.8, we expect that that initially the delta will receive sediment from the channel, which then develops further from its equilibrium position. This could result in the bump in the development of the channel, as illustrated in figure 6.1.

Hence, regarding the Marsdiep inlet it is expected that, based on the linear approximation and on rough estimated disturbances, a bump in the development of the channel could occur and the delta is expected to evolve monotonously towards equilibrium (according to situation (1), appendix C).

When we consider the data of the Marsdiep, the delta is not likely to increase directly. This could be because of the coastal regression which will be elaborated in section 6.3 Furthermore, a bump in the channel development is not directly recognisable. The smaller system time-scale is about 25 years, which makes it likely that a bump is visible in the evolution since the closure. That we do not see the bump could be due to the combination of disturbances as discussed above. But, it could also be that because of the sparsety of the available field data, this development is not directly clear. This could be a great advantage of the linearised equations: the data-points of the elements do not directly show the initial development, but based on the model, we could *know* what the expected response would be.

Finally we make a remark considering the time-scale of elements. In section 4.3, we discussed this time-scale in the case of monotone developments or overshoots. However, in the case of a bump in the development, the term 'time-scale of an element' is not to be preferred. Figure 6.1 shows that the initial adaptation capacity of the channel, which is directly related to the time-scale of an element, appears high for the channel. Actually, the

channel actual moves in opposite direction, which results in a slower process towards equilibrium. In such a case, it is better to use the system time-scales as characteristics of the system than time-scale of elements.

6.2.3 Conclusion

From the linearised equations we derived system time-scales for Vlie and Marsdiep. For both Vlie and Marsdiep, it holds that the intensities of the responses corresponding to the smallest two time-scales have reduced with some 85% or more after about half a century. Then, the largest time-scale will dominate the morphological development. The actual values could change due to a change of the input parameters of Asmita.

Furthermore, the linear approximation, together with a rough estimation of the disturbances, point out that a bump in the morphological development of the channel is expected for the Marsdiep, and the delta is expected to grow monotonously towards its equilibrium (situation 1, figure 4.8).

6.3 Changing boundaries

6.3.1 Introduction

The closure of the Zuiderzee and in particular the responses of the Marsdiep and Vlie inlet systems to this closure, has been chosen as a reference case for the present study. However, the development that these two inlets have exhibited since the closure contains also a component related to sea level rise. As we are not interested in this component, we have developed a method to remove it from volume changes derived from field observations as well as from Asmita computations. The crux of this method is to take into account that spatial boundaries of elements (used in deteming their volumes) may vary as the sea level rises. This will be explained here after.

Sea level rise is one of the reasons that the boundaries to which the volumes of the elements are defined, change. Because we want to simulate the actual development of the elements, their volumes, as defined in Asmita and as derived from field data, should be related to the actual (changing) boundaries.

With respect to the channel and the flat, the changing boundary comprises the rising of the water level and the change of watersheds. The changing basin boundaries due to a change in watersheds are already taken into account in the interpretation of field data (see section 5.4). It is assumed that the changing watersheds do not have a significant influence on the sediment import in the tidal inlet and hence, this effect is not taken into account in the Asmita formulation. Furthermore, because it is assumed that the basin can follow the present sea level rise, the actual volume of the flat and the channel does not change, relative to the actual sea level. Hence, as long as the volumes are relative to the actual boundaries, no modifications are necessary in Asmita. Regarding the delta, the change in boundaries comprises the change of coastal profile. Because of this, the actual volume of the delta

increases, which should be taken into account. This effect is analysed in more detail and will be discussed in the subsequent section.

Summarising:
- boundaries change (among other things due to sea level rise) of all elements
- as a consequence of changing boundaries due to sea level rise, the channel and flat are assumed not to increase
- as a consequence of changing boundaries the delta does increase

Then, two aspects are necessary for the Asmita simulation:
- defining volumes of all elements related to actual boundaries, in Asmita and field data interpretation
- take into account the increase in delta in Asmita and in the interpretation of the field data

6.3.2 Boundaries in interpretation of field data

As explained in the previous section, the volumes of the elements based on field data should be based on actual boundaries. This means actual water levels (MLW) regarding flat and channel, and actual coastal profiles with respect to the delta. In the previous chapter we already related the volumes of channel and flat to the actual water level (section 5.5). As mentioned in the previous section, the sea level rise does not change the actual volume, because it is assumed that the basins can keep up with the present sea level rise. Regarding the delta, we must modify our interpretation of the field data for the change in reference coastal profile. This will be done in the same way in Asmita and will be discussed in the subsequent section.

6.3.3 Change delta due to changed boundaries

On a time-scale, which we consider to describe the morphological development of tidal inlets with Asmita, we generally cannot consider the coast adjacent to the delta as time-invariant. This is problematic, because we use this coast as a reference for determining the size of the delta.

This forms a serious point of attention when interpreting the field data. We have seen in the previous chapter that the development of the delta, shows an unexpected decrease. This might be an artefact of using the results of the 1972 field campaign as a reference for all delta volume computations, whereas according to Asmita definitions this reference should follow the cross-shore profile developments in the coast stretches adjacent to the delta. A recession of the coast for instance, yields a growth of the delta volume, irrespective of the actual erosion or sedimentation in that element. Hereafter, this effect will be looked at in detail.

We will first explain the different reasons for a change in the delta volume, and then we will discuss how we can take into account these changes in Asmita and in interpreting the field data.

We can distinguish three causes for changes in delta volume:
1. ordinary erosion and sedimentation
2. change of coastal profile (reference) due to sea level rise
3. change of coastal profile due to sediment demand of the tidal system (flat-channel-delta)

For the coastal profile an equilibrium shape exists which mainly depends on the wave conditions and the average grain size. (see Bruun, 1954). The time-scale for the cross-shore transport near the coast is assumed to be much smaller than that of the transport between delta and basin. So, the coast is assumed to have a fixed shape when looking at inlet evolution. Furthermore, the cross-shore transport is assumed to have no influence on the supply of sediment to the inlet, which confirms the presence of a constant equilibrium concentration in the 'outside world' as used in Asmita. In this way, we can assume that the coast only *supplies* sediment and does not *need* sediment to reach equilibrium.

1. *ordinary erosion and sedimentation*

This comprises the processes which are described by Asmita: no sea level rise and import/export of sediment of the system does not result in noticeable erosion or sedimentation of the coast adjacent to the delta.

2. *change of coastal profile (reference) due to sea level rise*

At the time-scale of sea level rise we may consider the cross-shore profile as shape-fixed. In that case, the response of this profile to sea level rise is limited to a translation in the cross-shore plane. This is realised by cross-shore transport only. It is assumed that the delta is able to follow this translation, so that the volume of the delta, relative to the actual coastal profile, does not change. This is illustrated in the following figure:

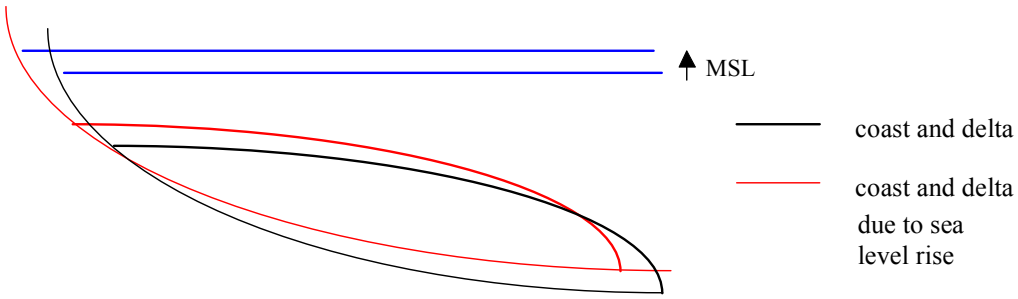

Figure 6-2 Change coastal profile due to sea level rise

3. *change of coastal profile due to sediment demand of the tidal inlet system*

Sediment is demanded by the tidal inlet due to two forcings, viz. the sea level rise and the closure. To follow the sea level rise, the channel and flat need sediment. We assume that satisfaction of this need is completely provided by the coast adjacent to the delta. This results in landward displacement of the coastal profile, which in turn results in an increase of the delta volume. After all, according to the definition of the delta volume as used in Asmita, the coastal profile is the reference relative to which the volume of the delta is computed. The second cause of sediment demand is related to the response of the system (flat, channel, delta) to the closure of the Zuiderzee. As a consequence of this closure, the system demands sediment, which, in the same way as the sea level rise, is provided by the coast adjacent to the delta. This will result also in a cross-shore displacement of the coastal profile and a

corresponding effect on the volume of the delta. The change of the coastal profile due to the demand of the basin is illustrated in figure 6.3.

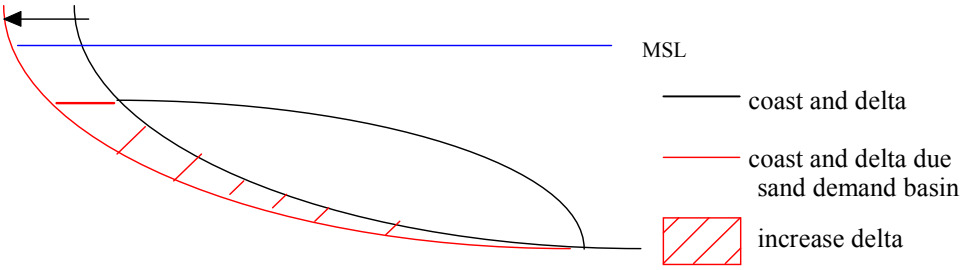

Figure 6-3 Change coastal profile due to demand basin

Summarised, the direct effect of a change of the coastal profile due to a rise of the sea level does not affect the delta volume. The demand of the basin due to sea level rise and the demand of the delta and basin due to the closure of the Zuiderzee result in a landward shift of the coastal profile, which leads to an increase of the delta volume. This is a purely geometric effect, that occurs even though no sedimentation takes place in the delta.

The above mentioned effects could have a significant impact, which we cannot neglect. This is confirmed by interpreted field data on the delta by Biegel (1992). Biegel calculated volumes of the delta relative to a fixed coastal profile, assuming that this fixed reference profile is also representative for other years. These results show a decrease of the volume in time, which is unexpected (see chapter 5). Based on the data-analysis, we expect an increase of the delta due to the closure of the Zuiderzee.

If we assume that the sediment demand of the basin and the delta is satisfied at the expense of the coast, then this sedimentation should be directly related to an increase of the delta. The present Asmita formulation does not cover this. In the subsequent section, we will consider Asmita and discuss a theoretical approach to relate the regression of the coast to an increase of the delta.

We conclude this section with a note on the coastal regression. In 1990, the government set up a agreement and defined a Basis Kustlijn (Basal Coastline). This comprises that from 1990 the coastline is maintained at its then position by carrying out beach nourishments. We assume in the present study that the coastline after 1990 is invariable. So the following extension in Asmita is applied till 1990. Actually, nourishments are carried out periodically, which means that the coastline is variable between certain ranges, which requires a different kind of adjustment of the delta, but this will not be elaborated in the present study.

6.3.4 Extension Asmita with respect to coast

In the original formulation of Asmita, changes of volumes of the elements are related to exchange of sediment between the elements, and between the delta and adjacent coast. Implicitly, it is assumed that the references, relative to which the volumes are determined, are time-invariant. In the previous section, we explained that this assumption is not correct regarding the development of Marsdiep and Vlie prior to the introduction in 1990 of

nourishments to maintain the Basal Coastline. Herafter, we will elaborate a method to adapt the Asmita formulation in this respect.

Suppose that the coast adjacent to the delta supplies the sediment which is demanded by the system (flat, delta, channel). This will cause erosion and hence a landward shift of the coasltal profile at rate R (m/s). The amount of sediment which is provided by the coast to the inlet system equals in that case:

$$R \cdot H \cdot L \tag{6.1}$$

where:
H = 'active' height coastal profile, which means the height of the coastal zone where sediment activity takes place (m)
L = length of coastal area (longshore), which supplies sediment to the system (m)

The sediment demand of the system consists of contributions of flat, channel and delta.

- flat:

If V_f is the flat volume as defined in Asmita, then the total sediment demand of this element equals (assuming that it keeps up with the sea level rise):

$$\frac{dV_f}{dt} + s \cdot A_f \tag{6.2}$$

where
s = sea level rise (m/s)
A_f = flat area (m2)
The term $s*A_f$ in the expression above results from our assumption that the flat will demand sediment to keep up with the rising sea level. Then, the actual volume does not change due to the sea level rise.

- channel:

The total sediment demand of this element equals

$$-\frac{dV_c}{dt} + s \cdot A_c \tag{6.3}$$

where
V_c = wet volume of channel (m3)
A_c = channel area (m2)

- delta

The actual sediment demand of the delta comprises that part of its volume change that is not related to a shift of the reference relative to which this volume is computed. It is reflected by:

$$\frac{dV_d}{dt} - R \cdot h \cdot b \tag{6.4}$$

where

h = 'active' height of the delta (m)
b = width of the delta (longshore) (m)

Based on conservation of sediment it follows, that the sediment supplied by the coast equals the sediment demand of the system:

$$R \cdot H \cdot L = \left(\frac{dV_f}{dt} + s \cdot A_f - \frac{dV_c}{dt} + s \cdot A_c + \frac{dV_d}{dt} - R \cdot h \cdot b \right) \cdot \lambda \qquad (6.5)$$

where
λ = fraction of the total sediment demand of the inlet system that is satisfied at the expense of the coast (-)

or

$$R \cdot \left(\frac{H \cdot L}{\lambda} + h \cdot b \right) = \frac{dV_f}{dt} - \frac{dV_c}{dt} + \frac{dV_d}{dt} + s \cdot A_b \qquad (6.6)$$

with
A_b $= A_f + A_c$, the surface area of the tidal basin (m2)

The original Asmita equations, where the geometric increase of the delta is added yield:

$$\frac{dV_f}{dt} = w_s \cdot A_f \left(c_f - c_{fe} \right) = \delta_{fc} \cdot \left(c_c - c_f \right) \qquad (6.7)$$

$$-\frac{dV_c}{dt} = w_s \cdot A_c \left(c_c - c_{ce} \right) = -\delta_{fc} \cdot \left(c_c - c_f \right) + \delta_{dc} \cdot \left(c_d - c_c \right) \qquad (6.8)$$

$$\frac{dV_d}{dt} - R \cdot h \cdot b = w_s \cdot A_d \left(c_d - c_{de} \right) = -\delta_{dc} \cdot \left(c_d - c_c \right) + \delta_{do} \cdot \left(c_E - c_d \right) \qquad (6.9)$$

If we substitute the equations 6.7-6.9 into the conservation equation 6.6, we find that:

$$R \cdot \left(\frac{H \cdot L}{\lambda} + h \cdot b \right) = \delta_{od} \cdot \left(c_E - c_d \right) + R \cdot h \cdot b + s \cdot A_b \qquad (6.10)$$

This means that we can eliminate the expression for the coastal regression *R* from equation 6.10:

$$R = \frac{\lambda}{H \cdot L} \cdot \left(\delta_{do} \cdot \left(c_E - c_d \right) + s \cdot A_b \right) \qquad (6.11)$$

Finally, we can adjust the change of the volume of the delta and add the geometric increase due to a change of the reference:

$$\frac{dV_d}{dt} = w_s \cdot A_d \cdot \left(c_d - c_{de}\right) + R \cdot h \cdot b \qquad (6.12)$$

substituting equation 6.11 for *R*, results in:

$$\frac{dV_d}{dt} = w_s \cdot A_d \cdot \left(c_d - c_{de}\right) + \beta \cdot \left(\delta_{do} \cdot \left(c_E - c_d\right) + s \cdot A_b\right) \qquad (6.13)$$

where

$$\beta = \frac{\lambda \cdot h \cdot b}{H \cdot L} \qquad (6.14)$$

β = 'adjustment factor' regarding delta due to changed boundaries (-)

Equation 6.13 illustrates that changes in the delta occur due to the three aspects as discussed in section 6.3.3, namely:

- ordinary sedimentation/erosion ($w_s A_d(c_d-c_{de})$)
- sediment demand of the inlet due to closure ($\beta\delta_{do}(c_E-c_d)$)
- sediment demand of the basin due to sea level rise ($\beta s A_b$)

The latter two terms illustrate the adjustment which is applied for the delta These terms indicate that the delta grows geometrically due to the changed boundary, which comprises the regression of the adjacent coastal profile.

By extending the sediment balance, we have actually added a fourth element 'coast' to the model, with the assumption that the cross-shore profile is in equilibrium. Hence, we assume that at the time-scale of the morphological evolution of the inlet, the equilibrium concentration in the 'outside world', c_E, indeed is a constant, provided that the wave climate in the coastal area remains unchanged. The fourth element is linked to the other elements via the sediment balance (equation 6.6). The four elements form a closed system if λ=1. After all, in that case, all sediment demand is supplied by the adjacent coast.

This expression for β is convenient, because this includes all possible uncertainties with respect to λ, H, L, h and b in one parameter. This adjustment factor β depends on the height and width ratio of delta and coast segment and on the amount of sediment imported by the inlet system at the expense of the coast. For the length of the coast segment, it is assumed that half of the island on both sides of the delta supply the sediment. These widths, together with the widths of the deltas are derived from Steetzel (1995) and are presented in table 6.2. The width of the delta is based on the location of the seawards bending of the NAP -5m depth contour. The heights H and h, are heights of the active profile where sediment transport takes place. For the delta the active zone ranges roughly from NAP to NAP -20 m. Regarding the coastal profile, the zone from the dunes towards the seaward end of the breaker zone is considered as the active zone. This area begins at the dunes at NAP +10 m and ends at a depth of approximately NAP -8m to NAP -10 m. So the active height ratio of

delta and coast is approximately h/H=20/18 or 20/20. With λ=1, these values result in β = 1.1 and 1.25 for respectively Vlie and Marsdiep.

Inlet	b, width delta (km)	coast west (km)	coast east (km)	L, length coast segment (km)
Marsdiep	18 km	8 (NH)	8 (Texel)	16
Vlie	15 km	5 (Vlieland)	8.5 (Terschelling)	13.5

Table 6.2: Width coast and delta segment (Steetzel, 1995)

This adjustment factor β contains several uncertainties. We estimated the length and height of the coast segment and the delta, but we do not have detailed field data to confirm this measures. Moreover, we do not know exactly which part of the sediment demanded by the inlet is withdrawn from the coast adjacent to the delta. It is also possible that part of the sediment comes from the wave-driven longshore sediment transport. To take into account these uncertainties, two different scenarios are used for β in the calibration. One scenario with the width and height ratio of coast and delta as indicated in the previous paragraph. This can be seen as an upper limit of adjustment, where β equals approximately 1.15. For the other scenario, it is assumed that λ=0.7, which means that 70 % of the sediment demand is taken from the adjacent coast. Furthermore, it is assumed that in an extreme case, the height of the active coastal profile reaches NAP -20m, which is the same height as the delta adjacent to this coast segement. This leads to a smaller height ratio. (20/30). Adjustment factor β in the second scenario has reduced to approximately 0.6. This scenario is a lower limit of adjustment. During the calibration, it will be analysed what the differences are between these two scenarios and which scenario results in the most plausible calibration (section 6.3.4).

To see the effect of adjustment on the morphological development of the elements, the change in sediment exchange due to the applied adjustment will be described

Sediment Transport due to adjustment delta

We will briefly discuss the effect of the applied extension of Asmita on the sediment exchange between the elements. We take an example where the delta and the flat tend to increase and the channel tends to decrease to reach equilibrium. In the figure 6.4, the sediment exchange with and without adjustment of the delta due to coastal regression is illustrated.

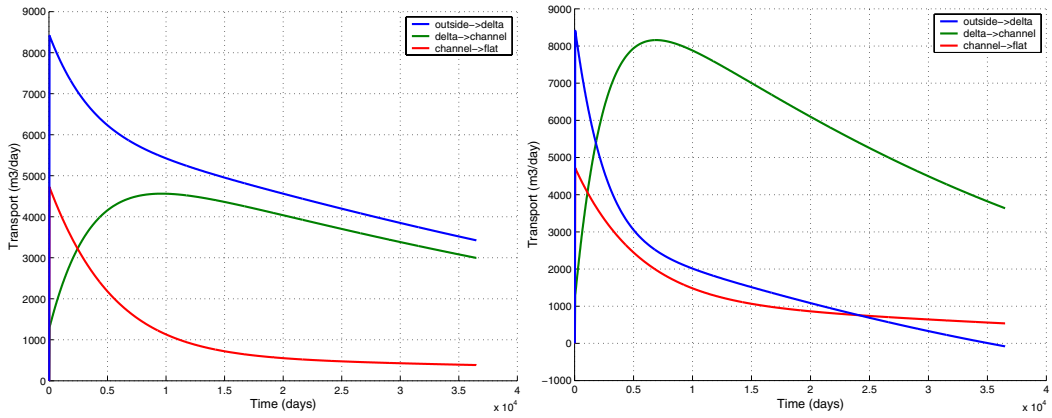

Figure 6-4 Transport between elements without (left) and with adjustment for delta

The left figure represents a situation for a fixed coast, thus without any adjustment for the delta. In this figure it is illustrated that sediment is transported from the outside world towards the delta. The delta needs this sediment to grow and as a consequence only a relatively small part of the imported amount of sediment is available for the channel. Also the flat requires sediment. Because of this, the channel has the largest difficulties to obtain sediment. In the right part of the figure, the adjustment for the delta volume is applied. As a consequence of the adjustment, the delta grows geometrically, and needs less sediment. This means that the channel can obtain sediment easier. The exchange between the channel and the delta is even larger than the exchange between the delta and the outside world. Because the geometrical increase of the delta is larger than the difference between the incoming and outgoing sediment in the delta, the net effect is an increase of the delta. From figure 6.4 it can be derived also that the flats are also influenced by the adjustment of the delta, though less than the channel.

So the effect of coastal regression on sediment exchange, and thus on the morphological development is clearly present. Due to the geometric increase of the delta, the basin can obtain sediment easier. However, after 1990, the coast line is kept in position by nourishments and then, this effect will not hold anymore. This will be made clear in the calibration.

6.4 Calibration Asmita

We will calibrate Asmita, on the morphological development of the Vlie and the Marsdiep inlets after the closure of the Zuiderzee. Besides, some information is derived on the future development towards equilibrium. First we will discuss the equilibrium relations which form an important basis for the Asmita modelling. Subsequently, the input and calibration parameters will be discussed. Finally, the closure of the Zuiderzee will be simulated and some conclusions considering the possible future development will be given.

6.4.1 Equilibrium relations

The Asmita concept is based on the assumption that the various morphological elements of an inlet system evolve towards an equilibrium state. If the length scale of the tidal basin is small compared to that of the tidal wave, this equilibrium state is determined primarily by

the tidal prism of the inlet. In particular logarithmics of equilibrium volumes of elements and prism are, by fair approximation, directly proportional to one another. The proportionality is indicated with empirical coefficients which depend on the shape and geometry of the inlet (see empirical relations in section 3.4). These coefficients can be determined for a certain inlet, assuming that the system was in equilibrium before the interruption. Given the (equilibrium) volume and tidal volume, the corresponding equilibrium coefficients can be determined.

However, before closure of the Zuiderzee, the basin was relatively large and Eysink's equilibrium relations for the Wadden (section 3.4) with respect to the channel and flat do not apply. As a consequence the equilibrium coefficient from the empirical relations cannot be calibrated with the situation before closure. This means that the equilibrium volumes cannot be estimated based on those relations, and should be used therefore as calibration parameters in Asmita.

In contradiction to the channel and the flat, we can estimate the equilibrium volumes of the delta, based on the change in tidal volume. Despite the fact that the system before closure contained a large basin, it is likely that the equilibrium volume of the delta before closure, was related to the tidal volume. Hence, we assume that we can use the equilibrium relation between delta and prism (equation 3.8) provided that we replace the prism by half the tidal volume. If we assume that the delta was in equilibrium before closure, then an increase in the delta should occur, related to the increase in tidal prism (see equation 3.8, $\Delta V_{de} \sim (\Delta P)^{1.23}$).

Summarising, it can be stated that equilibrium relations for the channel and flats are not valid for large basins, and thus cannot be used for predictions of the equilibrium situation after closure. Regarding the delta a rough estimation can be made based on the proportionality between the equilibrium relation and the delta volume before closure. We will use the equilibrium volumes as calibration parameters. Based on the field data and the equilibrium relations, we estimated ranges of the equilibrium volumes regarding the Vlie and Marsdiep elements. Within these ranges, the calibration will be carried out by tuning the equilibrium volumes. These ranges are presented in appendix G1.

6.4.2 Input parameters

In the previous section we concluded that the equilibrium volumes should be used as calibration parameters. Considering the available field data, which comprised eight data-points per element, the three equilibrium volumes are the only calibration parameters which we will use. Thus all other input parameters, require a proper estimation and will then be fixed during the calibration.

The sensitivity analysis in chapter 4 showed that of all model parameters, diffusion coefficients, concentration in the outside world and equilibrium volumes have the largest influence on the system time-scales and thus on the prediction of the morphological development. These parameters should be estimated carefully. Van Goor (2001) carried out a detailed study regarding the equilibrium concentration in the outside world (c_E). It turned out that with a value of $2 * 10^{-4}$ a fair reconstruction of the morphological behaviour can be

obtained for the Borndiep inlet. The concentration outside the inlet actually depends on the wave climate. Despite the slight different wave conditions near the Marsdiep and Vlie inlets (different angle of approach), the same value will be used henceforth in the calibration. Regarding the diffusion coefficients, further analysis is required.

Regarding the other input parameters rough estimates are made. For areas of elements, time-averaged values will be used. The vertical exchange coefficient (w_s) and the n-parameter are based on studies of Buisman (1997) and Van Goor (2001), see appendix G1. The average tidal range is derived from tidal data (Jaarboek Rijkswaterstaat, 1998). Finally the initial volumes of the elements should be given as input in Asmita. With respect to these values, the interpreted volumes derived from field data of 1933 are used. For the Marsdiep delta, the average of two volumes in 1925 and 1933 is used as initial value in Asmita.
All these input values which are used in the calibration can be found in appendix G1.

Diffusion coefficients

Van Goor (2001) optimised diffusion coefficients from field data on the Zoutkamperlaag, regarding the closure of the Lauwerszee. Buisman (1997) derived similar coefficients for the Zoutkamperlaag. We will use their results to arrive at estimates of diffusion coefficients of the Vlie and Marsdiep inlet. Therefore, we will discus the meaning of the diffusion coefficient in some more detail.

The diffusion coefficients originate from the mass-balance equation and are used also in Estmorf, ((Wang and Karssen, 1992), basis for Asmita concept). In Estmorf , a one-dimensional network schematisation is made for a basin, containing channels and adjacent flats. The exchange rate between flat and channel is defined as:

$$F = D \cdot h \cdot \frac{c_f - c_c}{L} \tag{6.15}$$

F = horizontal sediment flux per unit width (m2/s)
D = dispersion coefficient (m2/s)
h = time averaged water depth (m)
L = distance between centre of channel and centre of flat (m)

If we integrate this over the total width of the channel and flat, the area A_c, or cross-section is used instead of the water level:

$$T = D \cdot A_c \cdot \frac{c_f - c_c}{L} \tag{6.16}$$

T = total horizontal sediment flux (m^3/s)

Then, we derived the residual transport, in the same way as formulated in Asmita. In Asmita, the horizontal exchange is expressed as equation 6.17.

$$T = \delta \cdot \left(c_f - c_c\right) \tag{6.17}$$

This means that the diffusion coefficient equals:

$$\delta = \frac{D \cdot A_c}{L} \tag{6.18}$$

Thus, the diffusion coefficient depends on the dispersion coefficient, the cross-section which is available for sediment exchange between the elements, and the length between the centres of the elements. It represents the tide-averaged residual sediment transport between two elements, which takes place through a certain cross-section *Ac*, over a length of *L* metres.

The dispersion coefficient *D* represents the tide-residual sediment transport capacity per unit width. It is related to the tide averaged velocity and the fall velocity of the sediment particles. The tide averaged velocity is in equilibrium situation similar for the different inlets (~1 m/s). As the average grain size and related fall velocity for the different Wadden inlets are similar, the dispersion coefficient *D* is assumed to be the indifferent for the Wadden inlets.

So, to give an estimation of the diffusion coefficients in the Vlie and the Marsdiep, we can use values of Van Goor (2001), and scale them with the factor A_c/L. This scale-factor indicates that there is a kind of length-scale which determines the actual diffusion coefficient as defined in Asmita. The square root of the basin area might serve as such a length-scale, provided that the basins at hand do not differ substantially with respect to their shapes. The rate between the different characteristic lengths can be used as a scale factor for diffusion coefficients. Thus, for the diffusion coefficients of the Marsdiep it holds approximately that:

$$\delta_{mars} = \sqrt{\frac{A_{mars}}{A_{zoutk}}} \cdot \delta_{zoutk} \tag{6.19}$$

δ_{mars} = diffusion coefficient Marsdiep (m3/s)
δ_{zoutk} = diffusion coefficient Zoutkamperlaag (m3/s)
A = area (m2)

The same holds for the Vlie inlet. This scale factor can be used for exchange between delta and outside world δ_{do}, where the delta area plays a significant role, and for exchange between the delta and channel $\delta_{dc,}$ where the basin area is used in the scale factor.

For the exchange between flat and channel, the scale factor of area relations can be specified somewhat. The diffusion coefficient is a measure for the sediment exchange capacity between channel and flat. It is plausible that the exchange between channel and flat is related to the wet volume measured between flats and mean high water. Converting also into a length-scale, yields:

$$\delta_{mars} = \delta_{zout} \cdot \sqrt[3]{\frac{Qf_{mars}}{Qf_{zout}}} \tag{6.20}$$

where

$$Qf = A_f \cdot H - V_f \tag{6.21}$$

Qf = wet volume above flats and below MHW (m3)

Application of this scaling method yields the following diffusion coefficients, based on the diffusion coefficients derived for the Zoutkamperlaag:

Inlet	δ_{fc} (m3/s)	δ_{dc}(m3/s)	δ_{do} (m3/s)
Zoutkamperlaag	800	1000	1200
Marsdiep	980	2450	1550
Vlie	1300	2560	1770

Table 6.3: Diffusion coefficients

So, due to the larger size of the basins and deltas, the capability of exchanging sediment is larger, which results in diffusion coefficients for the Marsdiep and Vlie larger than those of the Zoutkamperlaag.

Change linear solution and time-scales

We have seen in the sensitivity analysis that system time-scales are more sensitive to variations in diffusion coefficients than to variations in other parameters. In that analysis we investigated the sensitivity of system time-scales for a variation of diffusion coefficient around a first estimate (see appendix B). The applied scaling (see table 6.3) results in diffusion coefficients which deviate from the first estimates, hence we may expect that the corresponding time-scales will be different also than what we concluded in the first estimates (see section 6.1). A comparison between the time-scales, based on first estimates of diffusion coefficients, and those, based on the scaled diffusion coefficients is given in table 6.4.

Inlet	T1 (years)	T2 (years)	T3 (years)
Marsdiep	3 (3)	198 (412)	12 (25)
Vlie	8.5 (10)	130 (253)	11 (15)

Table 6.4: New system time-scales due to changed diffusion coefficients
( ) =values former assumed time-scales

This table illustrates that the largest time-scales (T2) have reduced with about 50 percent to 198, respectively 130 years. Also the two smaller time-scales have decreased. This will result in a faster development of the system towards equilibrium state than expected on the basis of the first estimates.

6.4.3 Results calibration

Approach and assessment calibration

In this section we make an attempt to calibrate Asmita for the morphological development of the Marsdiep and Vlie inlets dueto the closure of the Zuiderzee. For this data covering 65 years are available. Besides, we are interested in the future development towards equilibrium. Therefore, we will simulate the future morphological development from the closure towards equilibrium, based on the calibrated equilibrium volumes.

Observations of 1933 serve as initial values for the simulation. Furthermore, all data-points are assumed to have the same weight. The volumes of the Vlie delta, interpreted from field data are related to the reference coast of 1972. Because we start our calibration and hence the adjustment of the delta in 1933, we want to use delta volumes relative to the coastal profile in 1933. Based on the estimated increase of the delta (V_0-V_{de}) and the actual volume of 1972, we carried out the calibration.

The equilibrium volumes will be calibration parameters. This means that these values will be varied together, between certain expected ranges (see appendix G1), till a plausible fit between the data and Asmita results. Between these boundaries, the Least Squares method is used to minimise the error (between observations and simulation results) and to optimise the equilibrium volumes of the elements. For this the Root Mean Square error is used (RMS value). The RMS error is defined as the root of the averaged square error:

$$RMS\_error = \sqrt{\frac{\sum_{i}^{1}\sum_{n}^{1}\left(V_{obs} - V_{asmi}\right)^2}{n \cdot i}} \qquad (6.22)$$

V_{obs} = actual volume element based on data (m3)
V_{asmita} = simulated actual volume (m3)
n = number of observation points per element (-)
i = number of elements (-)
For three elements eight observation points per element are available.

In the following section we will discuss the two scenarios for the adjustment of the delta, and the results of the calibration for the Vlie and Marsdiep inlets.

Two scenarios adjustment delta

For two different β's (equation 6.7) the inlet systems were calibrated, which implies a minimum and maximum adjustment for the delta. We will briefly discuss which adjusment factor is the most plausible. This is assessed based on the expected developments, and on the least squares between observations and simulations.

Using the lower limit (β=0.6) results in a minimum adjustment. For the Marsdiep this would imply a decrease of the delta, which is not expected (see appendix G3.1). Regarding Vlie

inlet, a reasonable calibration would be possible for the delta and flat, but then the calibration of the channel does not give acceptable results. If we consider the results in appendix G2.1 and G2.2, then we can see that the calibrated channel volumes do not fit the data if the lower limit for β is applied. It turned out that the upper limit, where all the sediment originates from the adjacent coast and the active coast height goes to approximately NAP -8/-10 m, is the most plausible scenario (β=1.1/1.2). This means that the upper limit for adjustment for the delta is applied for Marsdiep and Vlie. In the following section results of the calibration, using the upper limit of adjustment factor β, will be discussed.

Results Vlie inlet

Regarding all elements of the Vlie inlet, a plausible calibration of the morphological development is possible. This means that the equilibrium volumes are calibrated between the ranges (see appendix G) and optimised with Least Squares between these boundaries. The Vlie delta shows an increase as expected, based on the proportionality in the equilibrium relation. Also the flats show an increase as expected. A proper fit for the channel is also possible and indicates that especially the channel will accrete some more during the next century with 70 million m3. The calibrated equilibrium values are presented in table 6.5. The simulated morphological development is presented in appendix G2.

Despite the adjustment of the delta regarding coastal regression, the morphological development of the channel illustrates that in the first 20 years there were some difficulties to obtain sediment, which resulted in a small bump in the morphological development. So apparently, the prediction regarding the expected behaviour the Marsdiep (section 6.2) corresponds with the behaviour of the Vlie inlet. Furthermore, the flats react relatively fast. The largest system time-scale of 132 years, derived from the input parameters of Asmita, is of the same order as the overall morphological development of the system. It will take about 150 years before the total system has reached equilibrium (see appendix G2.4). The initial development of the flat and of the delta could correspond with the system time-scales of order 8.5 and 11 years, which do not play a role after 25 years. However, these time-scales could not be derived from the data (see section 4.6.3). Moreover, it should be noted that the applied adjustment influences the system time-scales somewhat, as the time-scales are based on morphological development due to sediment exchange.

In figures appendix G2.3 the cumulative adjusted volume of the delta is presented, due to sea level rise and due to closure. The adjustment due to sea level rise is constant in time. The adjustment due to closure decreases in time, as the demand of the delta and the basin also reduces. From figure G2.3a, it can be seen that the sediment, which is demanded from the adjacent coast due to closure, has reduced considerably till 1990. At that time, the flats and delta are not far from equilibrium. However, the channel still needs a lot of sediment to reach its estimated equilibrium (approximately 70 million m^3). Without nourishments at the adjacent coast, this sediment would originate partly from the delta, as the geometric increase due to sea level rise is larger than the demand of the delta to reach equilibrium. Because of the nourishments, the delta will not grow geometrically, as the reference coast does not change. Then, all sediment originates from the coast and hardly any sediment is available from the delta. This implies that in the case of nourishments, it will take longer for the basin,

especially the channel, to import sediment. Figures G2.2 and G2.4 show a bend in morphological development of especially the channel, which illustrates the delay in the morphological development due to nourishments.

In the case of a straight coastal profile, beach nourishments are required to compensate the response of the coast to sea level rise(as illustrated in figure 6.3). With respect to the Wadden coast adjacent to the Marsdiep and Vlie inlet, extra nourishments are required due to the sediment demand of the tidal system. The extra quantity of sediment which should be nourished can be derived by substituting equation 6.11 in 6.1, where the coastal regression is expressed as function of the demand of the inlet. Nourishments due to sea level rise comprise a constant amount in time (in the case of a constant sea level rise). Nourishments due to closure equal the exchange between the system and the coast, which results from calibration. These quantities result by integrating transport in time. The determination of these quantities with respect to nourishments is beyond the scope of this study.

Finally, a dynamic equilibrium will be reached, where the consequences of the closure are damped out and the channel and flats continue demanding sediment to keep up with the sea level rise.

	V_{de} (*10^6 m3)	V_{ce} (*10^6 m3)	V_{fe} (*10^6 m3)
Vlie	390	1130	190
Marsdiep	490	2050	50

Table 6.5: Calibrated equilibrium volumes

Results Marsdiep inlet

Regarding the Marsdiep inlet, also a proper calibration is possible for the morphological development of the elements after closure. The calibrated equilibrium volumes are presented in table 6.5. In appendix G3 the calibrated results are presented. The channel shows a plausible development and is likely to decrease more towards equilibrium in the future.

As discussed before (section 5.4) the calculated flat volumes of the Marsdiep are rather inaccurate, due to the relative small volume compared to the channel volume (2%). Moreover, the morphological development of channel and delta are not really sensitive to changes in equilibrium volume of the flat (see section 4.3.4). As a result, the calibrated equilibrium volume of the flat could deviate from the reality. Though a reasonable calibration is realised (see appendix figure G3.2).

Unexpected development is seen in the morphologic behaviour of the delta. The delta does not show the expected increase. It turns out that, even for the upper limit of the adjustment, the delta remained stable after closure.

It can be seen that the channel has less difficulties to obtain sediment than the channel of the Vlie inlet. This is because the need of the delta appears to be almost zero, and the demand of the flats is negligible. Therefore, the bump, as discussed in section 6.2 did not occur. The flat and delta are likely to be close to equilibrium, while the channel will need 100 million

m^3 to reach its estimated equilibrium. This sediment will be drawn from the coast. Nourishments delay this process, in the same way as discussed for the Vlie (see also figure G3.3, for adjustments delta in time). Figure G3.4 illustrates that it will take another 150 years before the system reaches equilibrium. This is of the same order of magnitude as the largest system time-scale of 198 years.

Then, the most important question is, why the delta has not increased since the closure, despite the increase in tidal volume of 25%? There are several possible reasons for this. One of them is that the data or applied adjustments in the model are not correct. Yet, according to personal communication with Mulder (RIKZ, march 2001), the preliminary results of the new calculations of the delta, show similar results. These new calculations comprise the determination of volumes of the Marsdiep delta from field data, related to the actual (changing) coastal profile. Hence, calculations of the delta based on field data, show the same results as the simulations with applied adjustment in Asmita. This indicates that the simulation and adjustment can be considered realistic.

Other possible explanations should be found for the calibrated results, which show a time-invariant delta volume in time. The reason for the fact that the delta has not increased, may be that at the time of the closure the volume of the delta was larger already than its equilibrium level. This could be caused by storm surges. Before the closure, a storm surge caused a set up in the entire Zuiderzee. This increased the tidal volume considerably. As a consequence, the accumulations in the delta during ebb were stronger than normal. This may have caused the delta to grow incidentally beyond its equilibrium size. The increase of the tidal volume due to the closure may have preserved this excess. The net effect could have been a stable delta. The reason that this effect has not occurred in the Vlie inlet could be the different orientation (north-south instead of east-west), and the fact that the Marsdiep basin was more dominantly connected with the Zuiderzee than the Vlie basin.

Finally, it must be noted that other factors could have played a role. Marsdiep inlet is everything but an ordinary inlet among the other (western) Wadden inlets. It is the first significant interruption in the dominating northwards longshore drift along the Wadden coast, it has an east-west orientation and finally, it is a long shaped basin with deep channels and little flat area. All these factors could have played a role in the deviating development of the delta of Marsdiep.

6.4.4 Uncertainties calibration

The equilibrium volumes are calibrated between the expected ranges and optimised with Least Squares between these boundaries. The calibrated morphological development is plausible, but still shows deviations. This means that the calibrated equilibrium volumes could deviate as well. Root mean square errors for Marsdiep and Vlie equal $2.6*10^7$ m^3 respectively $4.6*10^6$ m^3. These errors represent several uncertainties. Some of these were already explained in section 5.6. We concluded that the boundary assessment regarding the interpretation of the field data of the delta and flat, plays an important role in the calibration process. Besides, the estimated input parameters of Asmita could contribute to these uncertainties.

In this chapter, a possible adjustment for the changing boundaries of the delta was introduced. The adjustment factor β contains uncertainties with respect to the height and width of the coast and delta segment. Furthermore, it is uncertain whether all sediment is withdrawn from the coast. These uncertainties were analysed by calibrating two scenarios, but does not mean that the actual used factor is correct.

Despite the discussed uncertainties, the calibration with extension for coastal regression turned out to be reasonable. So, possible deviations are not expected to be significant. However, for a more detailed calibration of equilibrium volumes, it would be interesting if the aforementioned uncertainties could be reduced in further studies.

Finally, we will briefly evaluate the accuracy of empirical equilibrium relations (see equations 3.3 and 3.8). In this study it is essential to calibrate equilibrium volumes, as an apriori estimation, based on equilibrium relations was not possible. However, with the results of the calibration we can evaluate the equilibrium relations which hold for the Marsdiep and Vlie inlets. Based on the calibrated equilibrium volumes and the tidal prism we can derive the equilibrium coefficients as indicated in equation 3.3 and 3.8. Subsequent, the coefficients found with respect to the channel volume can be compared with the empirical coefficients derived for the Wadden inlets by Eysink and Biegel (1992). The coefficient found with respect to the delta volume can be compared with the relation derived by Walton and Adams (1976).

In table 6.6 the empirical coefficients according to the empirical equilibrium relations regarding delta and channel (equations 3.3 and 3.8) are presented, and the coefficients corresponding to the calibrated equilibrium volumes. To determine the equilibrium coefficients for the Marsdiep and Vlie, estimated values for prism in 1998 are used.

	P (10^6 m3)	**V_{de}** (10^6 m3)	**α_d calibr.** ($m^{-0.5}$)	**α_d emp.** ($m^{-0.5}$)	**V_{ce}** (10^6m3)	**α_c calibr.** ($m^{-0.23}$)	**α_c emp** ($m^{-0.23}$)
Vlie	1100	390	0.0030	0.0063	1130	1.1e-5	1.6e-5
Mars	980	500	0.0043	0.0063	2050	2.37e-5	1.6e-5

Table 6.6: Equilibrium coefficients derived from calibration (calib.), compared to empirical (emp.) coefficients according to Eysink and Biegel (1992) and Walton and Adams (1976).

In table 6.6 we can see that the coefficients found for the Marsdiep and Vlie deviate from the empirical coefficients according to Eysink and Biegel and Walton and Adams (1976). Large deviations between these coefficients illustrate that in general, we cannot predict equilibrium volumes, based on a relation only, and fix them in the calibration of Asmita. Estimating rough changes using the proportionality in the power relation, as done for the delta, may be justified, assuming that the power relation on itself is accurate enough. However, the results in table 6.6 indicate that we should carefully use empirical relations in (semi) empirical models. Using the equilibrium volumes as calibration parameters, as done in this study, is a good option.

6.5 Conclusion calibration

From the linearised equations we derived system time-scales for Vlie and Marsdiep. For both Vlie and Marsdiep, it holds that the intensities of the responses corresponding to the smallest two time-scales have reduced with some 85% or more after about half a century. Then, the largest time-scale will dominate the morphological development.

Due to coastal erosion the delta volume grows. This artefact of the Asmita definition of the delta is called geometric growth. This is taken into account in Asmita by adjusting the delta. This adjustment is determined by the demand of the inlet system due to the closure and the demand of the basin to keep up with the sea level rise. These adjustments are applied till 1990, as since then the coastline has been maintained at its then position by nourishments. Three equilibrium volumes have been used for the calibration of Asmita. It was necessary to calibrate these values, as it was not possible to estimate them at forehand, based on equilibrium relations. The other input parameters are estimated and fixed during the calibration. Diffusion coefficients calibrated for the Zoutkamperlaag, are scaled to diffusion coefficients for the Marsdiep and Vlie, using the length-scale ratios of the basins.

The equilibrium volumes are calibrated between the expected ranges and optimised with Least Squares between these boundaries. A plausible calibration of Asmita for the morphological development of Vlie and Marsdiep inlet is possible, including the extension for coastal regression. All elements show the expected development. Only the delta of the Marsdiep shows an unexpected, invariable development. Also, this same development is confirmed by preliminary data-calculations by RIKZ. A possible explanation for this effect is that the delta volume before closure already exceeded its equilibrium value, due to the storm surges in the former Zuiderzee.

Regarding both Marsdiep and Vlie inlets, the channel is the element which reacts the slowest. The delta and flat are close to their estimated equilibrium state. It will take at least a century before the channel, and thus the total system, reaches its equilibrium. About 170 million m^3 of sediment will be transported into the Vlie and Marsdiep basins. Beach nourishments slow down this process, because then the delta does not grow geometrically anymore which reduces the available sediment for especially the channel.

With respect to the Wadden coast adjacent to the Marsdiep and Vlie inlets, extra nourishments (compared to a straight coast) are required due to the sediment demand of the tidal system. The extra quantity of sediment to be nourished, can be derived based on the sediment demand of the inlet system due to closure, and the demand of the basin to keep up with the sea level rise. In the calibration a constant sea level rise of 17 cm per century has been assumed.

7 Conclusions and Recommendations

Hereafter, the conclusions from the present study are presented. Furthermore, some recommendations are given, for future research.

7.1 Conclusions

The conclusions concern three subjects: the use of a linear approximation of the Asmita model (chapter 4), the field-data analysis (chapter 5), and finally, the calibration of Asmita (chapter 6).

7.1.1 Conclusions linear approximation Asmita

- By linearising Asmita, the morphological development of a tidal inlet has been expressed explicitly in time-scales. The response of each element is described by a combination of system time-scales, which depend on geometric and exchange characteristics of the system (input parameters of Asmita).

- The linear approximation gives a simple analytical expression for the time-scale of an individual element, which indicates the initial adaptation capacity of an element for particular disturbances in a system. We concluded that factors like size of disturbances, size of relative disturbances (compared to volume) and the proximity of the outside world influence the time-scales of individual elements in a tidal system.

- The linearised equations are useful to predict the characteristic morphological response of the elements, given a certain combination of imposed disturbances in a tidal system. It has been demonstrated that in some situations an element does not evolve monotonously towards its equilibrium state, but first overshoots its equilibrium or initially moves away from it.

- In the present study it was not possible to derive system time-scales from the available field-data. Using the linearised equations, it may be possible to derive system time-scales from field observations, on the conditions that:
    1) period of interest is such that all system time-scales can be recognised.
    2) number of degrees of freedom are small compared to the number of data-points.

- It turned out that in the case of the calibration of the Marsdiep inlet, input parameters like the equilibrium volume, the diffusion coefficients and equilibrium concentration have a large influence on the system time-scales and thus on the morphological development, compared to the other Asmita parameters. These formed important parameters in the calibration.

7.1.2 Conclusions data-analysis regarding closure Zuiderzee

- Analysis of the tidal pattern before and after closure, and the maps of bed topography in the period 1933-1998, showed that especially in the Marsdiep and Vlie inlets considerable changes occurred. Eierlandse gat and Borndiep inlet have been less affected by the closure.

- Regarding the hydrodynamics in Vlie and Marsdiep basin, the character of the tidal wave along the basin changed from a more propagating character in the former Zuiderzee, into a more standing character after closure. While before closure the tidal range decreased from sea towards Nijkerk, the tidal range after closure increased from sea towards the Afsluitdijk. As a result the tidal volume in the Vlie and Marsdiep inlets increased after the closure.

- Considering the development of the volumetric data of Marsdiep and Vlie inlets, both the delta and the channel show a decrease of volume with time, which is not directly expected, based on the increase in tidal volume. The seeming decrease of the delta volume is the result of unjustly neglecting the regression of the coast. The decrease of the channel is result of a net sedimentation in the back, which is larger than the erosion near the throat of the inlet. The flats show an increase, due to the decreased basin area and the increased tidal range.

7.1.3 Conclusions calibration Asmita

- In the equilibrium relations the proportionality between the tidal prism and volume of the elements is given by empirical equilibrium coefficients. Analysing the equilibrium coefficients found in the calibration of equilibrium volumes, showed large deviations from the empirical coefficients by Eysink and Biegel (1992) and Walton and Adams (1976). Therefore, equilibrium relations should be used carefully as basis for predictions in large scale modelling.

- A plausible calibration of the morphological development of Vlie and Marsdiep inlets is possible with Asmita, including the extension for coastal regression. All elements show the expected development, as concluded from the data-analysis. Only the delta of the Marsdiep shows an unexpected, invariable development. This same development is confirmed by preliminary data-calculations by RIKZ (march 2001). A possible explanation for this effect is that the delta volume before closure was already larger than its equilibrium value. Before closure, storm surges caused set ups of the Zuiderzee, which could have increased the tidal prism considerably.

- It will take at least another century before the channels of Vlie and Marsdiep basin, and thus the total system, reaches its equilibrium. About 170 million m^3 of sediment will be transported into the Vlie and Marsdiep basins. Beach nourishments, which are carried out since 1990, slow down this process. Because then the delta does not grow geometrically anymore, the available sediment for especially the channel reduces.

- With respect to the Wadden coast adjacent to the Marsdiep and Vlie inlets, extra nourishments are required due to the sediment demand of the tidal system. The extra quantity of sediment to be nourished, can be derived based on the sediment demand of the inlet system due to closure, and the demand of the basin to keep up with the sea level rise.

- An error analysis concerning the calibration of Asmita to the closure of the Zuiderzee pointed out that uncertainties in the calibration process are expected with respect to the boundary interpretation of the elements (especially the delta) and the adjustment factor for the delta with respect to coastal regression.

7.2 Recommendations

- The applied adjustment for the delta for coastal regression could deviate because of the uncertainties in the adjustment factor. This factor contains length and height ratios of the delta and adjacent coast, which are based on rough estimates. Furthermore, it is uncertain whether all sediment actually originates from the coast adjacent to the delta. An investigation into coastal regression of the Wadden islands till 1990 could help to validate the applied correction.

- It was assumed that the coastal (cross-shore) profile is in equilibrium, as its adaptation time-scale is small compared to the system time-scales. The calibration results can turn out different, if the coast is not in equilibrium and may also demand sediment to reach equilibrium. Then, an interesting option may be to define the coast as a separate element with an equilibrium volume. Then, a more accurate calibration could be obtained.

- The boundaries of the basins and deltas form an important factor in the uncertainties of the total calibration process. Especially the delta and flat volumes are sensitive to deviations in boundaries. It is recommended that in further studies, more attention is given to the arbitrariness and uncertainties of these boundaries. This could result in a more accurate assessment and description of the evolution of the morphological elements.

- In the present study, the increase of the tidal range in time is not taken into account. This increase, in the same way as the rising sea level, influences the morphological development of tidal inlets on long term. The actual and future increase in tidal range and related causes should be investigated. This increase could be analysed with Asmita by introducing a constant forcing in time.

- Finally, more bathymetrical and tidal data of similar tidal systems like the Wadden inlets is desired, which describe the evolution after an imposed (human) interference. Then, the experience with a behaviour orientated model like Asmita may be extended which would definitely improve the knowledge and prediction capacity (better estimation parameters) of long-term modelling of tidal inlets.

References

Battjes, J.A., 1996. Stroming in open waterlopen. College handleiding ctwa331, faculteit der Civiele Techniek en Geowetenschappen, Technische Universiteit Delft.

Biegel, E.J., 1993. Morphological changes due to sea level rise in the Dutch Wadden Sea versus concepts morphological response model MORRES. Report IMAU-93.14. Institute for Marine and Atmosferic Research Utrecht, Utrecht University.

Bosch, drs. A., Ham, drs. W. van der, 1998. Twee eeuwen Rijkswaterstaat (1798-1998). Rijkswaterstaat.

Bruun, P., 1962. Sea level rise as a cause of shore erosion. ASCE Journal of the Waterways and Harbours Division., 88 (WW1), 1962. pp 117-130.

Bruun P., 1954. Coast Erosion and the development of beach profiles. Journal Memorandum No.44, US Army, Corps of Engineers, Beach Erosion Board, Washington D.C.

Buijsman, M.C. 1997, The impact of gas extraction and sea level rise on the morphology of the Wadden sea. Faculty of Civil Engineering, Delft University of Technology

De Vriend, H.J. 1998 On the Predictability of Coastal Morphology. In Proceedings 3rd Marine Science and Technology Conference, 23-27 May, Lisbon, Portugal.

De Vriend, H.J., J. Dronkers, M.J.F. Stive, A. van Dongeren en Z.B. Wang, 1999. Coastal inlets and Tidal basins. College handleiding ctwa5303, faculteit der Civiele Techniek en Geowetenschappen, Technische Universiteit Delft.

Doekes, J. 1985. Invloed van de afsluiting van de Zuiderzee op het getij in de Waddenzee. Nota GWIO 85.001. Dienst getijdewateren, Rijkswaterstaat.

Eysink W.D. and Biegel E.J., 1991. Impact of sealevel rise on the morphology of the Wadden Sea in the scoop of its ecological function. ISOS*2 Project, phase 1, Report H1300. DELFT HYDRAULICS, Delft.

Eysink W.D. and Biegel E.J., 1992. Impact of sealevel rise on the morphology of the Wadden Sea in the scoop of its ecological function. ISOS*2 Project, phase 2, Investigations on morphologic relations. Report H1300. DELFT HYDRAULICS, Delft.

Eysink W.D. and Biegel E.J., 1992. Impact of sealevel rise on the morphology of the Wadden Sea in the scoop of its ecological function. ISOS*2 Project, phase 3, Report H1300. DELFT HYDRAULICS, Delft.

Eysink W.D. and Biegel E.J. Impact of sealevel rise on the morphology of the Wadden Sea in the scoop of its ecological function. ISOS*2 Project, phase 4, Report H1300. DELFT HYDRAULICS, Delft.

Eysink, W.D., 1998. Effecten van bodemdaling door gaswinning in en rond Waddenzee. Morfologische, infrastructurele en economische aspecten. Rapport H3099. DELFT HYDRAULICS, Delft

Fokkink, R.J., 1996. A new evaluation of ESTMORF phase III, New physical relations and a refinement of the calibration. Report Z930. DELFT HYDRAULICS, Delft.

Gerritsen, F., 1990. Morphologic Stability of Inlets and Channels of the Western Wadden Sea. Nota GWAO-90.019. Dienst getijdewateren, Rijkswaterstaat.

Gerritsen, F., 1954. De waterbeweging in de Waddenzee. De Ingenieur Bouw- en Waterbouwkunde, 1954, no.37, blz B145-B154.

Gerritsen, F., 1997. Voorstudie naar een vakindeling van de zandbalans van het zeegat van Texel inclusief buitendelta en kombergingsgebied door middel van een tijdschalen analyse. Kust 2000, Rijkswaterstaat.

Hayes, M.O., 1979. Barrier island morphology as a function of tidal and wave regime. In Barrier Islands, S.P. Leatherman (editor), Academic Press, New York, 1-28.

Louters, T., en Gerritsen F., 1994. Riddle of the Sands. Report RIKZ 94.040, Rijks Instituut voor Kust en Zee, Rijkswaterstaat.

Marion, B.B. van, 1999. Zandbalansen van het Zeegat van Texel met het Invers Sediment Transport Model, 1931-1971. Rapport RIKZ/OS-99.116x. Project Kust*2000, Rijks instituut voor Kust en Zee/RIKZ, Rijkswaterstaat.

Mulder, J.P.M., 1999. Zandverlies op dieper water, samenvatting van de jongste inzichten, Rapport RIKZ/OS 99 165 X. RijksInstituut voor Kust en Zee, Rijkswaterstaat, Den Haag.

Rakhorst, H.D., 2000, draft Ontwikkeling van de westelijke Waddenzee. Erosie en Sedimentatie westelijke Waddenzee en aangrenzende Noordzee; 1926/1933-1982. Nota NH-ANV-2000-20. Directie Noord-Holland, Rijkswaterstaat

Rijkswaterstaat, 1998. Jaaboek monitoring rijkswateren 1998. Kentallen, kroniek en presentator. Rijkswaterstaat.

Ridderinkhof, H., 2000. Ferry observations on the transport of water through the Marsdiep tidal inlet between the North Sea and Wadden Sea (1998-2000). Artikel nav TESO metingen. NIOZ, Texel.

Sha 1990, Sedimental studies of the ebb-tidal deltas along the West Frisian Islands, the Netherlands. Universiteit van Utrecht

Sha L.P. and Van den Berg J.H., 1993. Variation in Ebb-tidal Geometry along the coast of the Netherlands and the German Bight, Journal of Coastal Research, 9(3), p730-746.

Smittenberg, T.J., 1999, Erosie en Sedimentatie balans tussen westelijke Waddenzee en aangrenzende kust. Stage verslag, Directie Noord-Holland, Rijkswaterstaat.

Staatscommissie Zuiderzee (Lorentz, H.A., Lely, C.W. et al), 1926. Verslag Staatscommissie Zuiderzee 1918-1926, 1926. ‘s Gravenhage.

Steetzel, H., 1995. Voorspelling ontwikkeling kustlijn en buitendelta’s Waddenkust over de periode 1990-2040. Rapport H1887. DELFT HYDRAULICS, Delft.

Stive, M.J.F., Capobianco, M., Wang, Z.B., Ruol, P. and Buijsman, M.C., 1998. Morphodynamics of a Tidal Lagoon and adjacent Coast. 8th International Biennial Conference on Physics of Estuaries and Coastal Seas, The Hague, September 1996, pp 397-407.

Thijsse, Prof.dr.ir. J. Th., 1972. Een halve eeuw Zuiderzeewerken 1920-1970. H.D. Tjeenk Willink B.V. Groningen.

Van Goor, M.A., 2001. Influence of Relative Sea Level Rise on Coastal Inlets and Tidal Basins. Note Z2822, DELFT HYDRAULICS, Delft.

Walton, T. L., and Adams, W.D., 1976. Capacity of Inlet outer bars to store sand, Proceedings of 15th Coastal Engineering Conference, ASCE, Honolulu, Hawai, p1919-1937.

Wang, Z.B. and Karssen, B., 1992. A dynamical/empirical model for the long-term morphological development of esturaries, Note Z473.20, DELFT HYDRAULICS, Delft.

Wang, Z.B. and Karssen, B., Fokkink, R.J. and Langerak, A., 1998. A dynamical/empirical model for the long-term morphological development of esturaries. 8th International Biennial Conference on Physics of Estuaries and Coastal Seas, The Hague, September 1996, pp 279-286.

Zagwijn, W.H., 1986. Nederland in het Holoceen, Rijks Geologische Dienst Haarlem, Staatsuitgeverij, ‘s-Gravenhage.